DISSERTATION

EXPLORING RADAR AS A TOOL FOR STUDYING MIGRATORY BIRDS AND THEIR RELATIONSHIPS WITH DYNAMIC LANDSCAPES

Submitted by

Miguel F. Jimenez

Graduate Degree Program in Ecology

In partial fulfillment of the requirements

For the Degree of Doctor of Philosophy

Colorado State University

Fort Collins, Colorado

Summer 2025

Doctoral Committee:

Advisor: Kyle G. Horton

Veronica Yovovich
David N. Koons
Kristen C. Ruegg

ABSTRACT

EXPLORING RADAR AS A TOOL FOR STUDYING MIGRATORY BIRDS AND THEIR RELATIONSHIPS WITH DYNAMIC LANDSCAPES

As a crisis-based discipline, conservation biology necessitates that we make timely management decisions to protect species based on the best available information. In effect, as new scientific tools become available, we must contend with simultaneously applying them in ways that provide novel insights and evaluating their limitations to assess the validity of those insights. The integration of radar with machine learning is one such tool that has revolutionized aeroecology, or the study of airborne organisms. Burgeoning methodologies leverage this integration, offering unique opportunities to understand how migratory birds are responding to large-scale environmental changes, such as urbanization and shifting light regimes. In this dissertation, my goal was to elucidate the promises and shortcomings of radar and machine learning as tools for informing migratory bird conservation management amid rapid global change.

As a first step, I focused on validating observations from a local weather radar station. Weather radar systems have become a central tool in the study of nocturnal bird migration. Yet, while studies have sought to validate weather radar data through comparison to other sampling techniques, few have explicitly examined the impact of range and topographical blockage on sampling detection—critical dimensions that can bias broader inferences. In my first chapter, I assess these biases with relation to the

Cheyenne, WY Next Generation Weather Radar (NEXRAD) site, one of the large-scale radars in a network of 160 weather surveillance stations based in the United States. I compared local density measures collected using a mobile, vertically looking radar with reflectivity from the NEXRAD station in the corresponding area. Both mean nightly migration activity and within night migration activity between NEXRAD and the mobile radar were strongly correlated ($r = 0.85$ and 0.70, respectively), but this relationship degraded with both increasing distance and beam blockage. Range-corrected NEXRAD reflectivity was a stronger predictor of observed mobile radar densities than uncorrected reflectivity at the mean nightly scale, suggesting that current range correction methods are somewhat effective at correcting for this bias. At the within night temporal scale, corrected and uncorrected reflectivity models performed similarly up to 65 km, but beyond this distance, uncorrected reflectivity became a stronger predictor than range-corrected reflectivity, suggesting range limitations to these corrections. Together, these findings further validate weather radar as an ornithological tool, but also highlight and quantify potential sampling biases.

In my second chapter, I focused on using NEXRAD to study habitat transitions by migratory birds. During migration, birds regularly transition between terrestrial and aerial habitats. Yet, much of our understanding of migratory behavior is centered around either terrestrial habitat quality or atmospheric conditions separately, at relatively coarse temporal scales. I employed NEXRAD to study the dynamic drivers and relative importance of terrestrial, aerial, and sampling predictors as birds transition between the terrestrial and airspace boundary. I found that atmospheric conditions were consistently strong predictors of migration activity throughout the night, and across spring and fall

seasons. Key sampling predictors, such as the time after local sunset, fluctuated throughout the night, with high importance shortly after sunset and diminishing importance in the middle of the night. Yet, terrestrial variables were not a strong predictor of nightly variation in migration activity. My results demonstrate that the importance of predictors of activity varies temporally, both within a single night and across seasons. These findings illuminate bird migration as a dynamic process, highlighting limitations and opportunities for employing weather surveillance radar to study transitions between terrestrial and aerial habitats.

In my third chapter, I used NEXRAD to study migratory stopover in urban areas. Despite global expansion, the role of cities in macroecological processes remains understudied. Using radar estimates of migratory bird stopover across the U.S., I assessed urban landscapes' contributions to stopover and links to social demographics for 2,130 parks across 88 cities. Stopover hotspots disproportionately occurred on urban landscapes relative to land area, with nearly 50% of spring migration hotspots falling within Metropolitan Statistical Areas. The relationship between urbanization and stopover varied regionally, correlating negatively in eastern flyways and positively in western flyways. Finally, stopover was positively correlated with income but varied considerably, with many cities showing no effect or an effect in the opposite direction. This study highlights the significance of cities in a hemispheric-scale ecological process and demonstrate radar as tool for studying urban social-ecological interactions.

Finally, in my fourth chapter, I investigated the effects of different light spectrums on birds in flight for the purpose of informing novel conservation management approaches. Artificial light at night (ALAN) has been shown to influence the behavior of

migratory birds, yet how different light spectra modulate these effects is somewhat unclear. I conducted a field experiment across 31 nights at a remote site in northern Colorado using LED floodlights with white, red, amber, and blue lighting treatments during fall migration in 2023 and 2024. Using a vertically looking radar system, I quantified avian in-flight responses in migration traffic rate, flight height, and flight direction. I found that short wavelength, white light significantly reduced flight height, and this response was stronger than red, amber, or blue lights. Beyond providing insight into avian biology, my results could have implications for the conservation management of ALAN. Further, the ability to detect behavior changes from a small point source in a low-density migration system supports the notion that ALAN may be more pervasive than is often recognized.

At its core, my dissertation is indicative of a broader shift in ecology and conservation science. Advances in remote sensing offer an opportunity to vastly expand the way we characterize social-ecological systems thereby diversifying the options we have for managing them. However, this “big data” approach must be validated and informed by local inference. My work emphasizes this point. As the integration of large datasets and machine learning become increasingly prominent in conservation biology, I urge the conservation community to explore their potential with creativity while remaining vigilant of the potential biases they may introduce.

ACKNOWLEDGEMENTS

As a firm believer that good scientific work is never the product of individual efforts, I have a long, non-exhaustive list of people that I would like to thank and acknowledge for helping me throughout my dissertation. First, I would like to thank Colorado State University's Graduate Degree Program in Ecology and Department of Fish, Wildlife, and Conservation Biology Department for supporting me throughout two graduate degrees. More specifically, I thank my advisor, Kyle Horton, and committee members, Veronica Yovovich, David Koons, and Kristen Ruegg, for their guidance as I developed my research questions, study designs, and analyses. I'd like to give additional thanks to Brian Gerber for his help while developing my analyses and Liba Pejchar for her continued mentorship.

I'd like to thank the various members of the Aeroeco Lab, past and present, for their support throughout my PhD, including Ali Khalighifar, Amy Collins, Hanna McCaslin, Maria Belotti, Yuting Deng, Victoria Simons and Carrie Ann Adams. I also thank everyone who helped me collect field data including Annika Abbott, Riana Zinn, Aitao Liu, and Christian Narby.

I estimate that I listened to approximately 120,000 minutes of music while reading, writing, collecting data, and writing code for my dissertation. Several artists emerged as particularly prominent components of the soundtrack that served as the backdrop for my research. I'd like to especially highlight (in no particular order) Stereolab, Noname, Saba, Haley Heynderickx, o.negative/timebandit, skozi.b, Nolen and Friends, Reckling, Gardens, Ahmad Jamal, Bill Evans Trio, Mort Garson, Big Thief,

Adrianne Lenker, Joanna Sternberg, Dijon, Sinead O'Connor, and Gorillaz. I also thank Cristyn Hypnar for providing the illustrations for Figure 3.1.

On a more personal note, I was fortunate to be surrounded by an incredible community that created space for fostering ideas, protecting my work-life balance, maintaining perspective beyond my research, and providing emotional support throughout my graduate career. For this, I thank the incredible group of graduate students in my cohort across Colorado State University's Graduate Degree Program in Ecology and Fish, Wildlife, and Conservation Biology Department. I thank the artist community of northern Colorado, especially FoCoMA and Wolverine Farm Publick House for providing a platform for me to explore the space between art and science. I thank Ryan Friebertshauser and Jacob Hoeffner for helping me create and perform my musical project, Swamp Candle, which was an artistic mirror for my dissertation.

I thank my parents, Francisco and Conception Jimenez, for their guidance and selflessness in providing me with opportunities throughout my career and life. I thank my sister, Elly Jimenez, for always providing an example of how to "dream big! Huge! outside of the current reality!" I, of course, give my deepest love and thanks to my fiancé, Dr. Sarah Jacobson, for her support and companionship throughout my career and personal life. I also thank our two feline sons, Ollivander and Pippin for waking me up every meowning.

Finally, I dedicate space in my work to my friend and colleague, Gabriel Trujillo. Gabe's ceaseless passion for nature and scientific understanding served as a guiding light since the beginning of my research career and I partially credit a lunch with him in Brooklyn for convincing me to return to graduate school. Gabe had the special moments

of finishing his PhD taken away from him. As I have the privilege of experiencing them myself, I hold space for and think of him.

TABLE OF CONTENTS

POSITIONALITY STATEMENT

I believe my positionality as a cis-gendered, first-generation Filipino-American male has provided me with a unique positionality within conservation biology and the broader scientific field. While my identity has granted me immense privilege in some spaces, it has also excluded me from others, forcing me to think critically about the intersectional nature of that exclusion. At the most basic level, conservation has historically been a predominantly affluent white male-dominated space. As such, I did not grow up viewing a place for myself in conservation science. As I have moved farther into this field, my commitment to conservation is often at odds with my recognition of its deep roots in racism and xenophobia. President Theodore Roosevelt, for instance, is often deemed “The Conservation President” but also ran on a campaign of explicitly dehumanizing and colonizing Filipinos. John James Audubon, the namesake of the bird conservation non-profit that employed me for over two years, was a slave-owner and held white supremacist views.

These contradictions have impacted my career in concrete ways. Unlike many of my colleagues, I did not grow up engaging in outdoor activities like camping or hiking. I did not have parents or family members with advanced degrees to guide me through academia and a career in STEM. I did not have the financial stability to pursue unpaid positions as a means for gaining professional experience. Yet, I also hold privileges that many of my colleagues don’t. Unlike many of my colleagues, I don’t believe I’ve ever been discriminated against on the basis of my gender, and I’ve never had to hide my sexual orientation. I believe the vantage point of holding some privileges but not others

has profoundly shaped the way I view conservation science. It has granted me access to corners of conservation spaces, but also a keen awareness of who isn't in those spaces and the conviction that I cannot effectively protect biodiversity without the

CHAPTER 1: QUANTIFYING RANGE- AND TOPOGRAPHICAL BIASES IN WEATHER SURVEILLANCE RADAR MEASURES OF MIGRATORY BIRD ACTIVITY

INTRODUCTION

The vast majority of bird migration occurs at night and cannot be directly observed (Larkin & Szafoni, 2008; McLaren et al., 2018). Ornithologists have attempted to overcome this challenge using various monitoring techniques, including moon watching (Liechti et al., 1995; Nisbet & Drury, 1969), acoustic monitoring (Evans & Mellinger, 1999), and the deployment of tracking devices on individual birds to monitor migration behavior (McKinnon & Love, 2018; Robinson et al., 2010). One approach that has become central in characterizing nocturnal migration activity, and more broadly throughout aeroecology, is the use of weather surveillance radar (Shamoun-Baranes et al., 2021). Radar has been used for more than 75 years for the study of migratory birds (Lack & Varley, 1945; Gauthreaux, 1970). Enhanced data access and the integration of machine learning, however, has led to a resurgence in the past decade in its use for quantifying movement of nocturnal migrants and driving predictions of where and when large migration events will occur across the continental United States (Van Doren & Horton, 2018). More broadly, radar-driven models are being used in a growing number of applications at multiple spatiotemporal scales including identifying key stopover locations (Cohen et al., 2021; Guo et al., 2023), estimating migratory bird exposure to anthropogenic light (Horton et al., 2019a; Weisshaupt et al., 2022), monitoring and forecasting nocturnal migration events (Horton et al., 2021; Kranstauber et al., 2022; Shi et al., 2023; Van Doren & Horton, 2018), and identifying phenological shifts (Deng et al., 2022; Haest et al., 2021b).

Given its increasingly prominent role in shaping our understanding of nocturnal bird migration, it is vital to identify and account for potential spatial and temporal biases in weather radar datasets. Cross-validation studies can be used to determine these biases and inform methods that account or correct for biases, such as range, blockage, and clutter contamination (Buler & Diehl, 2009a; Van Doren et al., 2023). Studies have found that time-referenced line-transect survey estimates of bird observations (Dokter et al., 2013) and visual bird migration counts (Schmidt et al., 2017) correspond well to radar reflectivity. As radar technology has progressed and dedicated bird radars, which are designed specifically to study avian activity, have become available, studies have compared across radar types, both validating weather radar as an ecological tool and illuminating the nuances of each radar system. For example, Dokter et al. (2010) used reference data collected by an X-band radar to validate an automated method for estimating real-time bird density altitude profiles from weather radar data. Gauthreaux et al. (2019) found that seasonal trends in L-band and S-band weather radars bird activity estimates were correlated, but suggested that this relationship was weakened by periods of low migration activity and differences in coverage volume and resolution. Nilsson et al. (2018) compared the observations across four different radar systems and found that weather radar measures of nightly migration intensity across a season correlated with high-resolution, vertically directed radars, particularly under clear sky conditions and at high altitudes. Together, cross-validation studies generally confirm that measures of avian biomass in the atmosphere correlate across different radar types, demonstrating the promise of weather surveillance systems as an ecological tool.

However, given these radar networks are designed to study weather conditions, there are inherent limitations for their use in aeroecology. For example, stations across the Next Generation Weather Radar (NEXRAD) system, a network of 160 weather surveillance stations based in the United States (Crum & Alberty, 1993), tend to be located at high elevation and thus may miss biological targets that reside beneath the radar's sampling pattern. Additionally, NEXRAD also has considerable spatial coverage gaps for biological use. These gaps are particularly pronounced across the Western flyways of the continental United States, where radars are less densely distributed. In recognition of this potential bias, range-corrective methods have been developed to account for the rising radar beam height that occurs with increasing range from the radar (Kranstauber et al., 2020). These methods seek to normalize detection probabilities of in-flight migrants and have been applied in practice to improve estimates of avian activity (Hoekstra et al., 2024; Horton et al., 2023). Yet, the limitations of these corrective measures have yet to be validated across various ranges.

Further, because the electromagnetic pulses emitted by radar can be blocked by landscape features, they are prone to missing aerial activity shaded by topographic blockage, such as mountains in high elevation regions. Based on estimates from clutter masking techniques (Buler et al., 2012), more than half of NEXRAD stations show some degree of blockage with this issue being more pronounced in the western continental United States. This combination of sparse NEXRAD radars and beam blockage due to topography leave the NEXRAD system potentially incapable of detecting important migration corridors in the western United States. Radar has also been used at increasingly varied temporal scales, ranging from analyses of within-night variation in

migration activity (Horton, Shriver, et al., 2016), to mean nightly estimate comparisons (Nilsson et al., 2018), and even to seasonal estimates of stopover intensity (Guo et al., 2024a). Given the temporal variation in NEXRAD-based studies, it may also be important to understand how these relationships change with temporal resolution.

I employed a high-precision, mobile X-band radar system designed to quantify animal movements in the lower atmosphere to address these limitations and enable filling spatial gaps in NEXRAD-based predictions across the continental United States. I compared migration intensity measured across two different, but complementary radar systems: the BirdScan MR1 and NEXRAD. More specifically, I collected data with the BirdScan MR1 at varying distances and elevations from the NEXRAD station in Cheyenne, WY, to quantify the relationship between these measurements and test how it varied with 1) the distance from the NEXRAD station and 2) beam blockage. I compared these relationships at the nightly and within-night temporal range, and with range-corrected and uncorrected NEXRAD data to understand how they are impacted by temporal resolution and the degree to which current range-correction efforts are affected. I predicted that NEXRAD measures of reflectivity would be less correlated with BirdScan MR1 measures of density as both distance and topographical blockage increased. Additionally, I predicted that relationships would be stronger at the nightly temporal scale and when range-corrections were applied.

MATERIAL AND METHODS

Study system

The NEXRAD station in Cheyenne, WY (41.15°N, 104.80°W; hereafter referred to by NEXRAD station code “KCYS”) monitors the atmosphere across large portions of

southeastern Wyoming and northern Colorado (Figure 1.1). The landscape of northeastern Colorado and southern Wyoming is dominated by a mix of rangeland and shortgrass prairie, which is relatively flat, whereas the foothills of the Rocky Mountains begin in north central Colorado. The region ranges from semi-arid plains to mid-elevation forests. Weather surveillance radar estimates of avian migration across the western United States, are likely prone to error (Ruth et al., 2012) and landscapes such as the one covered by the KCYS station remains ripe for testing the assumptions embedded in these methodologies.

Data collection with the BirdScan MR1

I collected nocturnal migration data with the BirdScan MR1, a vertically directed, mobile, 25 kW X-band (9.4 GHz, 3.2 cm wavelength) pulse radar system designed to monitor and quantify aerial animal movements (Haest et al., 2024; Swiss Birdradar, 2022; Zaugg et al., 2008). I used the short-pulse, antenna-rotating setting, which emits electromagnetic pulses with a pulse length of 81ns and shot frequency of about 1800 Hz. The pulses reflect off objects in the airspace and produce backscatter up to about 1500m, depending on the size of the object (Schmid et al., 2019; Weisshaupt et al., 2023). The temporal variation of the returned backscatter is then used to classify objects into bird types (unidentified, swift, passerine, wader, or flock), aerial insects, or precipitation based on echo features such as flight patterns, wingbeat frequency, and the radar cross section, which is a metric of target size (Haest et al., 2021a; Schmid et al., 2019; Zaugg et al., 2008).

During spring migration (April 1st-May 31st) in 2022 and 2023, I collected bird migration data along two 100km linear transects, both of which began at the KCYS station

and included five data collection sites located at varying distances (~20-100km) from the starting point of the transect for a total of 10 sites (Figure 1.1). To collect data across a diversity of topographies, one transect extended southeast into the relatively flat landscape of the Eastern Plains of Colorado and the other transect extended southwest into the foothills of the Rocky Mountain. I collected data at each site for two to three nights between civil twilights throughout each spring migration season. Visits were randomized with a random number generator, such that the order of site selection varied across both seasons.

I used the *birdscanR* R package (Haest et al., 2023) to extract and process measures of bird migration activity from the BirdScan MR1 in R (R Core Team, 2022). I used the *computeDensity()* function to calculate the density of targets flying in all directions within an altitudinal range of 25-1500m throughout the night for each 20-min period at each of the sampling sites, sum these values vertically across altitudinal bins, and filter out non-avian data to calculate migratory bird density (birds/km^2).

Downloading and processing NEXRAD data

I used data from NEXRAD as a comparison point for estimated migration densities. The NEXRAD network is jointly operated by the National Weather Service, the Federal Aviation Administration, and the U.S. Air Force. NEXRAD data are publicly accessible through Amazon Web Services (Amazon Web Services, 2023). Radar reflectivity (η) is a measure of the returned power from atmospheric activity, which can be used to estimate biomass within a volume of air (Chilson, Frick, et al., 2012). This radar product is commonly filtered to remove non-biological clutter and corrected to account for range bias

(Buler and Diehl, 2009). To understand the degree to which range-corrections improve the accuracy of NEXRAD estimates, I compared the migration density estimates derived from BirdScan MR1 to both the uncorrected and range-corrected radar reflectivity.

I downloaded level-II (NWS WSR-88D National Level II) radar scans to characterize migratory activity from local sunset to sunrise from April 1 to May 31 of 2022 and 2023. I used the *bioRad* R package to extract, process, and convert radar reflectivity factor (Z) into radar reflectivity (η), which is a more biologically relevant variable (Chilson, Frick, et al., 2012). I extracted data from the KCYS radar for each night of interest from scans at elevation angles ranging from 0°-4.5° and calculated the mean reflectivity over 20-minute sampling periods. I used the '*apply_mistnet*' function to filter out precipitation (Lin et al., 2019). To account for the NEXRAD station sampling an increasing height above ground level with increasing distance from the radar (Buler and Diehl, 2009), I compiled scans into vertical profiles of reflectivity and calculated the expected reflectivity at each pixel in each planned position indicator (PPI) using the '*integrate_to_ppi'* function in bioRad (Kranstauber et al., 2020). I omitted PPI pixels with a range adjustment factor (R) greater than 10 from my averaging. For uncorrected rasters, I summed the reflectivity values from the scans across elevation angles. Lastly, I changed the reflectivity values to 0 for volumes that were labeled as precipitation by MistNet for both corrected and uncorrected data. I used this process to output one range-corrected raster of migratory activity and one uncorrected raster of migratory activity. For each night that was sampled with the BirdScan MR1, I extracted reflectivity values within a 2km buffer of each sampling site from both the corrected and uncorrected rasters at a spatial resolution of approximately 0.0095 degrees in both latitude and longitude and averaged them into a

temporal resolution of 20-minute periods. I used these data to summarize mean nightly reflectivity at each site.

Covariate calculation, model-building and assessment

To assess the effects of sampling range, elevation, and beam blockage on the relationship between Birdscan MR1 traffic rates and NEXRAD reflectivity, I included them as covariates in my models. For range, I calculated the distance between survey points and the KCYS station using the *geosphere* package in R (Hijmans, 2022). To calculate elevation, I downloaded elevation raster data from the USGS GIS Data Download Application (United States Geological Survey, 2023) and extracted values at my sampling locations. To calculate blockage, I used the *geosphere* R package to produce a raster of the proportion of beam blockage with a beam angle of 0.5 degrees around the KCYS station following the methodology from Buler & Diehl (2009) and extracted the values at each of my points. Elevation and beam blockage were highly collinear (r=0.75), so I removed elevation as a predictor. I scaled and centered beam blockage and distance to avoid numerical instability. To ensure that unequal migration activity across sites and sample size reduction from range adjustment factor filtering were not driving my results, I used a one-way analysis of variance (ANOVA) to compare the mean nightly bird migration densities and the number of removed cells across my sites.

I assessed relationships between BirdScan densities and NEXRAD reflectivity at two temporal scales. I calculated the mean values of each radar system for each sampling night to capture nightly variation and used mean values of the 20-minute

sampling periods to capture within-night variation. Additionally, I built sets of models with both range-corrected and uncorrected NEXRAD reflectivity values. For both temporal scales, I square root transformed NEXRAD reflectivity and BirdScan densities to account for zero-inflation.

I calculated the Pearson's correlation coefficient between BirdScan densities and NEXRAD reflectivity, before and after filtering out insect detections. To test my hypothesis that both distance and blockage effect the relationship between BirdScan MR1 density and NEXRAD reflectivity, I used the *lme4* R package to fit a series of linear models and linear mixed models (Bates et al., 2015). For all models, I treated BirdScan MR1 density as my response variable predicted by NEXRAD reflectivity. Each model set included: 1) a null model, which included NEXRAD reflectivity as the sole fixed predictor, 2) a model that added two separate interactive terms for distance and NEXRAD reflectivity, and blockage and NEXRAD reflectivity to the null model, and 3) a model that added a three-way interactive term between distance, blockage, and NEXRAD reflectivity to the null model. For within-night variation models, I also included date as a random categorical intercept variable for each model set, with date corresponding to a full night from sunset to sunrise (i.e. including the morning of the following date).

I performed likelihood ratio tests (Tredennick et al., 2021) to assess whether or not the effects of distance and blockage had a significant effect on the relationship between BirdScan MR1 density and NEXRAD reflectivity relative to the null models. I used adjusted R^2 values to assess the relative performance between linear model sets and among linear models in the same set (Nakagawa & Schielzeth, 2013). I used

conditional R^2 values to assess linear mixed model performance because I was interested in the full explanatory power of the model and the random effect of date is fundamental to how migration density data are structured.

Lastly, to better understand the role of vertical sampling in the biases I examined, I compared the vertical profiles of migration activity across both radar systems. To do this, I used the elevation of each sampling site to convert BirdScan measurements to altitude (above sea level). I then summed BirdScan 20-minute sample densities into 100m vertical bins, calculated those densities as proportions of the entire sampling space, and aligned them with the altitudinal bins of the NEXRAD vertical profiles of reflectivity. I then calculated the correlation coefficient for all sites across each altitudinal bin.

RESULTS

Throughout two spring migration seasons, I recorded over 1,587,000 birds using the BirdScan MR1 across 44 nights of sampling. The mean density during sampling was 2.53 birds/km^2, with a minimum density of 0 and a maximum density of 43.84. Within sample periods, the mean nightly density of migrating birds as measured by the BirdScan MR1 did not significantly differ across sites ($F(9, 33) = 1.06$, $p = 0.414$). The mean number of cells removed from precipitation and range adjustment factor filtering did differ by site ($F(9, 795) = 13.41$, $p < 0.05$), however pairwise comparisons through Tukey's HSD tests revealed that these differences were, predictably, driven by the most blocked site and not by distance (Supplemental Table 1.1). In total, I was able to compare 803 20-minute sampling periods across my 10 sites.

Mean nightly models

Before filtering out insects from BirdScan density values, NEXRAD reflectivity was weakly correlated at the mean nightly scale (corrected: r=0.37; uncorrected: r=0.38). Upon applying an insect filter (Haest et al., 2023), NEXRAD reflectivity was more strongly correlated with BirdScan densities (corrected: r=0.85; uncorrected: r=0.71).

Consistent with correlation coefficients, models that included range-corrected NEXRAD reflectivity calculated as a nightly mean consistently outperformed uncorrected NEXRAD reflectivity models (Table 1.1). The model with two separate interactive terms for distance and NEXRAD reflectivity, and blockage and NEXRAD reflectivity had the highest adjusted R^2 (0.76) (Figure 1.2). The likelihood ratio test revealed that this model did provide a slight improvement to fit relative to the null model ($F(41, 37) = 2.571$, $p = 0.054$). The intercept for this model was significantly larger than zero (β=8.699, SE=1.483, t=5.865, p<0.01) and range-corrected NEXRAD reflectivity was a significant predictor, with a positive relationship to BirdScan density (β=1.185, SE=0.115, t=10.34, p<0.001). I include a model summary in Supplemental Table 1.2.

Within night models

Before filtering out insects from BirdScan density values, NEXRAD reflectivity was, again, weakly correlated at the within-night scale (corrected: r=0.31; uncorrected: r=0.25). Upon applying an insect filter, NEXRAD reflectivity was more strongly correlated with BirdScan densities (corrected: r=0.70; uncorrected: r=0.64).

In contrast to nightly means, the uncorrected NEXRAD reflectivity model set outperformed range-corrected model sets when data were analyzed within nights (Table 1.2). The three-way interactive term between distance, blockage, and NEXRAD reflectivity model explained the most variance for both corrected and uncorrected reflectivity, with the uncorrected model providing the highest R^2 value ($R^2_{marginal}$=0.36; $R^2_{conditional}$=0.67). The likelihood ratio test revealed that this model provided significantly better fit relative to the null model ($\chi^2(6)$=29.22, p<0.01). The intercept for this model was significantly larger than zero (β=15.140, SE=1.469, t=10.30, p<0.01). Uncorrected NEXRAD reflectivity was a significant predictor, with a positive relationship to BirdScan density (β=0.557, SE=0.057, t=9.813, p<0.01). Additionally, the interactive term for blockage and NEXRAD reflectivity was a negative predictor of BirdScan density (blockage: β=-0.317, SE=0.069, t=-4.581, p<0.01) (Figure 1.3). The three-way interactive term between distance, blockage, and NEXRAD reflectivity was also a negative predictor of BirdScan density (β=-0.309, SE=0.068, t=-4.507, p<0.01). Distance on its own as a non-interactive predictor had a positive relationship with BirdScan density (β=4.569, SE=1.491, t=3.068, p<0.01). I include a full model summary in Supplemental Table 1.3.

To further explore the discrepancy between correlation coefficient and linear mixed models results with respect to the relative performance of range-corrected and uncorrected NEXRAD model sets, I built subsequent three-way interaction models with subsets of data within 30km, 45km, 65km, 85km and calculated the conditional R^2 values for each model. I chose this model structure because it performed best with the full dataset for both range-corrected and uncorrected model sets. Models performed

similarly within 65km, with range-corrected models providing slight enhancements to performance ($R^2 \pm 0.004$). However, beyond 65km this pattern was reversed, with uncorrected models outperforming range-corrected models (Table 1.3).

Across all sites, I compared the vertical profiles at altitudes ranging from 1900m to 2900m above sea level. The vertical profiles of each radar system were most correlated at low altitudes and became decoupled at the highest altitudes (Supplemental Table 1.4), ranging from 0.68 to 0.08, respectively (mean=0.394, SD$\pm$0.189).

DISCUSSION

As weather radar surveillance systems continue to expand their role in aeroecology, it is crucial that we understand the potential sampling biases and limitations associated with these data (Bauer et al., 2019). I conducted a field-based ground-truthing experiment that quantifies the effects of range and topographical blockage on the NEXRAD system's ability to estimate bird migration activity. At both the nightly and within-night temporal scale, I found that NEXRAD reflectivity was highly correlated with measures of local density. I also found evidence to suggest that these reflectivity measures become less reliable with both increasing distance and beam blockage (Supplemental Table 1.3). However, I also found that uncorrected data are a better predictor of migration density than range-corrected data beyond a range of 65km at the within-night temporal scale, highlighting the spatiotemporal limitations of current range correction methods.

My finding that NEXRAD reflectivity correlates strongly with local measures of density adds to a growing body of literature demonstrating relatively consistent metrics

of migration across different monitoring systems (Dokter et al., 2011; Gauthreaux et al., 2019; Nilsson et al., 2018). The high level of correlation between weather radar and a dedicated bird radar monitoring system at multiple spatial and temporal scales is encouraging and supports assertions that radar systems can be used as a reliable tool for studying birds aloft (Kelly & Stepanian, 2020). On the whole, my results provide support for the continued use of NEXRAD-derived estimates of bird migration activity (Van Doren & Horton, 2018).

Beyond this overall support, my study design allowed us to explore nuances in how this relationship changes as a function of both range and blockage. With respect to range, my results support the long-held notion that bird detection is negatively impacted by distance as a result of increasing beam height (Buler & Diehl, 2009). This effect has long been recognized and my finding that models with distance outperformed null models emphasize the importance of accounting for range when sampling from stationary weather radars (Schmaljohann et al., 2008). To this end, I found that models with corrected data outperformed models with uncorrected data at the mean nightly scale, suggesting that current range correction measures are somewhat effective at reducing this bias (Dokter et al., 2019). Radar systems remained correlated at the within night scale as well, reinforcing the findings of Nilsson et al. (2018), which found that BirdScan and weather surveillance radars correlated well at a range of 20km. Within 65km, corrected and uncorrected models performed similarly. However, beyond this range, within night uncorrected models outperformed range-corrected models. This may suggest that current range-correction measures, which are applied increasingly across the radar aeroecology community (Hoekstra et al., 2024; Horton et al., 2023), may be

limited beyond this spatial scale and temporal resolution. Given the relatively limited scope of my study design, it is not clear how generalizable my results are to the entire NEXRAD system. I suggest that future study designs collecting data at finer distance steps may be able to explore this relationship more closely.

In addition to range, my finding that beam blockage was a negative predictor of migration activity is particularly notable given that the proportion of beam blockage across my study sites ranged between 0.00 and 0.30, which does not represent the full range of blockage exhibited by sites in more mountainous regions (Buler & Dawson, 2014). This could suggest that beam blockage may be a significant factor even at low levels and raises the possibility that we may be underestimating its importance. Further, I found a significant interaction between distance and blockage, which may suggest that corrective measures should incorporate both sources of bias. My study not only serves as a primary step in quantifying their effects at varying distances within a specific NEXRAD site coverage area, but also demonstrates a methodology with the potential to fine-tune existing range correction measures and inform the development of beam blockage corrective measures.

Temporally, I found that NEXRAD was a consistently stronger predictor of BirdScan densities at the nightly scale than the within-night scale, suggesting that increased temporal scale introduces additional variation. Many comparisons between radar systems have focused on metrics of nightly migration (Dokter et al., 2011; Nilsson et al., 2018). I find it encouraging that, even at the 20-minute scale, both radar systems remained relatively well correlated. However, particularly as we expand the usage of NEXRAD data in aeroecology (Bauer et al., 2019; Bauer et al., 2024), I recommend that

additional work should be done to understand the potential tradeoffs of using weather radar at fine temporal scales.

To this end, I also note several aspects of my study that I could not fully explore but may serve as important areas for future research. Although it was not the explicit goal of this study, it is notable that NEXRAD reflectivity was much more strongly correlated with BirdScan densities upon filtering out insects. This finding reinforces the fundamental differences between these two radar systems. While BirdScan radars are able to detect individuals within its sampling range, NEXRAD provides a measure of total reflected energy within a sampling volume. Thus, as suggested by Stepanian et al. (2016), significantly more insects would be needed to equate to the same reflector size of a bird. Additionally, as noted above, I explored the effects of distance in 20km steps and beam blockage of up to 0.30. Given I found effects at rather rough scales, I suggest that future studies at more detailed levels could further refine the relationships I describe. Relatedly, I found that vertical profiles between each radar system were most correlated at low altitudes across my sites. While this is consistent with pervious work (Nilsson et al., 2018), I show that it remains supported across a much broader range of distances. However, direct comparisons of vertical profiles remain challenging, as the BirdScan profiles I calculated are site specific and NEXRAD profiles are much more general. Studies that explicitly study the relationship between these profiles could be valuable in explaining the mechanisms that drive range- and blockage-induced biases.

Finally, due to the pulsated nature of bird migration and the bulk of migration activity occurring across only a few nights (Van Doren & Horton, 2018), I recognize that my field campaign may have been limited in its ability to capture the range of migration

activity at each site. This natural tradeoff of collecting data across multiple sites within a season may limit my ability to assess spatial variation separately from variation between nights. Studies that have collected ground-truthing data with a dedicated bird radar at a single site for a full migration season have been vital to advancing our knowledge of the biases across different radar systems (Nilsson et al., 2018) and I suggest that taking this approach in the western United States would offer further insight into the range and blockage biases I present here.

To my knowledge, I provide the first natural experiment that explicitly explores the effect of range and beam blockage on detection using two complementary radar systems. In essence, my results validate the use of the NEXRAD weather surveillance system as a tool for studying nocturnal bird migration and emphasize the importance of existing analysis techniques, such as range-correction. Moreover, these findings highlight the limitations of current analysis techniques, particularly with respect to distance. I suggest that further validation research in mountainous regions, such as the western United States, will serve to refine NEXRAD as a tool in aeroecology research.

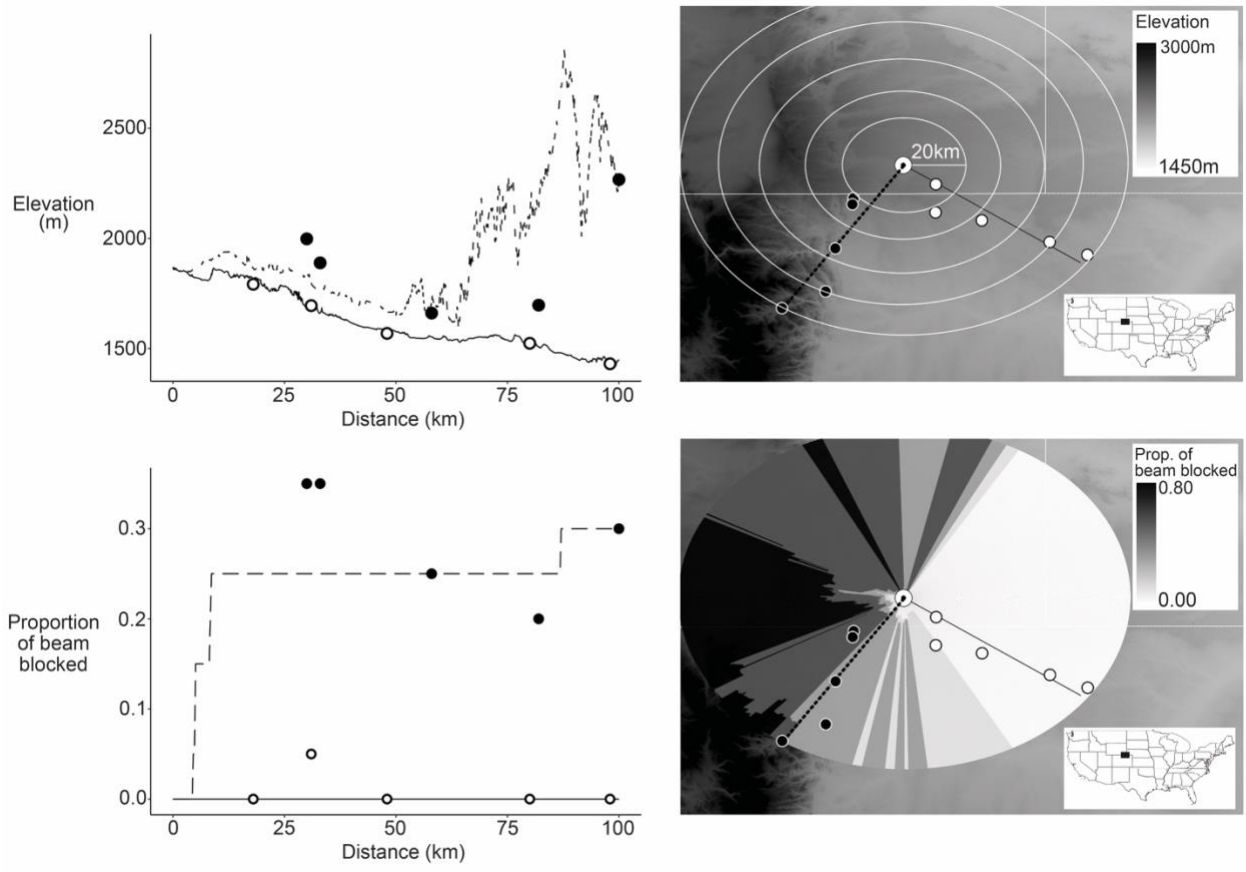

Figure 1.1 Overview of radar sampling design radiating out from the KCYS weather surveillance radar in Cheyenne, WY as a focal validation site. Sites were selected to span a wide range of elevations and distances from the KCYS radar station (left), with sites mapped out over concentric circles increasing their radii in increments of 20km (top right). Sites ran along flat (solid line) and elevated (dotted line) transects, one of which extended southeast into the plains of central Colorado (white points) and the other extended southwest into the foothills of the Rocky Mountains (black points) (right). Note that transect elevation profiles were taken along the straight radial line, whereas site locations were selected by accessibility and were not directly on transects.

Table 1.1 Summary of the adjusted R^2 values for six linear models used to characterize the relationship between mean nightly measures of BirdScan MR1 migration densities (birds/km^2) and NEXRAD reflectivity (cm^2/km^2). I include the model formula with its corresponding adjusted R^2.

Model	*Adjusted R^2*
BirdScan ~ $NEXRAD_{corrected}$ + block*$NEXRAD_{corrected}$ + dist*$NEXRAD_{corrected}$	0.758
BirdScan ~ $NEXRAD_{corrected}$ + block*dist*$NEXRAD_{corrected}$	0.748
BirdScan ~ $NEXRAD_{corrected}$	0.721
BirdScan ~ $NEXRAD_{uncorrected}$ + block*$NEXRAD_{uncorrected}$ + dist*$NEXRAD_{uncorrected}$	0.692
BirdScan ~ $NEXRAD_{uncorrected}$ + block*dist*$NEXRAD_{uncorrected}$	0.686
BirdScan ~ $NEXRAD_{uncorrected}$	0.497

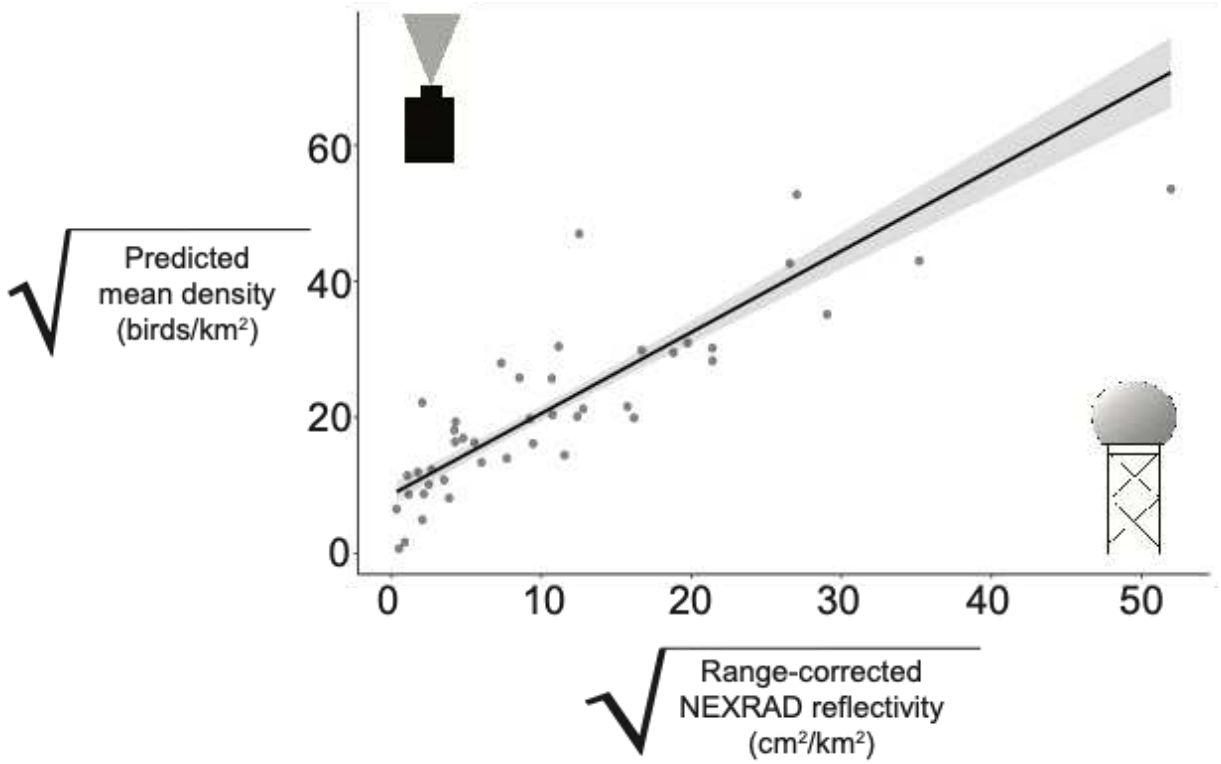

Figure 1.2. Mean nightly bird density (birds/km^2) as predicted by nightly range-corrected NEXRAD reflectivity (cm^2/km^2) from best-supported linear model. Shaded grey area denotes standard error and data points represent the observed values from the dataset used to develop the model from a dataset of 44 nights of field sampling.

Table 1.2 Summary of model performance for six linear mixed models used to characterize the relationship between within night measures of BirdScan MR1 migration densities (birds/km^2) and NEXRAD reflectivity (cm^2/km^2) in 20-minute intervals. I include the model formula with its corresponding marginal R^2 and conditional R^2 values.

Model	R^2 *marginal*	R^2 *conditional*
BirdScan ~ $NEXRAD_{uncorrected}$ + block*dist*$NEXRAD_{uncorrected}$ + (1|date)	0.364	0.674
BirdScan ~ $NEXRAD_{uncorrected}$ + (1|date)	0.361	0.667
BirdScan ~ $NEXRAD_{uncorrected}$ + block*$NEXRAD_{uncorrected}$ + dist*$NEXRAD_{uncorrected}$ + (1|date)	0.370	0.651
BirdScan ~ $NEXRAD_{corrected}$ + block*dist*$NEXRAD_{corrected}$ + (1|date)	0.354	0.646
BirdScan ~ $NEXRAD_{corrected}$ + block*$NEXRAD_{corrected}$ + dist*$NEXRAD_{corrected}$ + (1|date)	0.359	0.629
BirdScan ~ $NEXRAD_{corrected}$ + (1|date)	0.341	0.591

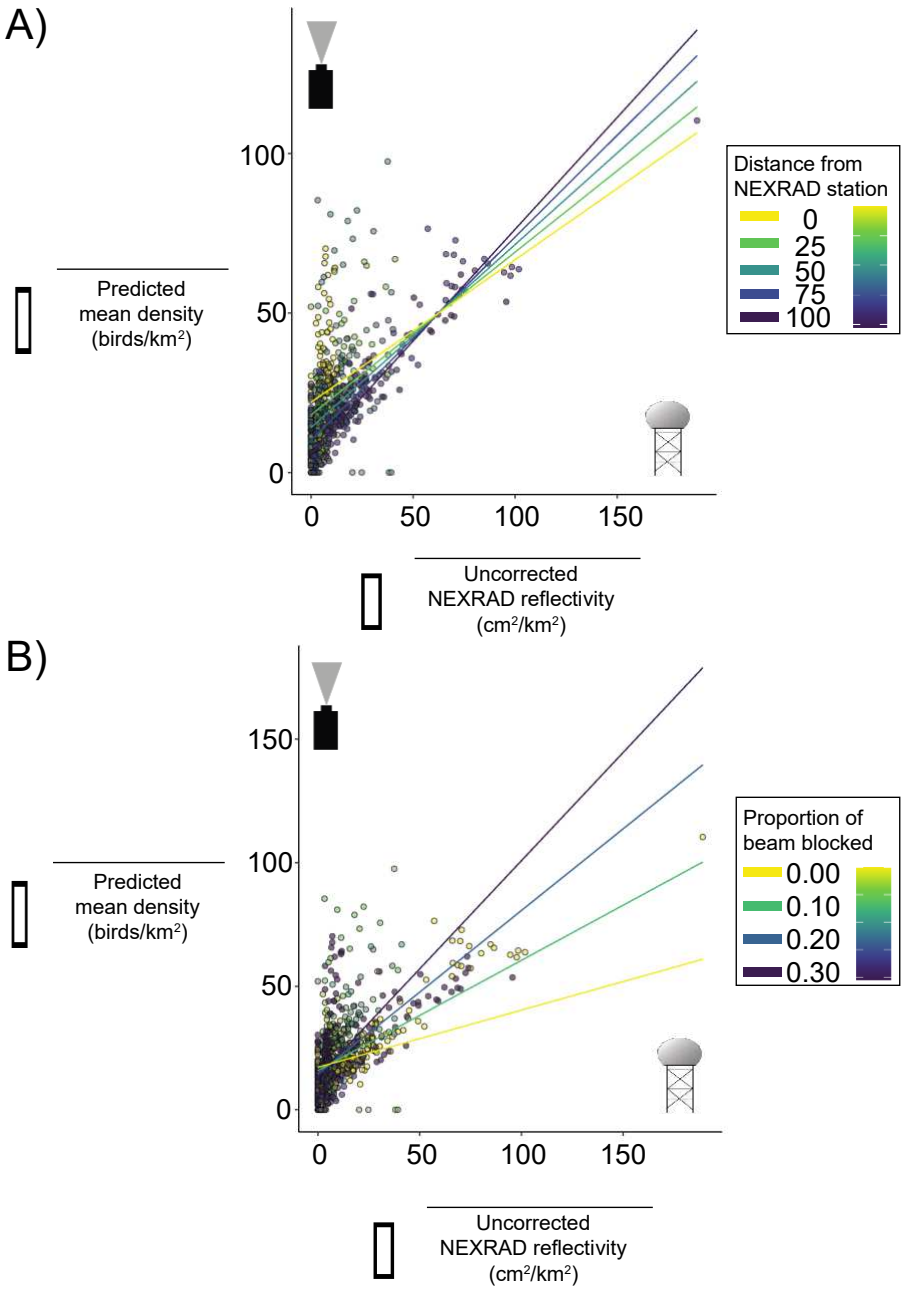

Figure 1.3 A) Within night, mean bird migration density (birds/km^2) as predicted by uncorrected NEXRAD reflectivity (cm^2/km^2) in 20-minute sampling periods from best-supported linear mixed model. Line color is used to denote predictions at varying distances from the KCYS NEXRAD station at mean beam blockage (0 when scaled) (A) and given varying proportions of beam blockage at mean distance from the station (B). Observed data points are plotted with color denoting distance and blockage as continuous variables.

Table 1.3 Summary of deviance explained for linear mixed models used to characterize the relationship between within night measures of BirdScan MR1 migration densities (birds/km^2) and NEXRAD reflectivity (cm^2/km^2) in 20-minute intervals. Models were built with a consistent model formula, but with subsets with varying maximum distances between the radar systems.

*Model: BirdScan ~ NEXRAD + block*dist*NEXRAD + (1 | date)*

	Conditional R^2	
Maximum distance (km)	Range-corrected	Uncorrected
30	0.844	0.841
45	0.848	0.846
65	0.745	0.742
85	0.682	0.703
100	0.646	0.674

LITERATURE CITED

Amazon Web Services, NEXRAD on AWS. Retrieved from https://s3.amazonaws.com/noaa-nexrad-level2/index.html

Bates D, Mächler M, Bolker B, Walker S (2015). “Fitting Linear Mixed-Effects Models Using lme4.” Journal of Statistical Software, 67(1), 1–48. doi:10.18637/jss.v067.i01.

Bauer, S., Shamoun-Baranes, J., Nilsson, C., Farnsworth, A., Kelly, J. F., Reynolds, D. R., Dokter, A. M., Krauel, J. F., Petterson, L. B., Horton, K. G., & Chapman, J. W. (2019). The grand challenges of migration ecology that radar aeroecology can help answer. Ecography, 42(5), 861–875. https://doi.org/10.1111/ecog.04083

Bauer, S., Tielens, E. K., & Haest, B. (2024). Monitoring aerial insect biodiversity: A radar perspective. Philosophical Transactions of the Royal Society B: Biological Sciences, 379(1904), 20230113. https://doi.org/10.1098/rstb.2023.0113

Buler, J. J., & Dawson, D. K. (2014). Radar analysis of fall bird migration stopover sites in the northeastern U.S. The Condor, 116(3), 357–370. https://doi.org/10.1650/CONDOR-13-162.1

Buler, J. J., & Diehl, R. H. (2009). Quantifying bird density during migratory stopover using weather surveillance radar. IEEE Transactions on Geoscience and Remote Sensing, 47(8), 2741–2751. IEEE Transactions on Geoscience and Remote Sensing. https://doi.org/10.1109/TGRS.2009.2014463

Buler, J. J., Randall, L. A., Fleskes, J. P., Jr, W. C. B., Bogart, T., & Kluver, D. (2012). Mapping Wintering Waterfowl Distributions Using Weather Surveillance Radar. PLOS ONE, 7(7), e41571. https://doi.org/10.1371/journal.pone.0041571

Chilson, P. B., Frick, W. F., Stepanian, P. M., Shipley, J. R., Kunz, T. H., & Kelly, J. F. (2012). Estimating animal densities in the aerosphere using weather radar: To Z or not to Z? Ecosphere, 3(8), art72. https://doi.org/10.1890/ES12-00027.1

Cohen, E. B., Horton, K. G., Marra, P. P., Clipp, H. L., Farnsworth, A., Smolinsky, J. A., Sheldon, D., & Buler, J. J. (2021). A place to land: Spatiotemporal drivers of stopover habitat use by migrating birds. Ecology Letters, 24(1), 38–49. https://doi.org/10.1111/ele.13618

Crum, T. D., & Alberty, R. L. (1993). The WSR-88D and the WSR-88D operational support facility. Bulletin of the American Meteorological Society, 74(9), 1669–1688. https://doi.org/10.1175/1520-0477(1993)074<1669:TWATWO>2.0.CO;2

Deng, Y., Belotti, M. C. T. D., Zhao, W., Cheng, Z., Perez, G., Tielens, E., Simons, V. F., Sheldon, D. R., Maji, S., Kelly, J. F., & Horton, K. G. (2022). Quantifying long-term phenological patterns of aerial insectivores roosting in the Great Lakes region using weather surveillance radar. Global Change Biology, n/a(n/a). https://doi.org/10.1111/gcb.16509

Dokter, A. M., Baptist, M. J., Ens, B. J., Krijgsveld, K. L., & Loon, E. E. van. (2013). Bird Radar Validation in the Field by Time-Referencing Line-Transect Surveys. PLOS ONE, 8(9), e74129. https://doi.org/10.1371/journal.pone.0074129

Dokter, A. M., Desmet, P., Spaaks, J. H., van Hoey, S., Veen, L., Verlinden, L., Nilsson, C., Haase, G., Leijnse, H., Farnsworth, A., Bouten, W., & Shamoun-Baranes, J. (2019). bioRad: Biological analysis and visualization of weather radar data. Ecography, 42(5), 852–860. https://doi.org/10.1111/ecog.04028

Dokter, A. M., Liechti, F., Stark, H., Delobbe, L., Tabary, P., & Holleman, I. (2010). Bird migration flight altitudes studied by a network of operational weather radars. Journal of The Royal Society Interface, 8(54), 30–43. https://doi.org/10.1098/rsif.2010.0116

Dokter, A. M., Liechti, F., Stark, H., Delobbe, L., Tabary, P., & Holleman, I. (2011). Bird migration flight altitudes studied by a network of operational weather radars. Journal of the Royal Society Interface, 8(54), 30–43.

Evans, R., & Mellinger, D. K. (1999). Monitorig Grassland Birds in Nocturnal Migration. Studies in Avian Biology, 19, 219–229.

Gauthreaux, S. A., Jr. (1970). Weather Radar Quantification of Bird Migration. BioScience, 20(1), 17–19. https://doi.org/10.2307/1294752

Gauthreaux, S. A., Shapiro, A.-M., Mayer, D., Clark, B. L., & Herricks, E. E. (2019). Detecting bird movements with L-band avian radar and S-band dual-polarization Doppler weather radar. Remote Sensing in Ecology and Conservation, 5(3), 237–246. https://doi.org/10.1002/rse2.101

Guo, F., Buler, J. J., Smolinsky, J. A., & Wilcove, D. S. (2023). Autumn stopover hotspots and multiscale habitat associations of migratory landbirds in the eastern United States. Proceedings of the National Academy of Sciences, 120(3), e2203511120. https://doi.org/10.1073/pnas.2203511120

Guo, F., Buler, J. J., Smolinsky, J. A., & Wilcove, D. S. (2024). Seasonal patterns and protection status of stopover hotspots for migratory landbirds in the eastern United States. Current Biology, 34(2), 235-244.e3. https://doi.org/10.1016/j.cub.2023.11.033

Haest, B., Hertner, F., Schmid, B., Preatoni, D., De Groeve, J., & Liechti, F. (2023). birdscanR: Migration Traffic Rate Calculation Package for Birdscan MR1 Radars [Computer software]. Zenodo. https://doi.org/10.5281/zenodo.7665531

Haest, B., Liechti, F., Hawkes, W. L., Chapman, J., Åkesson, S., Shamoun-Baranes, J., Nesterova, A. P., Comor, V., Preatoni, D., & Bauer, S. (2024). Continental-scale patterns in diel flight timing of high-altitude migratory insects. Philosophical Transactions of the Royal Society B: Biological Sciences, 379(1904), 20230116. https://doi.org/10.1098/rstb.2023.0116

Haest, B., Schmid, B., Hertner, F., Aschwanden, J., Früh, D., Kleger, D., Peter, D., Sapir, N., Troupin, D., Werber, Y., Yovel, Y., & Liechti, F. (2021)a. BirdScan Community Reference Dataset (Version 1.0.0) [Dataset]. Zenodo. https://doi.org/10.5281/zenodo.5734961

Haest, B., Stepanian, P. M., Wainwright, C. E., Liechti, F., & Bauer, S. (2021)b. Climatic drivers of (changes in) bat migration phenology at Bracken Cave (USA). Global Change Biology, 27(4), 768-780.

Hoekstra, B., Bouten, W., Dokter, A., van Gasteren, H., van Turnhout, C., Kranstauber, B., van Loon, E., Leijnse, H., & Shamoun-Baranes, J. (2024). Fireworks disturbance across bird communities. Frontiers in Ecology and the Environment, 22(1), e2694. https://doi.org/10.1002/fee.2694

Horton, K. G., Buler, J. J., Anderson, S. J., Burt, C. S., Collins, A. C., Dokter, A. M., Guo, F., Sheldon, D., Tomaszewska, M. A., & Henebry, G. M. (2023). Artificial light at night is a top predictor of bird migration stopover density. Nature Communications, 14(1), Article 1. https://doi.org/10.1038/s41467-023-43046-z

Horton, K. G., Nilsson, C., Van Doren, B. M., La Sorte, F. A., Dokter, A. M., & Farnsworth, A. (2019). Bright lights in the big cities: Migratory birds' exposure to artificial light. Frontiers in Ecology and the Environment, 17(4), 209–214. https://doi.org/10.1002/fee.2029

Horton, K. G., Shriver, W. G., & Buler, J. J. (2016). An assessment of spatio-temporal relationships between nocturnal bird migration traffic rates and diurnal bird stopover density. Movement Ecology, 4(1), 1. https://doi.org/10.1186/s40462-015-0066-1

Horton, K. G., Van Doren, B. M., Albers, H. J., Farnsworth, A., & Sheldon, D. (2021). Near-term ecological forecasting for dynamic aeroconservation of migratory birds. Conservation Biology, 35(6), 1777–1786. https://doi.org/10.1111/cobi.13740

Kelly, J. F., & Stepanian, P. M. (2020). Radar Aeroecology. Remote Sensing, 12(11), Article 11. https://doi.org/10.3390/rs12111768

Kranstauber, B., Bouten, W., Leijnse, H., Wijers, B.-C., Verlinden, L., Shamoun-Baranes, J., & Dokter, A. M. (2020). High-Resolution Spatial Distribution of Bird Movements Estimated from a Weather Radar Network. Remote Sensing, 12(4), Article 4. https://doi.org/10.3390/rs12040635

Kranstauber, B., Bouten, W., van Gasteren, H., & Shamoun-Baranes, J. (2022). Ensemble predictions are essential for accurate bird migration forecasts for conservation and flight safety. Ecological Solutions and Evidence, 3(3), e12158. https://doi.org/10.1002/2688-8319.12158

Lack, D., & Varley, G. C. (1945). Detection of Birds by Radar. Nature, 156(3963), Article 3963. https://doi.org/10.1038/156446a0

Larkin, R. P., & Szafoni, R. E. (2008). Evidence for widely dispersed birds migrating together at night. Integrative and Comparative Biology, 48(1), 40–49. https://doi.org/10.1093/icb/icn038

Liechti, F., Bruderer, B., & Paproth, H. (1995). Quantification of Nocturnal Bird Migration by Moonwatching: Comparison with Radar and Infrared Observations (Cuantificación de la Migración Nocturna de Aves Observando la Luna: Comparación con Observaciones de Radar e Intrarrojas). Journal of Field Ornithology, 66(4), 457–468.

Lin, T., Winner, K., Bernstein, G., Mittal, A., Dokter, A. M., Horton, K. G., Nilsson, C., Van Doren, B. M., Farnsworth, A., La Sorte, F. A., Maji, S., & Sheldon, D. (2019). M IST N ET: Measuring historical bird migration in the US using archived weather radar data and convolutional neural networks. Methods in Ecology and Evolution, 10(11), 1908–1922. https://doi.org/10.1111/2041-210X.13280

McKinnon, E. A., & Love, O. P. (2018). Ten years tracking the migrations of small landbirds: Lessons learned in the golden age of bio-logging. The Auk, 135(4), 834–856. https://doi.org/10.1642/AUK-17-202.1

McLaren, J. D., Buler, J. J., Schreckengost, T., Smolinsky, J. A., Boone, M., Emiel van Loon, E., Dawson, D. K., & Walters, E. L. (2018). Artificial light at night confounds broad-scale habitat use by migrating birds. Ecology Letters, 21(3), 356–364. https://doi.org/10.1111/ele.12902

Nakagawa, S., & Schielzeth, H. (2013). A general and simple method for obtaining R2 from generalized linear mixed-effects models. Methods in Ecology and Evolution, 4(2), 133–142. https://doi.org/10.1111/j.2041-210x.2012.00261.x

Nilsson, C., Dokter, A. M., Schmid, B., Scacco, M., Verlinden, L., Bäckman, J., Haase, G., Dell'Omo, G., Chapman, J. W., Leijnse, H., & Liechti, F. (2018a). Field validation of radar systems for monitoring bird migration. Journal of Applied Ecology, 55(6), 2552–2564. https://doi.org/10.1111/1365-2664.13174

Nilsson, C., Dokter, A. M., Schmid, B., Scacco, M., Verlinden, L., Bäckman, J., Haase, G., Dell'Omo, G., Chapman, J. W., Leijnse, H., & Liechti, F. (2018b). Field validation of radar systems for monitoring bird migration. Journal of Applied Ecology, 55(6), 2552–2564. https://doi.org/10.1111/1365-2664.13174

Nilsson, C., Dokter, A. M., Verlinden, L., Shamoun-Baranes, J., Schmid, B., Desmet, P., Bauer, S., Chapman, J., Alves, J. A., Stepanian, P. M., Sapir, N., Wainwright, C., Boos, M., Górska, A., Menz, M. H. M., Rodrigues, P., Leijnse, H., Zehtindjiev, P., Brabant, R., … Liechti, F. (2019). Revealing patterns of nocturnal migration using the European weather radar network. Ecography, 42(5), 876–886. https://doi.org/10.1111/ecog.04003

Nisbet, I. C. T., & Drury, W. H. (1969). A Migration Wave Observed by Moon-Watching and at Banding Stations. Bird-Banding, 40(3), 243–252. https://doi.org/10.2307/4511585

R Core Team. (2022). R Core Team (2022). R: A language and environment for statistical computing. R Foundation for Statistical Computing, Vienna, Austria. URL https://www.R-project.org/. [Computer software].

Robinson, W. D., Bowlin, M. S., Bisson, I., Shamoun-Baranes, J., Thorup, K., Diehl, R. H., Kunz, T. H., Mabey, S., & Winkler, D. W. (2010). Integrating concepts and technologies to advance the study of bird migration. Frontiers in Ecology and the Environment, 8(7), 354–361. https://doi.org/10.1890/080179

Ruth, J. M., Diehl, R. H., & Felix, R. K., Jr. (2012). Migrating Birds' use of Stopover Habitat in The Southwestern United States. The Condor, 114(4), 698–710. https://doi.org/10.1525/cond.2012.120020

Schmaljohann, H., Liechti, F., Bächler, E., Steuri, T., & Bruderer, B. (2008). Quantification of bird migration by radar – a detection probability problem. Ibis, 150(2), 342–355. https://doi.org/10.1111/j.1474-919X.2007.00797.x

Schmid, B., Zaugg, S., Votier, S. C., Chapman, J. W., Boos, M., & Liechti, F. (2019). Size matters in quantitative radar monitoring of animal migration: Estimating monitored volume from wingbeat frequency. Ecography, 42(5), 931–941. https://doi.org/10.1111/ecog.04025

Schmidt, M., Aschwanden, J., Liechti, F., Wichmann, G., & Nemeth, E. (2017). Comparison of visual bird migration counts with radar estimates. Ibis, 159(3), 491–497. https://doi.org/10.1111/ibi.12473

Shamoun-Baranes, J., Bauer, S., Chapman, J. W., Desmet, P., Dokter, A. M., Farnsworth, A., Haest, B., Koistinen, J., Kranstauber, B., Liechti, F., Mason, T. H. E., Nilsson, C., Nussbaumer, R., Schmid, B., Weisshaupt, N., & Leijnse, H. (2021). Weather radars' role in biodiversity monitoring. Science, 372(6539), 248–248. https://doi.org/10.1126/science.abi4680

Shi, X., Hu, C., Soderholm, J., Chapman, J., Mao, H., Cui, K., Ma, Z., Wu, D., & Fuller, R. A. (2023). Prospects for monitoring bird migration along the East Asian-Australasian Flyway using weather radar. Remote Sensing in Ecology and Conservation, 9(2), 169–181. https://doi.org/10.1002/rse2.307

Stepanian, P. M., Horton, K. G., Melnikov, V. M., Zrnić, D. S., & Gauthreaux, S. A. (2016). Dual-polarization radar products for biological applications. Ecosphere, 7(11).

Swiss Birdradar. (2022). https://www.swiss-birdradar.com/home.html

Tredennick, A. T., Hooker, G., Ellner, S. P., & Adler, P. B. (2021). A practical guide to selecting models for exploration, inference, and prediction in ecology. Ecology, 102(6), e03336. https://doi.org/10.1002/ecy.3336

United States Geological Survey. (2023). GIS Data Download. https://www.usgs.gov/the-national-map-data-delivery/gis-data-download

Van Doren, B. M., & Horton, K. G. (2018). A continental system for forecasting bird migration. Science, 361(6407), 1115–1118. https://doi.org/10.1126/science.aat7526

Van Doren, B. M., Lostanlen, V., Cramer, A., Salamon, J., Dokter, A., Kelling, S., Bello, J. P., & Farnsworth, A. (2023). Automated acoustic monitoring captures timing and intensity of bird migration. Journal of Applied Ecology, 60(3), 433–444. https://doi.org/10.1111/1365-2664.14342

Weisshaupt, N., Hervo, M., & Haest, B. (2023). Comparison of bird migration in a radar wind profiler and a dedicated bird radar. Remote Sensing in Ecology and Conservation, 9(6), 820-828.

Weisshaupt, N., Leskinen, M., Moisseev, D. N., & Koistinen, J. (2022). Anthropogenic Illumination as Guiding Light for Nocturnal Bird Migrants Identified by Remote Sensing. Remote Sensing, 14(7), Article 7. https://doi.org/10.3390/rs14071616

Zaugg, S., Saporta, G., van Loon, E., Schmaljohann, H., & Liechti, F. (2008). Automatic identification of bird targets with radar via patterns produced by wing flapping. Journal of The Royal Society Interface, 5(26), 1041–1053. https://doi.org/10.1098/rsif.2007.1349

CHAPTER 2: WEATHER SURVEILLANCE RADAR AS A TOOL FOR STUDYING THE DYNAMIC DRIVERS OF MIGRATORY BIRD TRANSITIONS BETWEEN TERRESTRIAL AND AERIAL HABITATS

INTRODUCTION

There is growing recognition that airspace represents a vast, understudied habitat that plays a vital role in many ecological processes (Diehl, 2013). Species across a variety of taxonomic groups rely on airspace for a portion of their life cycle, including birds (Horton et al., 2016; Peterson et al., 2015), bats (Hooton et al., 2022), insects (Aralimarad et al., 2011), and a diversity of microbial communities (Womack et al., 2010). Airspace also supports critical global ecosystem functions, such as pollination (Klein et al., 2006). Yet, because aeroecology is a relatively nascent sub-discipline within the field of ecology (Kunz et al., 2008), we still lack basic knowledge on many aerial ecosystems (Diehl et al., 2017). Beyond representing a distinct gap in our ability to describe biological systems, aerial ecosystems are often ignored in conservation assessment, frameworks, and planning despite growing evidence of their central role in supporting biodiversity (Davy et al., 2017; Lambertucci & Speziale, 2021). Together, our limited insight on these ecosystems constrains current ecological theory and conservation practice.

Bird migration is a large-scale ecological process that relies heavily on airspace habitat. Across North America, for example, 70% of species migrate between their breeding and non-breeding ranges (Horton et al., 2019). The degree of avian dependance on airspace ranges, with some species, such as the Common Swift (*Apus apus*), remaining airborne for up to 10 months of the year (Hedenström et al., 2016).

However, while migratory birds use airspace during flights, they also transition regularly between terrestrial and airspace habitats throughout their life cycle. Similarly to how amphibian life cycles oscillate between terrestrial and aquatic ecosystems (Diehl et al., 2017), terrestrial habitat supports many birds throughout their non-breeding and breeding phases, as well as during stopover events between migratory flights (Schmaljohann et al., 2022). This aspect of their biology makes birds an ideal study system for advancing our understanding of the connections between aerial ecosystems and terrestrial ecosystems.

During migration, birds make frequent decisions regarding the relative use of both habitats. Decades of research have revealed dynamic drivers of spatiotemporal use patterns within each habitat independently. For instance, it is well-supported that departure decisions and migration activity within the airspace are strongly tied to atmospheric conditions at multiple interacting scales (Cooper et al., 2023; Kranstauber et al., 2022; Shamoun-Baranes et al., 2017). In fact, we have leveraged our understanding of these relationships to develop bird migration forecasting systems at continental scales (Bradarić et al., 2024.; Van Doren & Horton, 2018). Within the context of migratory stopover, terrestrial habitat may serve many functions including allowing for physiological recovery from flights, providing areas where birds can avoid adverse weather conditions, or reducing predation risk (Schmaljohann et al., 2022). Birds likely select terrestrial stopover habitat to maximize these potential benefits (Bayly et al., 2013) and there is evidence that the quality of stopover habitat can have impacts on individual fitness (Gomez et al., 2017). Further, many studies highlight potential connections between the drivers of space use between aerial and terrestrial habitats.

For example, over-water flights are energetically costly to birds, causing dense stopover concentrations along large water bodies, such as the Gulf of Mexico and the Great Lakes (Bayly et al., 2018; Deppe & Rotenberry, 2005; Dunn, 2001), where migrants wait for favorable atmospheric conditions before advancing their aerial migration (Nourani et al., 2017). Additionally, some raptors make diurnal flights within migratory corridors that are funneled by the underlying topography, such as coastlines and ridgelines (Peterson et al., 2015). In essence, habitat use by migratory birds may be driven by a combination of both atmospheric and terrestrial factors. Yet, we lack a comprehensive understanding of the relative importance of each, particularly at fine temporal scales that may capture the transition between the terrestrial and airspace boundary.

Remote sensing has become a central tool in aeroecology with the use of radar systems, in particular, revealing major insights into how wildlife use airspace (Chilson et al., 2012) and being poised to make key contributions in describing aerial migration mechanisms (Bauer et al., 2019). The Next Generation Weather Radar (NEXRAD) is one such system that has been used to characterize macroecosystem airspace use across the continental United States (Kelly & Horton, 2016) and, more recently, to study the connections between terrestrial and aerial drivers of migration decisions. Clipp et al. (2020), for instance, were able to demonstrate that broad-scale weather conditions influenced the spatiotemporal patterns of stopover for trans-Gulf migratory birds. Cohen et al. (2021) further developed a stopover-to-passage ratio, which estimates the percentage of passage migrants that stop in a given area using NEXRAD data and found that stopover concentrates along forested coastal landscapes. These techniques have been adapted by others to quantify multi-scale drivers of stopover (Guo et al.,

2023) and illuminate gaps in stopover protection efforts (Guo et al., 2024). These methodological advancements and burgeoning applications of NEXRAD data present a unique opportunity to explicitly study migratory bird transitions between terrestrial and airspace habitats.

In this study, I employed the NEXRAD system to assess within-night changes in the relative importance of predictors of migratory bird airspace use. Specifically, my objective was to estimate the relative strength of terrestrial, atmospheric, and sampling variables in predicting bird migration activity to identify 1) patterns across a given night and 2) differences in those patterns between seasons. I predicted that terrestrial predictors would be more important closer to local sunset and sunrise, when birds are departing and arriving from terrestrial landscapes, respectively. Relatedly, I predicted that atmospheric predictors would be most important in the middle of each night, as birds are actively making flights through the airspace.

MATERIAL AND METHODS

I used supervised machine learning to determine the importance of variables in predicting within-night migration activity across the continental United States. Here, I describe the methods I used for data acquisition and processing, and my approach to model training, performance evaluation, and predictor importance determination.

Weather surveillance radar data

As a measure of migration activity, I used radar data collected through the NEXRAD network, which is operated by the National Weather Service, the Federal Aviation Administration, and the U.S. Air Force. The NEXRAD network consists of Doppler

weather radars (WSR-88D) that scan 360° at 0.5° azimuthal intervals (e.g., 720 azimuths) and multiple elevation angles (e.g. 0.5°, 1.5°... 4.5°) to monitor the airspace every 5–10 minutes. I downloaded level-II radar scans which are accessible through Amazon Web Services (https://registry.opendata.aws/noaa-nexrad/), in 30-minute intervals, or the closest available scan, between 0 and 12 hours after local sunset from 2012 to 2021 (Spring: March 1st -June 15th; Fall: August 1st-November 15th) to capture all hours of possible nocturnal migration. Within these periods, I downloaded polar volumes, or a collection of azimuthal scans, for all 143 stations in the continental United States.

I replicated the clutter mitigation methods of Horton et al (2023) through the R package *bioRad* (Dokter, et al. 2019) to reduce the influence of non-avian targets. Specifically, I applied the MistNet algorithm function to filter out precipitation from polar volumes (Lin et al., 2019), removing scans in which precipitation contamination exceeded 30% within a 5km range between an altitude of 7.5-80km. I also applied static binary clutter masks to remove topographical and ground-based clutter. To account for the angled radar beam sampling higher altitudes with increasing range, I constructed vertical profiles of reflectivity, which integrate reflectivity from multiple tilt angle sweeps (Lin, et al. 2019). With these vertical profiles of reflectivity, I range corrected planned position indicators (PPIs) using the integrate_to_ppi function in bioRad. This range correction reduces the bias associated with angled radar beams, which sample at increasing height above ground level with increasing distance from the radar (Buler & Diehl, 2009). I used this function to calculate the expected reflectivity at each pixel in each PPI as weighted by the vertical profile of reflectivity and exclude individual PPI

pixels that had range adjustment factors (R) greater than 10. The result of this processing was a range-corrected measure of vertically integrated reflectivity (cm^2/km^2), which I used as a raster of within-night bird migration intensity aggregated to ~3km resolution. For all models, I cube-root transformed this response variable to fit model assumptions.

Atmospheric predictors

I used the North American Regional Reanalysis (NARR) to calculate atmospheric predictors across the continental United States (Mesinger, et al. 2006). The NARR model provides measurements of variables at 29 pressure levels every 3 hours, with a 32 km resolution. I downloaded NARR data from 2012 through 2021. From this dataset, I extracted variables including air temperature (ºC), geopotential height (m), zonal (U, east/west) and meridional (V, north/south) wind components (m s-1), surface pressure (Pa), relative humidity (%), visibility (m), mean sea level pressure (Pa), and total cloud cover (%). For variables available at multiple pressure levels (air temperature and zonal and meridional wind speed), I extracted data from 1000 hPa to 800 hPa at 50 hPa intervals.

In addition to local conditions surrounding each 2.9 km sampling pixel, I extracted atmospheric predictors from spatially distant areas. That is, for each atmospheric predictor, I calculated conditions at locations 150 km from each focal point in all cardinal directions. I included distant predictors to reflect conditions at a set range away from the focal area to capture the possibility that birds respond to environmental cues at a macroscale. This distance is twice the distance used to characterize “remote” predictors

by Kranstauber et al (2022) and within the range of average nightly flight distances of Swainson's Thrush *(Catharus ustulatus)* (Wikelski et al., 2003).

Sampling predictors

For each radar scan, I calculated several sampling predictors that have been shown to have a relationship with NEXRAD-derived measures of bird migration activity (Van Doren & Horton, 2018). I calculated the ordinal date and time after local sunset for each NEXRAD station during which data were collected. I also estimated the distance of each pixel to the NEXRAD station collecting data and used NASA's Digital Elevation Model and Associated Products data to calculate the elevation of each pixel at a 30m resolution (Crippen et al., 2016).

Terrestrial predictors

I calculated terrestrial predictors in three categories: land cover, vegetative phenology, and artificial light at night. I used the MODIS Land Cover Type Product (MCD12Q1 v 6.0; Sulla-Menashe and Friedl 2018) to estimate land cover predictors. This product includes six distinct land cover classifications at ~500 m resolution and annual time. I used the University of Maryland classification scheme, which provides 16 classes/types of land cover. I summed all associated land cover types by combining the Cropland and Cropland/Natural Vegetation classes as cropland cover, Evergreen Needleleaf Forests, Evergreen Broadleaf Forests, Deciduous Needleleaf Forests, Deciduous Broadleaf Forests, and Mixed Forests as forest cover, Closed and Open

Shrublands as shrub cover, and Savannas and Woody Savannas as savanna cover. I calculated percent cover for each cover type at a 2.9 km resolution.

I used the MODIS Vegetation Index (VI) to calculate the mean enhanced vegetation index (EVI) at a resolution of ~500m (Didan, et al. 2015). I used the MOD13A1 v6.0 layer to extract EVI and aggregated EVI values to 2.9 km resolution (6 x 6 cells). I then calculated the mean and standard deviation of EVI per grid cell. I used NASA's visible infrared imaging radiometer suite (VIIRS; the "vcm" version of tiled monthly cloud-free DNB composites) dataset as an index of anthropogenic light at night at a 15 arc second (~500m) spatial resolution (available at the Colorado School of Mines' Earth Observation Group webpage: https://eogdata.mines.edu/products/vnl/). I applied the same method as EVI to this dataset to calculate the mean and standard deviation values of radiance derived from VIIRS. In total, this process added four vegetative phenology and artificial light at night predictors for a total of 13 terrestrial predictors across all three categories to be included in my forecasting model.

I aggregated all terrestrial predictors into ~500m cells by 6 x 6 (2.9 x 2.9 km) quadrants and calculated the mean and standard deviation for each aggregate cell. Resampling these datasets allowed us to project terrestrial predictors onto a common resolution of 2.9 x 2.9 km.

A full list of predictors can be found in Supplemental Table 2.1.

Model training and performance evaluation

I used gradient boosted trees via the *LightGBM* R package to analyze the associations between bird migration intensity and my predictor variables. I fit models for

each two-hour interval following local sunset (i.e. hours 0-2, 2-4, 4-6, 6-8, 8-10, and 10-12). Across all training locations, the mean night length for both spring and fall fell between 10-12 hours (spring=10.6±1.1; fall=11.9±1.2), ensuring my models primarily captured nocturnal periods. To assess differences between seasons, I built separate models for spring and fall migration.

To represent spatial heterogeneity across the country while accounting for computing limitations, I subsampled the area within each NEXRAD station domain. Specifically, I randomly selected 20%, or approximately 2,020 pixels, of each NEXRAD station's coverage and used the full 10 years of data across those pixels to build a dataset for model training, validation, and holdout experiments. Within this dataset, I allocated 70% for model training, 15% for validation to tune hyperparameters, and the remaining 15% for evaluating model performance. I identified objective, learning rate, max depth, number of leaves, type of tree learner, and training steps as the most important hyperparameters for model performance and used a grid search to test a range of values for each. I trained models to determine the best value for each hyperparameter (objective=regression, learning rate=0.1, max depth=30, number of leaves=500, type of tree learner=serial, and training steps=10). To prevent overfitting during training of my model, I employed early stopping using the root mean square error (RMSE) as the monitoring metric. Model predictive performance was evaluated using the R-squared values. Additionally, I calculated the predictive gain as a percentage of contribution by each predictor variable for every two-hour period to interpret their relative importance in predicting migration activity.

RESULTS

I trained and evaluated the performance of 10 models for each season per two-hour time interval, for a total of 120 gradient boosting regression models. Each model was trained on over 13 million observations across 10 years of NEXRAD data.

Model performance

The model performance for both spring and fall was stable throughout the night (spring: median R^2=0.73, SD±0.08; fall: median R^2=0.74, SD±0.03), with slight increases between hours two and six and a slight drop off after hour eight. The range of model performance was consistent between seasons (spring: R^2_{min}=0.53f, R^2_{max}=0.76; fall: R^2_{min}=0.66, R^2_{max}=0.76) and are summarized in Table 2.1.

Atmospheric predictors

For both seasons, atmospheric predictor variables composed the majority of predictive gain across all timesteps (spring: median=63%, SD±4%; fall: median=75%, SD±4%) (Figure 2.1). Atmospheric importance was lowest between 0-2 hours after sunset but increased between 2-4 hours after sunset (spring: Δ_{gain}=7%; fall: Δ_{gain}=10%). During the spring, atmospheric gain peaked at 64% between 6-8 hours after sunset. During the fall, the percentage of atmospheric gain peaked at 77% between 2-4 hours after sunset.

In spring, air temperature was consistently a top atmospheric predictor, followed by the V-component of wind speed (north/south), surface pressure, the U-component of

wind speed (east/west), and geopotential height in varying order. In fall, the V-component of wind speed was consistently a top atmospheric predictor, followed by surface pressure, air temperature, geopotential height, and the U-component of wind speed in varying order (Figure 2.2). With respect to multi-scale atmospheric predictors, spatially distant predictors composed a much larger proportion of mean gain than local predictors and their relative gains stayed stable throughout the night (Figure 2.2). With respect to directional variables, north and easterly conditions were stronger predictors in the fall season, whereas south and westerly conditions were stronger predictors in the spring season (Figure 2.3).

Sampling predictors

Sampling variables consistently composed the second most predictive gain (spring: median=34%, SD±4%; fall: median=22%, SD±4%) (Figure 2.1). Sampling gain peaked between 0-2 hours after sunset for both seasons (spring: peak gain=43%; fall: peak gain=30%). In the spring, sampling gain steadily decreased between 2-8 hours after sunset, before increasing again from 8-10 hours after sunset (8-10 median=34%, SD±1%). Similarly, in the fall, sampling gain steadily decreased between 2-8 hours after sunset, with the second highest gain between 8-10 hours after sunset (8-10 median=22%, SD±1%). Across all timesteps, sampling gain was higher in the spring than the fall.

Ordinal date was the strongest sampling predictor across both seasons and all timesteps (Figure 2.4). Time after sunset was most important between 0-2 hours after

sunset. Both time after sunset and distance to radar importance increased between 10-12 hours after sunset.

Terrestrial predictors

Across both seasons, terrestrial predictor variables composed a relatively small proportion of predictive gain throughout the night (spring: median=3%, SD<1%; fall: median=3%, SD<1%). In spring, terrestrial importance stayed relatively consistent throughout the night but peaked between 10-12 hours after local sunset (10-12 median=4%, SD±<1%). In fall, terrestrial importance peaked between 0-2 hours after sunset (8-10 median=3%, SD±<1%) and steadily declined for the remainder of the night. Across both seasons, VIIRS nighttime light was the strongest terrestrial predictors, followed by forest cover and water bodies in varying order.

DISCUSSION

Birds regularly transition between terrestrial and aerial habitat, and advances in radar aeroecology provide a novel methodology for studying this ecological process. I used weather radar to study the dynamic drivers of migratory bird activity across different portions of the night. I found that atmospheric predictors were consistently the strongest predictors of activity throughout the night for both spring and fall seasons. Sampling predictors fluctuated, with high importance shortly after local sunset, and terrestrial variables showed marginal predictive importance throughout the night. To my knowledge, this study is the first to explicitly study the dynamic drivers of migratory bird activity between the terrestrial and aerial boundary. Together, this study provides

unique insight into the dynamic use of aerials habitats, and I discuss the potential implications of my findings on future research.

My finding that atmospheric variables were a major, consistent predictor of migration activity supports decades of research suggesting that weather conditions strongly influence avian migratory behavior and timing (Åkesson & Hedenström, 2000; Cooper et al., 2023; McCabe et al., 2018). Few studies have explicitly compared the relative importance of different predictor types, and my study helps illuminate the drivers of bird migration through this lens. My results are consistent with Cohen et al. (2021), who used a suite of predictors to estimate spatial drivers of stopover and found that weather variables were stronger predictors of migratory stopover than landcover variables. Additionally, the top atmospheric predictors (namely air temperature and wind speed components) were consistent with previous migration forecasting efforts (Van Doren & Horton, 2018). Beyond this, my study design allowed us to consider variables as dynamic predictors and provide additional nuance within these relationships. For example, I found some support for my prediction that atmospheric conditions would be most important in the middle of the night, as atmospheric predictive gain was highest between 2-8 hours after sunset. Seasonally, I also found that atmospheric variables were more important in the fall than the spring across all timesteps, which may reflect the faster, pulsated pace of spring migration (Nilsson et al., 2018) often thought to be reliant on favorable wind assistance. Further, I found that atmospheric conditions 150km from each focal point were more important than local conditions for both seasons, but that southwestern predictors were more important in the spring and northeastern conditions were more important in the fall. Overall, my results refine existing notions of

how migratory birds use airspace and suggest that some aspects of this relationship change at varying temporal scales.

Sampling variables were the second most important predictor in my models and their relative importance showed considerable variation throughout the night. Similar to atmospheric variables, my findings are consistent with previous studies (e.g., Van Doren & Horton, 2018), for example, ordinal date was a consistently strong predictor of aerial activity, which reflects the strong seasonality of migration. On the contrary, time after sunset was highly dynamic, with strong importance early in the night and much weaker importance throughout the rest of the night. I suggest that this change in importance is likely reflective of birds taking off shortly after local sunset and entering the radar beam. That is, sunset serves as a cue for nocturnal migrants to begin their flights en masse (Coppack et al., 2008; Schmaljohann et al., 2011) and, consequently, the period following sunset is when weather radar begins to detect birds aloft. However, during the middle of the night, activity is relatively steady and becomes detached from sunset timing. To this end, I also observed an increase in the importance of the time after sunset at the end of the night in the spring and, to a lesser extent, in the fall. This may be indicative of a similar, inverse sampling effect as birds land shortly after sunrise and leave the radar beam. This temporal pattern of take-off and landing with local sunset and sunrise, respectively, has been well documented (Dinevich et al., 2003) and my findings suggest a related variability in the importance of different sampling variables throughout the night, which have implications for interpreting weather radar data and forecasting efforts.

My top terrestrial predictors of VIIRS nighttime light, forest cover, and water cover were similar to previous work on migration stopover (Cohen et al., 2021; Guo et al., 2023; Horton et al., 2023). Yet, contrary to my predictions, terrestrial predictors held relatively little predictive gain across the night. While I did see a very slight peak in terrestrial importance late in the night (hours 8-10) for spring and early (hours 0-2) for fall, overall terrestrial variable importance was marginal relative to atmospheric variables. This doesn't necessarily mean that terrestrial habitat isn't important, but that it isn't a central driver in predicting nightly variation in migration activity. While I am cautious not to discount the importance of terrestrial habitat on migratory behavior (Bayly et al., 2016; Buler et al., 2007), I submit that my findings may stress the importance of including airspace in habitat when trying to understand migratory behavior. A review of migratory stopover research, for example, highlighted remarkably inconsistent support for the relationship between terrestrial habitat quality and stopover duration (Schmaljohann et al., 2022). My results may suggest that the migratory assistance provided by atmospheric conditions weighs heavily against the refueling potential offered by terrestrial resources. While I recognize the importance of considering terrestrial habitat quality across the avian full annual cycle (Gunnarsson et al., 2005; Johnson, 2007), I suggest that explicitly integrating the role of atmospheric conditions may provide a more holistic model for understanding avian migratory decisions and tradeoffs.

While my goal was to determine the relative importance of terrestrial and aerial variables in predicting bird migration activity, I note that there are fundamental differences between how these predictors were captured in my model. I based my

predictions on evidence that birds make decisions about where to land based on key terrestrial habitat features, such as forest cover, at multiple spatial scales (Buler et al., 2007; Guo et al., 2023). Yet at the within-night scale, unlike atmospheric conditions, landcover is not a dynamic predictor. I suspect that, while landcover may not be a predictor of within-night activity, key landcovers like forest shape the baseline of migration activity levels, whereas atmospheric conditions predict deviations from that baseline. A hierarchical approach to that nests aerial conditions within terrestrial cover could be a valuable next step for this work. Relatedly, while I chose to design my study at the continental scale, region-specific models may reveal spatial variation in terrestrial and aerial importance. For instance, terrestrial habitat may be more important in areas surrounding large migration barriers, such as large bodies of water along the Gulf Coast (Deppe & Rotenberry, 2005) or cropland in the midwestern United States (Guo et al., 2023).

Migration is the least understood portion of the avian life cycle, which is highlighted by our limited understanding of their transition between terrestrial and airspace habitat. Here, I provide insights on the relative importance of these variables in predicting migration activity and shed new light onto how they may change over the course of a given night. My research underlines the importance of advancing our understanding of airspace as habitat and validates the value of bird migration as a system for doing so.

FIGURES AND TABLES

Table 2.1 Summary of the model performance (R^2) of gradient boosted regression tree models that were used to predict bird migration activity for each timestep after sunset during spring and fall migration.

Season	Timestep (hours after sunset)	Median R^2 (±SD)
Spring		
	0-2	0.734 (±0.001)
	2-4	0.757 (±0.001)
	4-6	0.752 (±0.002)
	6-8	0.740 (±0.002)
	8-10	0.715 (±0.002)
	10-12	0.537 (±0.003)
Fall		
	0-2	0.722 (±0.002)
	2-4	0.761 (±0.001)
	4-6	0.757 (±0.002)
	6-8	0.733 (±0.002)
	8-10	0.688 (±0.003)
	10-12	0.658 (±0.002)

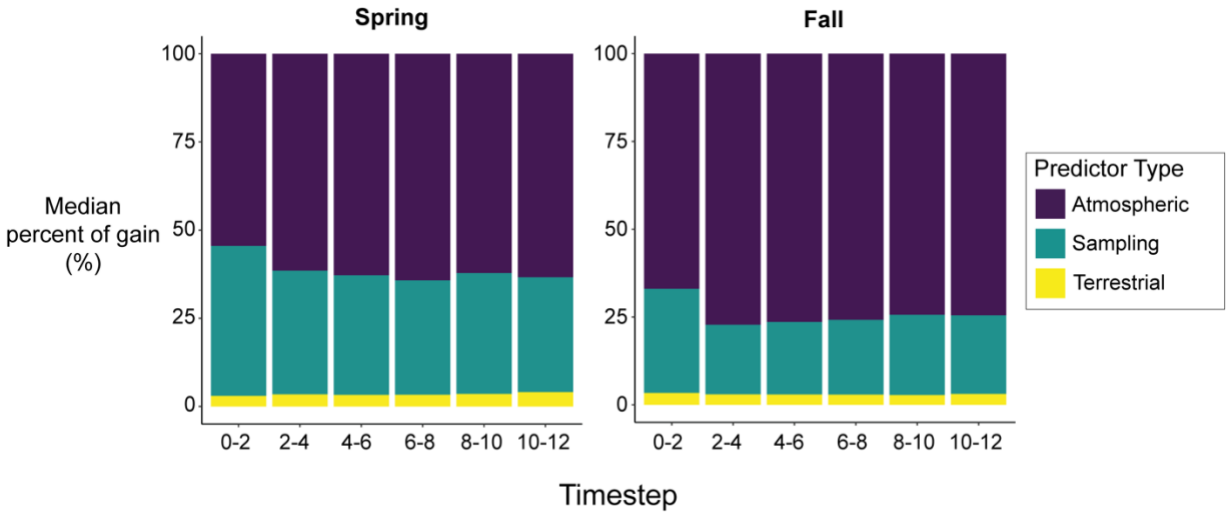

Figure 2.1 Bar chart summarizing median percent of gain contributed by each predictor type (atmospheric, sampling, and terrestrial) for each timestep after sunset for both spring (left) and fall (right) bird migration seasons. Predictor types are denoted by different colors.

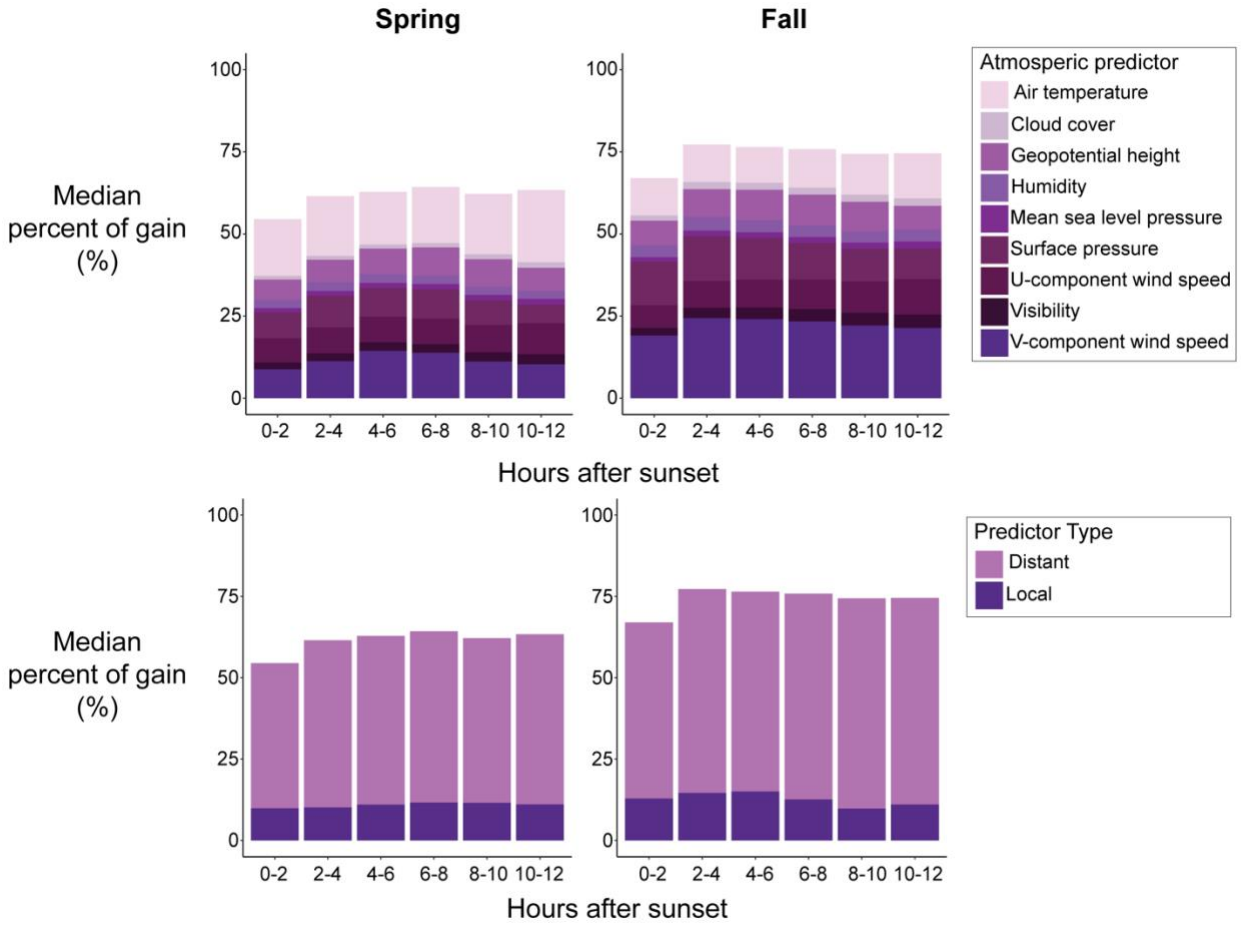

Figure 2.2 Bar chart summarizing median percent of gain contributed by each atmospheric predictor in models used to predict bird migration activity throughout the night. Predictors are aggregated by different atmospheric conditions (top) and spatial scale (bottom) for both spring (left) and fall (right) migration seasons.

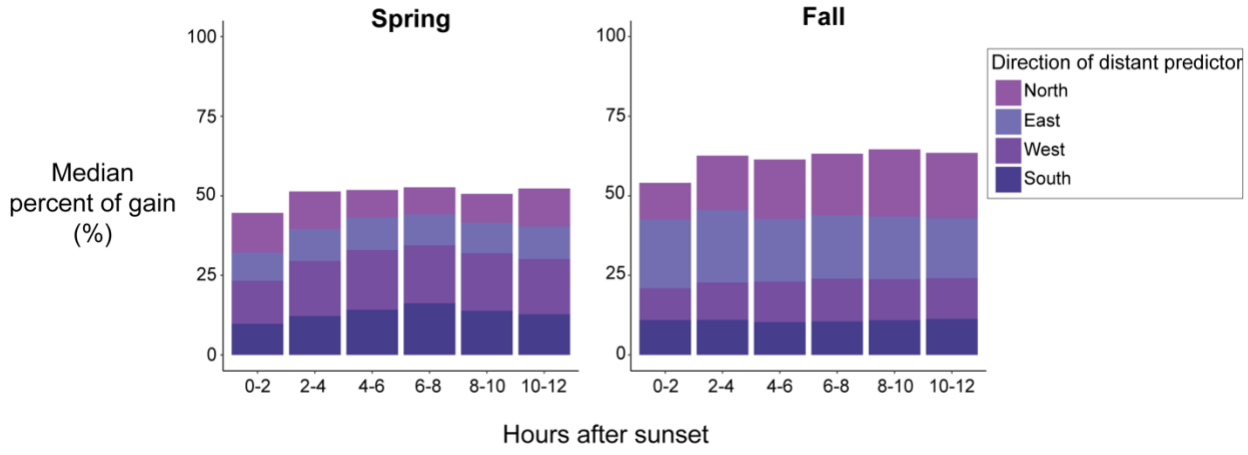

Figure 2.3 Bar chart summarizing the median percent of gain contributed by directional predictors in models used to predict bird migration activity throughout the night. Model results are organized by spring (left) and fall (right).

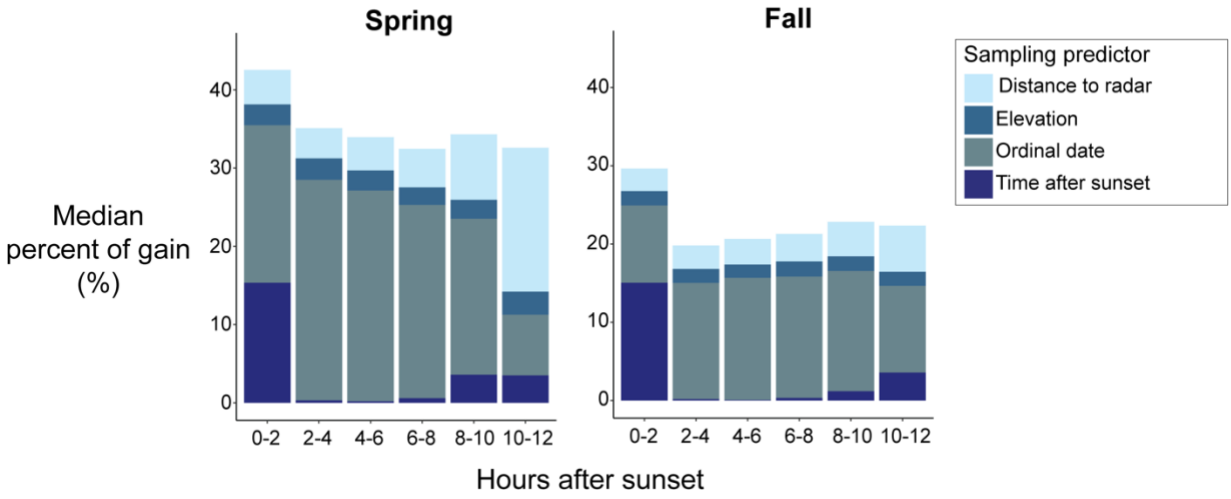

Figure 2.4 Bar chart summarizing the median percent of gain contributed by each sampling predictor in models used to predict bird migration activity throughout the night. Model results are organized by spring (left) and fall (right). The percentage range is scaled down to a maximum of 45% to make small percentage contributions more visible. su

LITERATURE CITED

Åkesson, S., & Hedenström, A. (2000). Wind selectivity of migratory flight departures in birds. *Behavioral Ecology and Sociobiology*, *47*(3), 140–144. https://doi.org/10.1007/s002650050004

Aralimarad, P., Reynolds, A. M., Lim, K. S., Reynolds, D. R., & Chapman, J. W. (2011). Flight altitude selection increases orientation performance in high-flying nocturnal insect migrants. *Animal Behaviour*, *82*(6), 1221–1225. https://doi.org/10.1016/j.anbehav.2011.09.013

Bauer, S., Shamoun-Baranes, J., Nilsson, C., Farnsworth, A., Kelly, J. F., Reynolds, D. R., Dokter, A. M., Krauel, J. F., Petterson, L. B., Horton, K. G., & Chapman, J. W. (2019). The grand challenges of migration ecology that radar aeroecology can help answer. *Ecography*, *42*(5), 861–875. https://doi.org/10.1111/ecog.04083

Bayly, N. J., Gómez, C., & Hobson, K. A. (2013). Energy reserves stored by migrating Gray-cheeked Thrushes Catharus minimus at a spring stopover site in northern Colombia are sufficient for a long-distance flight to North America. *Ibis*, *155*(2), 271–283. https://doi.org/10.1111/ibi.12029

Bayly, N. J., Gómez, C., Hobson, K. A., & Rosenberg, K. V. (2016). Prioritizing tropical habitats for long-distance migratory songbirds: An assessment of habitat quality at a stopover site in Colombia. *Avian Conservation and Ecology*, *11*(2), art5. https://doi.org/10.5751/ACE-00873-110205

Bayly, N. J., Rosenberg, K. V., Easton, W. E., Gómez, C., Carlisle, J., Ewert, D. N., Drake, A., & Goodrich, L. (2018). Major stopover regions and migratory bottlenecks for Nearctic-Neotropical landbirds within the Neotropics: A review.

Bird Conservation International, *28*(1), 1–26. https://doi.org/10.1017/S0959270917000296

Bradarić, M., Kranstauber, B., Bouten, W., & Shamoun-Baranes, J. (2024). Forecasting nocturnal bird migration for dynamic aeroconservation: The value of short-term datasets. *Journal of Applied Ecology*, *n/a*(n/a). https://doi.org/10.1111/1365-2664.14651

Buler, J. J., & Diehl, R. H. (2009). Quantifying Bird Density During Migratory Stopover Using Weather Surveillance Radar. *IEEE Transactions on Geoscience and Remote Sensing*, *47*(8), 2741–2751. IEEE Transactions on Geoscience and Remote Sensing. https://doi.org/10.1109/TGRS.2009.2014463

Buler, J. J., Moore, F. R., & Woltmann, S. (2007). A Multi-Scale Examination of Stopover Habitat Use by Birds. *Ecology*, *88*(7), 1789–1802. https://doi.org/10.1890/06-1871.1

Chilson, P. B., Bridge, E., Frick, W. F., Chapman, J. W., & Kelly, J. F. (2012). Radar aeroecology: Exploring the movements of aerial fauna through radio-wave remote sensing. *Biology Letters*, *8*(5), 698–701.

Clipp, H. L., Cohen, E. B., Smolinsky, J. A., Horton, K. G., Farnsworth, A., & Buler, J. J. (2020). Broad-Scale Weather Patterns Encountered during Flight Influence Landbird Stopover Distributions. *Remote Sensing*, *12*(3), Article 3. https://doi.org/10.3390/rs12030565

Cohen, E. B., Horton, K. G., Marra, P. P., Clipp, H. L., Farnsworth, A., Smolinsky, J. A., Sheldon, D., & Buler, J. J. (2021). A place to land: Spatiotemporal drivers of

stopover habitat use by migrating birds. *Ecology Letters*, *24*(1), 38–49. https://doi.org/10.1111/ele.13618

Cooper, N. W., Dossman, B. C., Berrigan, L. E., Brown, J. M., Cormier, D. A., Bégin-Marchand, C., Rodewald, A. D., Taylor, P. D., Tremblay, J. A., & Marra, P. P. (2023). Atmospheric pressure predicts probability of departure for migratory songbirds. *Movement Ecology*, *11*(1), 23. https://doi.org/10.1186/s40462-022-00356-z

Coppack, T., Becker, S. F., & Becker, P. J. J. (2008). Circadian flight schedules in night-migrating birds caught on migration. *Biology Letters*, *4*(6), 619–622. https://doi.org/10.1098/rsbl.2008.0388

Crippen, R., Buckley, S., Agram, P., Belz, E., Gurrola, E., Hensley, S., Kobrick, M., Lavalle, M., Martin, J., Neumann, M., Nguyen, Q., Rosen, P., Shimada, J., Simard, M., & Tung, W. (2016). NASADEM GLOBAL ELEVATION MODEL: METHODS AND PROGRESS. *The International Archives of the Photogrammetry, Remote Sensing and Spatial Information Sciences*, *XLI-B4*, 125–128. XXIII ISPRS Congress, Commission IV (Volume XLI-B4) - 12–19 July 2016, Prague, Czech Republic. https://doi.org/10.5194/isprs-archives-XLI-B4-125-2016

Davy, C. M., Ford, A. T., & Fraser, K. C. (2017). Aeroconservation for the Fragmented Skies. *Conservation Letters*, *10*(6), 773–780. https://doi.org/10.1111/conl.12347

Deppe, J. L., & Rotenberry, J. T. (2005). Temporal Patterns in Fall Migrant Communities in Yucatan, Mexico. *The Condor*, *107*(2), 228–243. https://doi.org/10.1093/condor/107.2.228

Diehl, R. H. (2013). The airspace is habitat. *Trends in Ecology & Evolution*, *28*(7), 377–379. https://doi.org/10.1016/j.tree.2013.02.015

Diehl, R. H., Peterson, A. C., Bolus, R. T., & Johnson, D. H. (2017). Extending the Habitat Concept to the Airspace. In P. B. Chilson, W. F. Frick, J. F. Kelly, & F. Liechti (Eds.), *Aeroecology* (pp. 47–69). Springer International Publishing. https://doi.org/10.1007/978-3-319-68576-2_3

Dinevich, L., Matsyura, A., & Leshem, Y. (2003). Temporal Characteristics of Night Bird Migration Above Central Israel—A Radar Study. *Acta Ornithologica*, *38*(2), 103–110. https://doi.org/10.3161/068.038.0206

Dunn, E. H. (2001). MASS CHANGE DURING MIGRATION STOPOVER: A COMPARISON OF SPECIES GROUPS AND SITES. *Journal of Field Ornithology*, *72*(3), 419–432. https://doi.org/10.1648/0273-8570-72.3.419

Gomez, C., Bayly, N. J., Norris, D. R., Mackenzie, S. A., Rosenberg, K. V., Taylor, P. D., Hobson, K. A., & Daniel Cadena, C. (2017). Fuel loads acquired at a stopover site influence the pace of intercontinental migration in a boreal songbird. *Scientific Reports*, *7*(1), Article 1. https://doi.org/10.1038/s41598-017-03503-4

Gunnarsson, T. G., Gill, J. A., Newton, J., Potts, P. M., & Sutherland, W. J. (2005). Seasonal matching of habitat quality and fitness in a migratory bird. *Proceedings of the Royal Society B: Biological Sciences*. https://doi.org/10.1098/rspb.2005.3214

Guo, F., Buler, J. J., Smolinsky, J. A., & Wilcove, D. S. (2023). Autumn stopover hotspots and multiscale habitat associations of migratory landbirds in the eastern

United States. *Proceedings of the National Academy of Sciences*, *120*(3), e2203511120. https://doi.org/10.1073/pnas.2203511120

Guo, F., Buler, J. J., Smolinsky, J. A., & Wilcove, D. S. (2024). Seasonal patterns and protection status of stopover hotspots for migratory landbirds in the eastern United States. *Current Biology*, *34*(2), 235-244.e3. https://doi.org/10.1016/j.cub.2023.11.033

Hedenström, A., Norevik, G., Warfvinge, K., Andersson, A., Bäckman, J., & Åkesson, S. (2016). Annual 10-Month Aerial Life Phase in the Common Swift *Apus apus*. *Current Biology*, *26*(22), 3066–3070. https://doi.org/10.1016/j.cub.2016.09.014

Hooton, L. A., Moretto, L., & Davy, C. M. (2022). Aerial Habitats for Urban Bats. In L. Moretto, J. L. Coleman, C. M. Davy, M. B. Fenton, C. Korine, & K. J. Patriquin (Eds.), *Urban Bats: Biology, Ecology, and Human Dimensions* (pp. 95–105). Springer International Publishing. https://doi.org/10.1007/978-3-031-13173-8_7

Horton, K. G., Buler, J. J., Anderson, S. J., Burt, C. S., Collins, A. C., Dokter, A. M., Guo, F., Sheldon, D., Tomaszewska, M. A., & Henebry, G. M. (2023). Artificial light at night is a top predictor of bird migration stopover density. *Nature Communications*, *14*(1), Article 1. https://doi.org/10.1038/s41467-023-43046-z

Horton, K. G., Nilsson, C., Van Doren, B. M., La Sorte, F. A., Dokter, A. M., & Farnsworth, A. (2019). Bright lights in the big cities: Migratory birds' exposure to artificial light. *Frontiers in Ecology and the Environment*, *17*(4), 209–214. https://doi.org/10.1002/fee.2029

Horton, K. G., Van Doren, B. M., Stepanian, P. M., Farnsworth, A., & Kelly, J. F. (2016). Where in the air? Aerial habitat use of nocturnally migrating birds. *Biology Letters*, *12*(11), 20160591. https://doi.org/10.1098/rsbl.2016.0591

Johnson, M. D. (2007). Measuring Habitat Quality: A Review. *The Condor*, *109*(3), 489–504. https://doi.org/10.1093/condor/109.3.489

Kelly, J. F., & Horton, K. G. (2016). Toward a predictive macrosystems framework for migration ecology. *Global Ecology and Biogeography*, *25*(10), 1159–1165. https://doi.org/10.1111/geb.12473

Klein, A.-M., Vaissière, B. E., Cane, J. H., Steffan-Dewenter, I., Cunningham, S. A., Kremen, C., & Tscharntke, T. (2006). Importance of pollinators in changing landscapes for world crops. *Proceedings of the Royal Society B: Biological Sciences*, *274*(1608), 303–313. https://doi.org/10.1098/rspb.2006.3721

Kranstauber, B., Bouten, W., van Gasteren, H., & Shamoun-Baranes, J. (2022). Ensemble predictions are essential for accurate bird migration forecasts for conservation and flight safety. *Ecological Solutions and Evidence*, *3*(3), e12158. https://doi.org/10.1002/2688-8319.12158

Kunz, T. H., Gauthreaux, S. A., Jr, Hristov, N. I., Horn, J. W., Jones, G., Kalko, E. K. V., Larkin, R. P., McCracken, G. F., Swartz, S. M., Srygley, R. B., Dudley, R., Westbrook, J. K., & Wikelski, M. (2008). Aeroecology: Probing and modeling the aerosphere. *Integrative and Comparative Biology*, *48*(1), 1–11. https://doi.org/10.1093/icb/icn037

Lambertucci, S. A., & Speziale, K. L. (2021). Need for global conservation assessments and frameworks to include airspace habitat. *Conservation Biology*, *35*(4), 1341–1343. https://doi.org/10.1111/cobi.13641

Lin, T.-Y., Winner, K., Bernstein, G., Mittal, A., Dokter, A. M., Horton, K. G., Nilsson, C., Van Doren, B. M., Farnsworth, A., La Sorte, F. A., Maji, S., & Sheldon, D. (2019). MistNet: Measuring historical bird migration in the US using archived weather radar data and convolutional neural networks. *Methods in Ecology and Evolution*, *10*(11), 1908–1922. https://doi.org/10.1111/2041-210X.13280

McCabe, J. D., Olsen, B. J., Osti, B., & Koons, P. O. (2018). The influence of wind selectivity on migratory behavioral strategies. *Behavioral Ecology*, *29*(1), 160–168. https://doi.org/10.1093/beheco/arx141

Nilsson, C., Dokter, A. M., Schmid, B., Scacco, M., Verlinden, L., Bäckman, J., Haase, G., Dell'Omo, G., Chapman, J. W., Leijnse, H., & Liechti, F. (2018). Field validation of radar systems for monitoring bird migration. *Journal of Applied Ecology*, *55*(6), 2552–2564. https://doi.org/10.1111/1365-2664.13174

Nourani, E., Yamaguchi, N. M., & Higuchi, H. (2017). Climate change alters the optimal wind-dependent flight routes of an avian migrant. *Proceedings of the Royal Society B: Biological Sciences*, *284*(1854).

Peterson, A. C., Niemi, G. J., & Johnson, D. H. (2015). Patterns in diurnal airspace use by migratory landbirds along an ecological barrier. *Ecological Applications*, *25*(3), 673–684. https://doi.org/10.1890/14-0277.1

Schmaljohann, H., Becker, P. J. J., Karaardic, H., Liechti, F., Naef-Daenzer, B., & Grande, C. (2011). Nocturnal exploratory flights, departure time, and direction in

a migratory songbird. *Journal of Ornithology*, *152*(2), 439–452. https://doi.org/10.1007/s10336-010-0604-y

Schmaljohann, H., Eikenaar, C., & Sapir, N. (2022). Understanding the ecological and evolutionary function of stopover in migrating birds. *Biological Reviews*, *97*(4), 1231–1252. https://doi.org/10.1111/brv.12839

Shamoun-Baranes, J., Liechti, F., & Vansteelant, W. M. G. (2017). Atmospheric conditions create freeways, detours and tailbacks for migrating birds. *Journal of Comparative Physiology A*, *203*(6), 509–529. https://doi.org/10.1007/s00359-017-1181-9

Van Doren, B. M., & Horton, K. G. (2018). A continental system for forecasting bird migration. *Science*, *361*(6407), 1115–1118. https://doi.org/10.1126/science.aat7526

Wikelski, M., Tarlow, E. M., Raim, A., Diehl, R. H., Larkin, R. P., & Visser, G. H. (2003). Costs of migration in free-flying songbirds. *Nature*, *423*(6941), Article 6941. https://doi.org/10.1038/423704a

Womack, A. M., Bohannan, B. J. M., & Green, J. L. (2010). Biodiversity and biogeography of the atmosphere. *Philosophical Transactions of the Royal Society B: Biological Sciences*, *365*(1558), 3645–3653. https://doi.org/10.1098/rstb.2010.0283

CHAPTER 3: DIVERGENT EFFECTS OF URBANIZATION AND SOCIAL LANDSCAPES ON CONTINENTAL MIGRATORY BIRD STOPOVER

INTRODUCTION

With 66% of the world expected to live in cities by 2050 (*1*), urbanization is a global process that has rapid and widespread impacts on ecological systems. Urban ecology has emerged as a field of research dedicated to studying these impacts in various forms (*2*) and, despite scientific interest in the field steadily increasing for decades (*3*), substantial gaps remain in our understanding of cities in an ecological context. Yet, in contrast to their influence as a global process, cities are typically studied in isolation, as singular landscapes. Urban ecology is dominated by a single-city approach (*4*), limiting our insight into the role of cities in large-scale, macroecological processes and our ability to compare differences in the drivers of biodiversity between cities (*5*). As a critical example, there is growing recognition that historical biases in social processes, such as inequitable city planning, influence urban ecosystems today (*6*) and research that connects social landscapes to patterns of biodiversity in cities is a noted priority for the field (*7*). However, it is difficult to draw broader patterns in urban social-ecological relationships because these studies primarily assess these relationships within a single urban landscape or across a handful of cities in the same region. The relatively few studies that have employed multi-city comparisons to understand these connections highlight remarkable variability between cities (*8*, *9*), suggesting that a stronger focus on inter-city variation may help uncover social-ecological drivers of urban biodiversity. Thus, a multi-city framework appears to be

crucial to advance our understanding of the cumulative ecological impacts of urbanization and large-scale patterns of biodiversity in cities (*10*).

One of the central challenges of multi-city study designs is the lack of urban biodiversity data that are comparable across a broad spatial extent. Several multi-city ecological networks have been established with the explicit goal of developing a shared protocol that can be used to collect standardized data, yet these networks remain relatively sparse in distribution due to the logistical constraints of expanding such a network (*4*). Semi-structured, crowd-sourced biodiversity data are another tool often used for large-scale ecological research. However, there is growing evidence that these data are biased, with substantially more survey effort in densely populated areas (*11*, *12*). Moreover, even within cities, it is increasingly clear that crowd-sourced data are heavily biased by many of the same social inequities associated with urban biodiversity patterns (*13*, *14*), making it difficult to decouple social-ecological mechanisms from survey effort. These challenges and biases have hindered our ability to move beyond a single-city paradigm and study urbanization holistically, as a large-scale process.

The application of large-scale remote sensing has been recognized as a promising pathway for moving multi-city research forward (*10*). The use of weather surveillance radar is one such remote sensing tool that has become integral to studying aerial macroecosystems (*15*). The Next Generation Weather Radar (NEXRAD) system, for example, has been leveraged to characterize and forecast aerial habitat use in migratory birds across the continental United States (CONUS) (*16*). While this system has been used in an urban context, such as studying aerial habitat use above cities and conservation risks that urban areas pose to aerial organisms (*17*, *18*), it has not been

used explicitly as a tool for studying social-ecological systems. One key advancement radar aeroecologists have developed is the application of radar data to estimate the density of migratory bird stopover, a critical phase of their migratory cycles during which birds rest and refuel in terrestrial habitat between migratory flights (*19*, *20*). More recently, aeroecologists have scaled this approach up by integrating machine learning, effectively expanding the landscape for which we can estimate stopover density (*21*, *22*). By implementing this technique across the CONUS (*23*), we have devised a method for quantifying urban habitat use that is both widespread and untainted by human-driven biases in sampling effort that are tied to the underlying social landscape of the city.

I employed NEXRAD data to conduct a multi-city study on the social-ecological drivers of migratory bird stopover in urban areas across the CONUS, representing a merging of concepts that are central to the fields of aeroecology (*24*) and urban ecology (*6*) (Figure 3.1). Specifically, I used estimates of stopover density for both spring and fall migration seasons derived from 143 NEXRAD sites to investigate 1) the relative contribution of urban areas to migratory stopover and 2) the relationships of that stopover with the underlying social landscape that supports it.

RESULTS AND DISCUSSION

Urban areas overrepresented across continental migration hotspots

To measure the extent to which migratory birds use urban habitat for stopover, I developed a resource selection ratio. I calculated the percentage of high-density stopover hotspots, defined by Horton et al. as the top 10% of stopover density within a

circular focal window radius of 265km (23), that fell within an urban area and divided by the percentage of land area in the CONUS comprised by increasingly strict definitions of “urban” area, which ranged from 4 to 35% (Figure 3.2). Across all definitions and both seasons, ratios were greater than one (1.26-1.96), meaning that urban areas were overrepresented in stopover hotspots relative to their CONUS land area (Figure 3.2). Moreover, selection ratio values increased we used increasingly restrictive definitions of urban boundaries for both seasons, with the percentage of fall stopover hotspots falling in urban areas nearly doubling the land area comprised by the U.S. Census Bureau Urban Area designation. This result suggests that migratory birds are disproportionately using urban centers to support their stopover at a continental scale.

The use of weather surveillance radar to quantify stopover density across broad extents is expanding in its application, including to understand spatiotemporal drivers of regional stopover habitat use (20), multiscale habitat associations (22), and assess the conservation status of critical stopover habitat (25). At the most relaxed definition of “urban,” 48% and 44% of spring and fall stopover hotspots, respectively, fall within a U.S. Census Bureau Metropolitan Statistical Area. At the most restrictive definition, despite only comprising 3.6% of the CONUS land area, U.S. Census Bureau Urban Areas comprised nearly twice that percentage of stopover hotspot area for spring (6.5%) and fall (7.0%). While urban stopover has been studied on a more local scale (26–28), the large-scale nature of my results provides broader context for this work and suggests that a substantial proportion of stopover habitat falls within cities.

Although the goals of this study were not explanatory, many recent studies provide important context that may explain my findings. For instance, artificial lights

such as those emitted by highly developed areas have long been known to attract migratory birds aloft (29) and are a top predictor of continental stopover density (23), which may represent an ecological trap that explains my findings at a more proximate level. I also note that there is spatial congruence between human population density and biodiversity, such that cities often arise in biodiverse regions (30) like coastlines or riparian areas, which may provide a more ultimate, long-term explanation for this pattern. Regardless of what drives the overrepresentation of urban areas in high-density stopover hotspots, I contend that this finding underscores the importance of cities in large-scale migratory bird conservation strategies. While cities, of course, pose various major threats to migratory birds (18, 31), there is a growing body of literature uncovering that cities can also provide benefits to birds (32) and other wildlife (33). My results highlight that migratory bird use of urban landscapes is substantial, and the development of bird-friendly practices in cities could play a prominent role in migratory bird conservation (34).

Divergent effects of urbanization and social landscapes on stopover

To test the hypothesis that the level of urbanization predicts stopover density, I constructed a series of regression models using the National Center for Health Statistics Urban-Rural Classification Scheme (35) as an ordinal predictor of mean stopover density across 3,108 counties. My CONUS model did not show a significant relationship in spring (Estimate = -0.04, 95% CI = [-0.12, 0.05]) nor fall (Estimate = -0.02, 95% CI = [-0.12, 0.09]), suggesting that there is not a consistent effect of urbanization on stopover density across the CONUS. However, regional migration flyway-specific models did

show strong variation in the size and direction of posterior regression coefficients between flyways (Figure 3.3). In the spring, Pacific and Central Flyways of the western CONUS showed a positive relationship between stopover density and urbanization (Pacific: Estimate = 0.97, 95% CI = [0.71, 1.24]; Central: Estimate = 0.41, 95% CI = [0.19, 0.66]), whereas the Atlantic Flyway of the eastern CONUS showed a negative relationship (Estimate = -0.34, 95% CI = [-0.44, -0.23]). This trend was similar for the fall with the Central Flyway showing a positive relationship (Estimate = 0.58, 95% CI = [0.35, 0.85]) and Atlantic showing a negative one (Estimate = -0.29, 95% CI = [-0.41, -0.17]). However, the Pacific Flyway did not show a significant relationship in the fall.

My analysis highlights that the relationship between stopover density and urbanization is not uniform – rather, it varies considerably across migratory flyways. Across regions in the CONUS, I found that stopover density had an opposite relationship with urbanization, with density increasing in western flyways and decreasing in the eastern flyways. I suspect that this may reflect divergent effects of urbanization across different regional contexts. For example, water is a much more limited resource across the western CONUS and studies have shown that urbanization has divergent effects on various hydrologic processes (36, 37), with water being consolidated in densely populated areas in arid regions. Cities in water-limited regions can be greener than their surrounding areas (38), potentially providing key resources for local bird communities (39). Beyond the specific impacts to migratory birds, my results suggest that urbanization may exhibit region-specific effects on a macroecological process. While remote sensing data has been employed to study regional vegetation

changes across the CONUS in response to urbanization (38, 40), my approach demonstrates how it may be applied to higher trophic levels.

To test the prediction that stopover density increases with household income, I fit a hierarchical model for 2,130 city parks across 88 cities using social demographic data on the population surrounding each park (41). I calculated the mean stopover density for each urban park as a response variable and the proportion of high-income residents within walking distance of that park as a fixed-effect predictor. I found an overall positive relationship, such that at the CONUS level, mean stopover density in urban parks increased with a higher proportion of high-income residents (Estimate = 0.42, 95% CI = [0.31, 0.54]). However, I also found remarkably wide variability in city-level effects with most cities showing no significant relationship and some showing distinctly negative relationships (Figure 3.4).

My hypothesis was guided by the “luxury effect,” which predicts that measures of biodiversity tend to increase with key social predictors, such as race and household income. This concept is commonly used to characterize our understanding of social-ecological relationships in cities (42). Various studies have found support for this prediction with respect to urban avian bird diversity (43, 44) and, indeed, the global effect of my models suggests that avian stopover density in urban parks is linearly proportional to the percentage of high-income residents in the area. Yet, more recently, the luxury effect has come under scrutiny as an oversimplification of the complex drivers of urban biodiversity (45). Multi-city studies continually highlight remarkably high levels of variability in what this relationship looks like across different cities (8, 9) and the estimates of my city-level effects strongly support this notion. While some cities in this

analysis appear to exhibit a luxury effect with respect to stopover density (n=4), I did not detect a directional relationship in the vast majority of cities (n=82) and found that some cities even show an opposite directional effect (n=2).

Beyond the scientific community, I assert that this variability could have important implications for the implementation of conservation in cities. Even when planned at a large scale (46), conservation strategies must be linked to much more local action and outreach (47). As noted above, given their prevalence in stopover hotspots, bird-friendly cities could be a critical component of this link (34). The efficacy of urban conservation programs hinges on understanding the relationship between city residents and urban wildlife. My results highlight remarkably broad variability in that relationship. I stress that effective urban conservation must account for these distinctions between cities. In doing so, I echo many of my colleagues in suggesting that a stronger understanding of the historical and current processes that drive inter-city variability in social-ecological relationships is a critical next step in advancing both urban ecology theory and urban conservation.

Conclusion

I used stopover densities as estimated by 10 million remote sensing observations to assess stopover patterns in urban areas across the CONUS. My results not only highlight the extent to which migratory birds use stopover habitat across urban landscapes but, more broadly, demonstrate the utility of weather surveillance radar for developing multi-city social-ecological research. While the NEXRAD system has been used within an urban context, I show that it may further be employed to explicitly study

social-ecological relationships across cities. I submit that weather radar could play a prominent role in advancing our understanding of urban ecosystems.

As cities continue to expand across the globe, ecologists must develop theory and practice that address the scope of these changes in urban ecosystems. Our ability to develop multi-city research will be essential to this development, yet the logistical hurdles of collecting comparable ecological data across different cities remains a challenge. Here, I demonstrate how weather surveillance radar may play a pivotal role in that advancement. In addition to estimating the extent to which birds use urban landscapes for migratory stopover across the CONUS, I illustrate how radar can reveal regional patterns in the effects of urbanization and inter-city variation in social-ecological relationships. Ultimately, my approach underscores the potential of weather radar as a scalable tool for advancing the field of urban ecology.

METHODS

Estimating stopover density

I obtained stopover estimates as calculated and provided by Horton et al (23). The NEXRAD system is a network of weather surveillance stations operated jointly by the National Weather Service, Federal Aviation Administration, and Air Force. There are 143 stations located within the CONUS, which scan the lower atmosphere horizontally every 5-10 minutes, between an elevation angle of 0.5-19.5°. Each radar station operates in a super-resolution format, providing spatial data at a 250m range resolution and 0.5° azimuthal resolution. The NEXRAD network has long been recognized as an

ornithological tool (48) and integrations with machine learning have rapidly expanded its application in the quantification of bird migration activity (15).

Horton et al (23) leveraged 10 million NEXRAD observations to estimate stopover densities across the CONUS. Broadly, this approach entailed downloading and processing NEXRAD data, fitting generalized additive models to select sampling timing, and using niche models to predict stopover densities across the CONUS. Specifically, they downloaded radar reflectivity data during spring and fall migration seasons from 2016 through 2020, using established methods to remove non-avian clutter and correct for range biases. They fit generalized additive models to these data to determine the peak rate of increase in reflectivity. Given that birds depart shortly after local sunset, this period represented the peak exodus of birds from terrestrial habitat and into migratory flights. They used this period to estimate stopover densities within NEXRAD coverage. Using a composite of those estimates across scans, they randomly selected 1 million locations and extracted stopover densities. By combining these data with a suite of 49 terrestrial and sampling predictors, they used an ensemble of boosted regression models to identify associations and predict densities in areas uncovered by NEXRAD. Horton et al then used these models to develop seasonal layers of bird migrant stopover density across the CONUS at a spatial resolution of 1km. Additionally, these layers were used to calculate stopover “hotspots,” which represent areas of high stopover intensity quantiles at the scale of a night’s flight distance. For further details on this methodology, see Horton et al. (23).

Calculating stopover and area proportions

I developed selection ratios of urban stopover, which represent the proportion of migratory bird stopover hotspots falling within urban areas relative to the CONUS land area comprised by urban areas using three “urban” definitions (Supplemental Table 3.1). I downloaded public spatial data and cropped them to the CONUS. I reprojected all spatial layers to a common projected coordinate system (EPSG:5070, NAD83 / Conus Albers) to ensure spatial compatibility.

For both spring and fall seasons, I first calculated the land area comprised by urban areas across each definition. I then used the top 90th quantile of stopover density within a 265km buffer, as defined by Horton et al. (23), and calculated the overlap between this spatial layer and urban areas across each definition. I divided the overlap by its respective land area to calculate a selection ratio, whereby values above 1 represent overselection and values below 1 represent underselection. All spatial analyses were conducted in R Version 2024.04.2+764 (49).

Modeling stopover as function of urbanization

I assessed the relationship between stopover density and urbanization at the spatial scale of the United States administrative county. To do this, I used rasters of stopover density to extract the mean stopover density for each of the 3,108 counties for both spring and fall migration seasons. I obtained NCHS Urban-Rural Classification Scheme at the county level from the Center for Disease Control’s Data Analysis Tools (Supplemental Table 3.1). This classification scheme ranks every United States county on an ordinal Urban-Rural scale from 1-6.

I fit a series of Bayesian ordinal regression models to assess the effect of urbanization on stopover density. All models were implemented using the 'brms' package in R (50), which employs Hamiltonian Monte Carlo for Bayesian inference. I modeled stopover density as a function of urbanization on the NCHS ordinal scale. All models were specified using a Gamma distribution with a log link function, suitable for modeling the positive, right-skewed values exhibited by stopover densities. I applied weakly informative normal priors (mean = 0, SD = 10) on the coefficients and intercept, and each model was run with four Markov chains, 2,000 iterations per chain, and a 1,000-iteration warmup phase. I used model summaries provided by the brms package to generate posterior estimates and infer the relationship between urbanization levels and stopover density, with credible intervals quantifying uncertainty.

I built five separate models across different spatial scales and extents. My first model represented the entire CONUS. The subsequent four models were run for each Migratory Bird Program Administrative Flyway, as delineated by the U.S. Fish & Wildlife Service (51). Across these extents, I built models for both spring and fall, for a total of 10 models.

Modeling stopover as function of household income

I assessed the relationship between stopover density and household income at the scale of individual parks and cities, and across the CONUS. I used a hierarchical modeling structure to account for nested spatial scales between these estimates.

For this analysis, city parks served as the smallest unit of interest. Urban parks are a useful comparison across cities, given their relatively similar recreational land use and, relatedly, land management practices. I downloaded spatial and social

demographic data on city parks from ParkServe, which is an inventory of parks for every urban area in the U.S., including Puerto Rico (41). This inventory can be downloaded as a shapefile, which, in addition to delineating over 145,000 parks, provides demographic data derived from census block group data. With respect to income, the database calculates the number of low-, middle-, and high-income households around each park. These are defined as households within a 10-minute walking distance to a park that are <75%, 75-125%, and >125% of their city's median income, respectively. For each park, I calculated the number of high-income households as a proportion of the total households within a 10-minute walking distance and used this as my predictor variable. For this analysis, I decided to focus on large metropolitan areas, or counties categorized as 1 or 2 by the NCHS Urban-Rural Classification Scheme. I used the layers of stopover density to extract the mean density of each park within these boundaries and used this value as the response variable in my models.

I fit three Bayesian hierarchical models to evaluate the relationship between mean stopover density of each park and the proportion of high-income households around that park again using the 'brms' package in R (50). I fit these models in a Gamma regression framework with a log link to account for the continuous and positively skewed nature of the stopover density data. Given the coarse 1km grain size of the stopover density layers relative to the size of many city parks, I suspected my models may be subject to spatial autocorrelation. Thus, I conducted a two-step sensitivity analysis. First, I fit one model with all city parks within large metropolitan areas (n=80,449) and one model with only parks larger than the 1km grain size (n=2,526). Both models estimated global effects in the same direction, but with the

subset model exhibiting a stronger effect size (Full Model: Estimate = 0.15, 95% CI = [0.10, 0.20]; Subset Model 1: Estimate = 0.24, 95% CI = [0.11, 0.36]) (Supplemental Figure 3.1). Second, to ensure robust city-level estimates, I fit a third model, removing cities that had less than five parks larger than the 1km grain size. This final model included 2,130 parks across 88 cities and, again, estimated global effects in the same direction (Subset Model 2: Estimate = 0.42, 95% CI = [0.31, 0.54]) (Supplemental Figure 3.1). Using this model, I extracted the city-level effect estimates along with their 95% credible intervals and report those results in my main text.

FIGURES AND TABLES

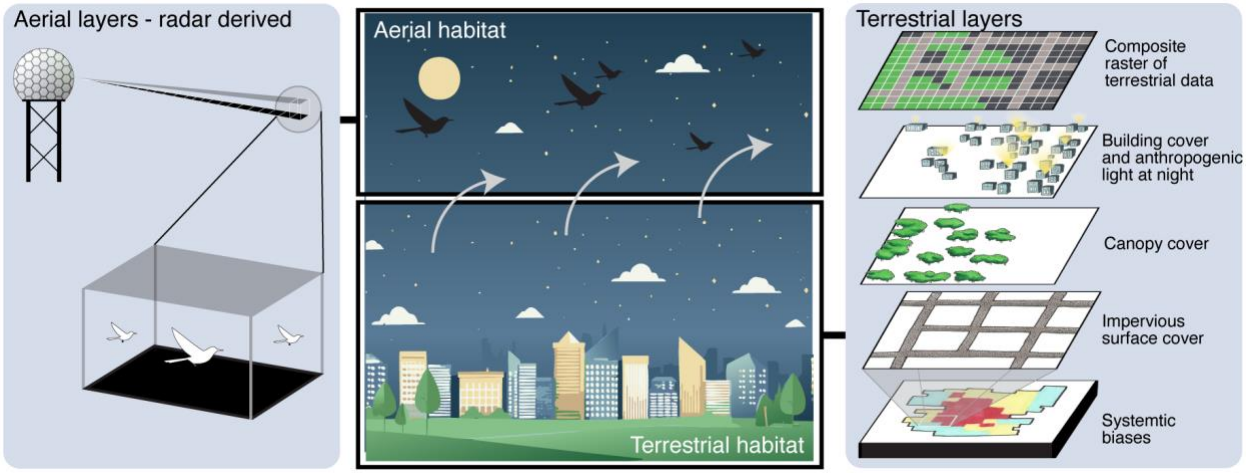

Figure 3.1 *Conceptual diagram of weather surveillance radar used as a tool for studying urban social-ecological landscapes. The radar sweep (left) of departing birds is connected to the terrestrial urban landscape, which is connected to underlying systemic biases (right) that drive landscape heterogeneity. Illustrations by Cristyn Hypnar.*

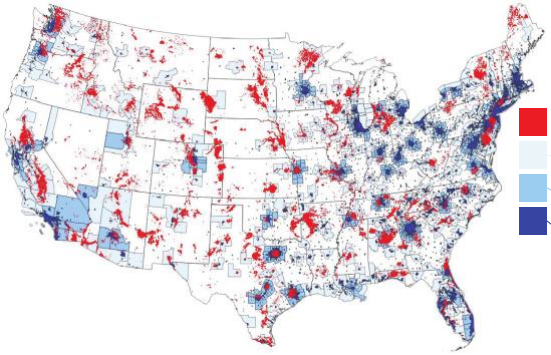

Definition (Institution)	Land area (%)	Spring Hotspot (%)	Fall Hotspot (%)	Spring Selection Ratio	Fall Selection Ratio
Metropolitan Statistical Area (United States Census Bureau)	35.33	48.17	44.37	1.36	1.26
Large Metropolitan Area (National Center for Health Statistics)	9.80	17.12	13.21	1.75	1.35
Census Urban Area (United States Census Bureau)	3.58	6.46	7.01	1.81	1.96

Figure 3.2 *Left)* Continental United States (U.S.) map of three overlayed delineations of "urban," as defined by the U.S. Census Bureau and the National Center for Health Statistics and fall high-density avian stopover hotspots, defined as the top 10% of stopover density within a circular focal window radius of 265km. *Right)* Table summarizing the percentage of land area that is urban, the percentage of fall and spring migration hotspots that fall within that urban landscape, and the fall and spring selection ratio across three definitions of "urban." The seasonal selection ratios are calculated by dividing the hotspot percentage by the land area percentage.

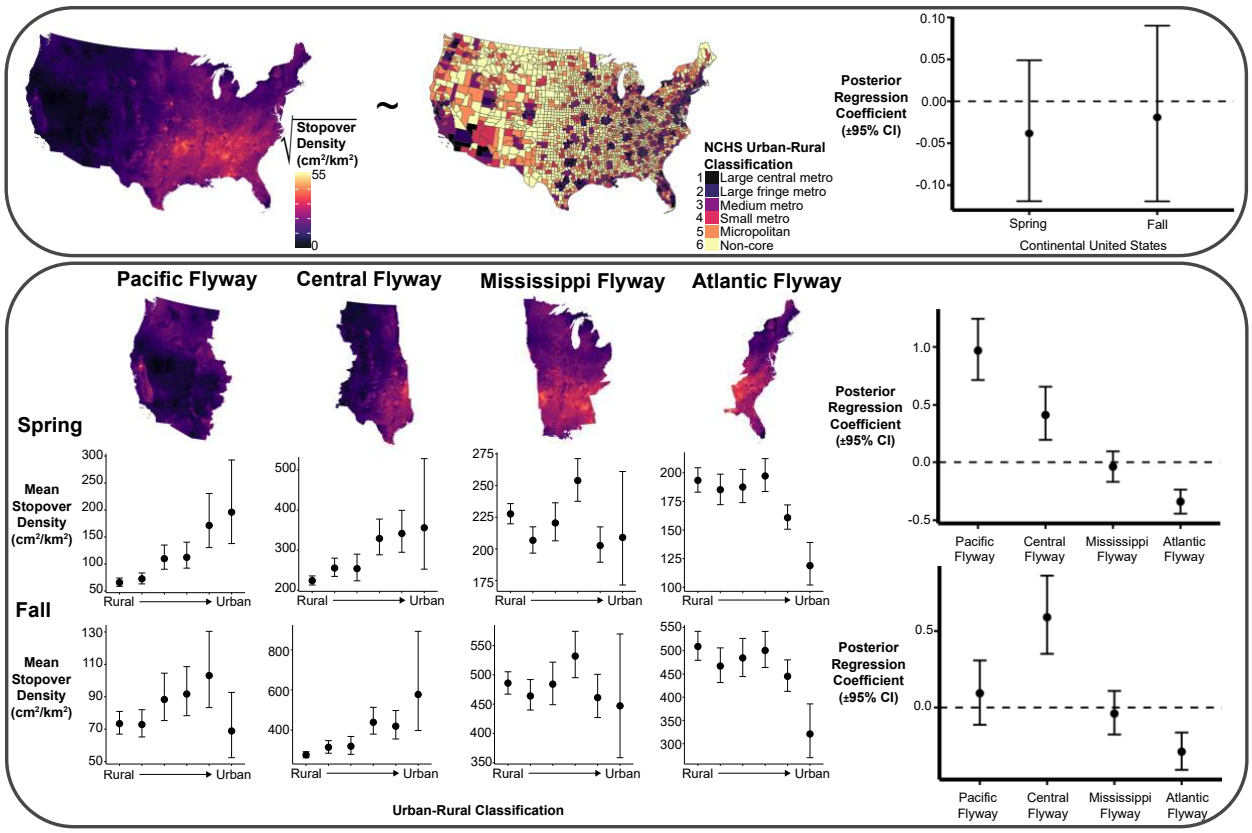

Figure 3.3 Summary of posterior regression coefficients from a series of generalized linear models used to assess the relationship between migratory bird stopover density and urbanization across the continental United States (CONUS). Top panel: A map of stopover density (left), which was used as the response variable, a map of the National Center for Health Statistics Urban-Rural Classification Scheme by county (middle), which was used as a predictor variable. Posterior regression coefficients for the CONUS model are plotted for both the spring and fall migration seasons (right). Bottom panel: The conditional effects for each flyway model are plotted for each season, showing the relationship between stopover density and urbanization on an ordinal scale (left). Posterior regression coefficients for each flyway model are plotted for both seasons (right).

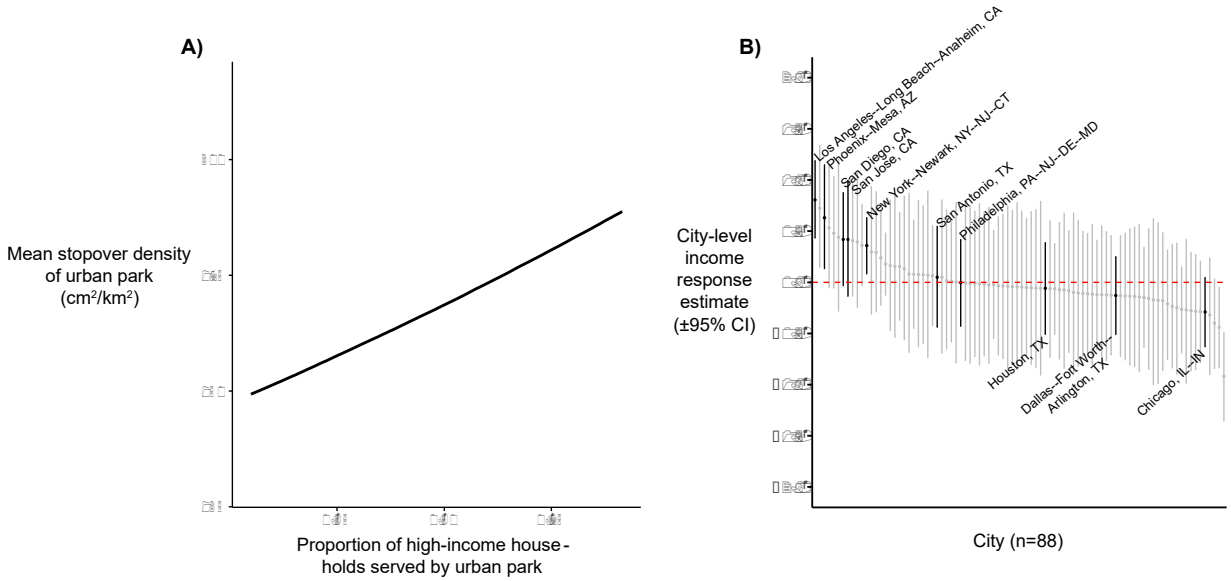

Figure 3.4 Plot summarizing the relationship between mean migratory bird stopover density in city parks and the proportion of residents within walking distance of that park that are low income as estimated by a hierarchical model. (A) Global conditional effects of the proportion of high-income households within a 10-minute walking distance of a park on the estimated mean spring stopover density of migratory birds for that park. Shaded areas represent the 95% credible intervals. A log link and Gamma family were used to model the positively skewed response variable. (B) City-level estimates are represented by a point, which is the posterior mean of the coefficient estimate for each of the 88 cities included in the model, and 95% credible intervals. Response estimates are on the log scale and cities are ordered in decreasing income response. A positive relationship denotes cities in which park stopover density increases with the proportion of high-income residents living near a park and negative relationship denotes cities in which stopover density decreases. The top 10 most-populous urban areas are highlighted in black and labeled.

LITERATURE CITED

1. United Nations, Department of Economic and Social Affairs, Population Division (2018). World Urbanization Prospects: The 2018 Revision, Key Facts. ESA/P/WP/248.

2. S. T. A. Pickett, M. L. Cadenasso, D. L. Childers, M. J. Mcdonnell, W. Zhou, Evolution and future of urban ecological science: ecology in, of, and for the city. *Ecosyst. Health Sustain.* **2**, e01229 (2016).

3. M. K. Collins, S. B. Magle, T. Gallo, Global trends in urban wildlife ecology and conservation. *Biol. Conserv.* **261**, 109236 (2021).

4. S. B. Magle, M. A. Fidino, E. W. Lehrer, T. Magle, M. F. J. Aronson, “Multicity Ecological Networks for Addressing Urban Biodiversity Conservation” in *Urban Biodiversity and Equity* (2023).

5. S. B. Magle, M. Fidino, E. W. Lehrer, T. Gallo, M. P. Mulligan, M. J. Ríos, A. A. Ahlers, J. Angstmann, A. Belaire, B. Dugelby, A. Gramza, L. Hartley, B. MacDougall, T. Ryan, C. Salsbury, H. Sander, C. Schell, K. Simon, S. St Onge, D. Drake, Advancing urban wildlife research through a multi-city collaboration. *Front. Ecol. Environ.* **17**, 232–239 (2019).

6. C. J. Schell, K. Dyson, T. L. Fuentes, S. Des Roches, N. C. Harris, D. S. Miller, C. A. Woelfle-Erskine, M. R. Lambert, The ecological and evolutionary consequences of systemic racism in urban environments. *Science* **369**, eaay4497 (2020).

7. S. Knapp, M. F. J. Aronson, E. Carpenter, A. Herrera-Montes, K. Jung, D. J. Kotze, F. A. La Sorte, C. A. Lepczyk, I. MacGregor-Fors, J. S. MacIvor, M. Moretti, C. H. Nilon, M. R. Piana, C. C. Rega-Brodsky, A. Salisbury, C. G. Threlfall, C. Trisos, N. S. G.

Williams, A. K. Hahs, A Research Agenda for Urban Biodiversity in the Global Extinction Crisis. *BioScience* **71**, 268–279 (2021).

8. S. B. Magle, M. Fidino, H. A. Sander, A. T. Rohnke, K. L. Larson, T. Gallo, C. A. M. Kay, E. W. Lehrer, M. H. Murray, S. A. Adalsteinsson, A. A. Ahlers, W. J. B. Anthonysamy, A. R. Gramza, A. M. Green, M. J. Jordan, J. S. Lewis, R. A. Long, B. MacDougall, M. E. Pendergast, K. Remine, K. C. Simon, C. C. St. Clair, C. J. Shier, T. Stankowich, C. J. Stevenson, A. J. Zellmer, C. J. Schell, Wealth and urbanization shape medium and large terrestrial mammal communities. *Glob. Change Biol.* **27**, 5446–5459 (2021).

9. M. Fidino, H. A. Sander, J. S. Lewis, E. W. Lehrer, K. Rivera, M. H. Murray, H. C. Adams, A. Kase, A. Flores, T. Stankowich, C. J. Schell, C. M. Salsbury, A. T. Rohnke, M. J. Jordan, A. M. Green, A. R. Gramza, A. J. Zellmer, J. Williamson, T. D. Surasinghe, H. Storm, K. L. Sparks, T. J. Ryan, K. R. Remine, M. E. Pendergast, K. Mullen, D. E. Minier, C. R. Middaugh, A. L. Mertl, M. R. McClung, R. A. Long, R. N. Larson, M. T. Kohl, L. R. Harris, C. T. Hall, J. D. Haight, D. Drake, A. M. Davidge, A. O. Cheek, C. P. Bloch, E. G. Biro, W. J. B. Anthonysamy, J. L. Angstmann, M. L. Allen, S. A. Adalsteinsson, A. G. Short Gianotti, J. M. LaMontagne, T. A. Gelmi-Candusso, S. B. Magle, Gentrification drives patterns of alpha and beta diversity in cities. *Proc. Natl. Acad. Sci.* **121**, e2318596121 (2024).

10. G. Chen, Y. Zhou, J. A. Voogt, E. C. Stokes, Remote sensing of diverse urban environments: From the single city to multiple cities. *Remote Sens. Environ.* **305**, 114108 (2024).

11. E. M. Geurts, J. D. Reynolds, B. M. Starzomski, Turning observations into biodiversity data: Broadscale spatial biases in community science. *Ecosphere* **14**, e4582 (2023).

12. C. T. Callaghan, J. J. L. Rowley, W. K. Cornwell, A. G. B. Poore, R. E. Major, Improving big citizen science data: Moving beyond haphazard sampling. *PLOS Biol.* **17**, e3000357 (2019).

13. A. M. Grade, N. W. Chan, P. Gajbhiye, D. J. Perkins, P. S. Warren, Evaluating the use of semi-structured crowdsourced data to quantify inequitable access to urban biodiversity: A case study with eBird. *PLOS ONE* **17**, e0277223 (2022).

14. D. Ellis-Soto, M. Chapman, D. Locke, Uneven biodiversity sampling across redlined urban areas in the United States. (2022).

15. S. Bauer, J. Shamoun-Baranes, C. Nilsson, A. Farnsworth, J. F. Kelly, D. R. Reynolds, A. M. Dokter, J. F. Krauel, L. B. Petterson, K. G. Horton, J. W. Chapman, The grand challenges of migration ecology that radar aeroecology can help answer. *Ecography* **42**, 861–875 (2019).

16. B. M. V. Van Doren, K. G. Horton, A continental system for forecasting bird migration. *Science*, doi: 10.1126/science.aat7526 (2018).

17. J. A. Elmore, C. S. Riding, K. G. Horton, T. J. O'Connell, A. Farnsworth, S. R. Loss, Predicting bird-window collisions with weather radar. *J. Appl. Ecol.* **58**, 1593–1601 (2021).

18. K. G. Horton, C. Nilsson, B. M. Van Doren, F. A. La Sorte, A. M. Dokter, A. Farnsworth, Bright lights in the big cities: migratory birds' exposure to artificial light. *Front. Ecol. Environ.* **17**, 209–214 (2019).

19. D. N. Bonter, S. A. Gauthreaux Jr, T. M. Donovan, Characteristics of Important Stopover Locations for Migrating Birds: Remote Sensing with Radar in the Great Lakes Basin. *Conserv. Biol.* **23**, 440–448 (2009).

20. J. J. Buler, R. H. Diehl, Quantifying bird density during migratory stopover using weather surveillance radar. *IEEE Trans. Geosci. Remote Sens.* **47**, 2741–2751 (2009).

21. E. B. Cohen, K. G. Horton, P. P. Marra, H. L. Clipp, A. Farnsworth, J. A. Smolinsky, D. Sheldon, J. J. Buler, A place to land: spatiotemporal drivers of stopover habitat use by migrating birds. *Ecol. Lett.* **24**, 38–49 (2021).

22. F. Guo, J. J. Buler, J. A. Smolinsky, D. S. Wilcove, Autumn stopover hotspots and multiscale habitat associations of migratory landbirds in the eastern United States. *Proc. Natl. Acad. Sci.* **120**, e2203511120 (2023).

23. K. G. Horton, J. J. Buler, S. J. Anderson, C. S. Burt, A. C. Collins, A. M. Dokter, F. Guo, D. Sheldon, M. A. Tomaszewska, G. M. Henebry, Artificial light at night is a top predictor of bird migration stopover density. *Nat. Commun.* **14**, 7446 (2023).

24. R. H. Diehl, The airspace is habitat. *Trends Ecol. Evol.* **28**, 377–379 (2013).

25. F. Guo, J. J. Buler, J. A. Smolinsky, D. S. Wilcove, Seasonal patterns and protection status of stopover hotspots for migratory landbirds in the eastern United States. *Curr. Biol.* **34**, 235-244.e3 (2024).

26. D. N. Pennington, J. Hansel, R. B. Blair, The conservation value of urban riparian areas for landbirds during spring migration: Land cover, scale, and vegetation effects. *Biol. Conserv.* **141**, 1235–1248 (2008).

27. S. N. Matthews, P. G. Rodewald, Urban Forest Patches and Stopover Duration of Migratory Swainson's Thrushes. *The Condor* **112**, 96–104 (2010).

28. P. G. Rodewald, S. N. Matthews, Landbird use of Riparian and Upland Forest Stopover Habitats in an Urban Landscape. *The Condor* **107**, 259–268 (2005).

29. C. S. Burt, J. F. Kelly, G. E. Trankina, C. L. Silva, A. Khalighifar, H. C. Jenkins-Smith, A. S. Fox, K. M. Fristrup, K. G. Horton, The effects of light pollution on migratory animal behavior. *Trends Ecol. Evol.* **38**, 355–368 (2023).

30. G. W. Luck, A review of the relationships between human population density and biodiversity. *Biol. Rev.* **82**, 607–645 (2007).

31. B. M. Van Doren, D. E. Willard, M. Hennen, K. G. Horton, E. F. Stuber, D. Sheldon, A. H. Sivakumar, J. Wang, A. Farnsworth, B. M. Winger, Drivers of fatal bird collisions in an urban center. *Proc. Natl. Acad. Sci.* **118**, e2101666118 (2021).

32. R. Pacheco-Muñoz, A. Ceja-Madrigal, J. E. Schondube, Migratory birds benefit from urban environments in a highly anthropized Neotropical region. *PLOS ONE* **20**, e0311290 (2025).

33. C. A. Lepczyk, M. F. Aronson, F. A. La Sorte, Cities as sanctuaries. *Front. Ecol. Environ.* **21**, 251–259 (2023).

34. R. P. Snep, J. L. Kooijmans, R. G. Kwak, R. P. Foppen, H. Parsons, M. Awasthy, H. L. Sierdsema, J. M. Marzluff, E. Fernandez-Juricic, J. de Laet, Y. M. van Heezik, Urban bird conservation: presenting stakeholder-specific arguments for the development of bird-friendly cities. *Urban Ecosyst.* **19**, 1535–1550 (2016).

35. CDC, NCHS Urban-Rural Classification Scheme for Counties, *National Center for Health Statistics* (2024). https://www.cdc.gov/nchs/data-analysis-tools/urban-rural.html.

36. J. Chen, L. Theller, M. W. Gitau, B. A. Engel, J. M. Harbor, Urbanization impacts on surface runoff of the contiguous United States. *J. Environ. Manage.* **187**, 470–481 (2017).

37. C. Li, G. Sun, P. V. Caldwell, E. Cohen, Y. Fang, Y. Zhang, L. Oudin, G. M. Sanchez, R. K. Meentemeyer, Impacts of Urbanization on Watershed Water Balances Across the Conterminous United States. *Water Resour. Res.* **56**, e2019WR026574 (2020).

38. L. Bounoua, P. Zhang, G. Mostovoy, K. Thome, J. Masek, M. Imhoff, M. Shepherd, D. Quattrochi, J. Santanello, J. Silva, R. Wolfe, A. M. Toure, Impact of urbanization on US surface climate. *Environ. Res. Lett.* **10**, 084010 (2015).

39. B. W. Schleder, “Residential irrigation as a driver of urban bird community structure,” thesis, California State University, Fresno, United States -- California (2010).

40. X. Li, Y. Zhou, G. R. Asrar, J. Mao, X. Li, W. Li, Response of vegetation phenology to urbanization in the conterminous United States. *Glob. Change Biol.* **23**, 2818–2830 (2017).

41. The ParkServe® database, *Trust for Public Land*. https://www.tpl.org/parkserve/about.

42. M. Leong, R. R. Dunn, M. D. Trautwein, Biodiversity and socioeconomics in the city: a review of the luxury effect. *Biol. Lett.* **14**, 20180082 (2018).

43. E. M. Wood, S. Esaian, C. Benitez, P. J. Ethington, T. Longcore, L. Y. Pomara, Historical racial redlining and contemporary patterns of income inequality negatively affect birds, their habitat, and people in Los Angeles, California. *Ornithol. Appl.* **126**, duad044 (2024).

44. C. O. Estien, M. Fidino, C. E. Wilkinson, R. Morello-Frosch, C. J. Schell, Historical redlining is associated with disparities in wildlife biodiversity in four California cities. *Proc. Natl. Acad. Sci.* **121**, e2321441121 (2024).

45. R. Poulton Kamakura, J. Bai, V. Sheel, M. Katti, Biodiversity is not a luxury: Unpacking wealth and power to accommodate the complexity of urban biodiversity. *Ecosphere* **15**, e70049 (2024).

46. C. A. Runge, J. E. M. Watson, S. H. M. Butchart, J. O. Hanson, H. P. Possingham, R. A. Fuller, Protected areas and global conservation of migratory birds. *Science* **350**, 1255–1258 (2015).

47. W. V. DeLuca, N. E. Seavy, J. Grand, J. Velásquez-Tibatá, L. Taylor, C. Bowler, J. L. Deppe, E. J. Knight, G. M. Lentijo, T. D. Meehan, N. L. Michel, S. P. Saunders, N. Schillerstrom, M. A. Smith, C. Witko, C. B. Wilsey, A framework for linking hemispheric, full annual cycle prioritizations to local conservation actions for migratory birds. *Conserv. Sci. Pract.* **5**, e12975 (2023).

48. S. A. Gauthreaux Jr., Weather Radar Quantification of Bird Migration. *BioScience* **20**, 17–19 (1970).

49. R Core Team, R Core Team (2022). R: A language and environment for statistical computing. R Foundation for Statistical Computing, Vienna, Austria. URL https://www.R-project.org/., (2024).

50. P.-C. Bürkner, Bayesian Item Response Modeling in R with brms and Stan. arXiv arXiv:1905.09501 [Preprint] (2020). https://doi.org/10.48550/arXiv.1905.09501.

51. Migratory Bird Program Administrative Flyways | U.S. Fish & Wildlife Service (2025). https://www.fws.gov/partner/migratory-bird-program-administrative-flyways.

CHAPTER 4: WHITE LIGHT REDUCES FLIGHT HEIGHT OF BIRDS RELATIVE TO OTHER LIGHT SPECTRA IN LOW-DENSITY MIGRATION CORRIDOR

INTRODUCTION

For millions of years, animals have evolved with a light cycle that followed a predictable diurnal pattern. However, a growing human footprint across much of the globe has drastically altered this light cycle by emitting high levels of artificial light at night (ALAN), illuminating nocturnal landscapes that would otherwise be dark (Seymoure et al., 2025). Given that this development is relatively recent in human and evolutionary history (Aulsebrook et al., 2018), we are only beginning to understand the full impacts on animal behavior and ramifications for wildlife conservation (Grubisic & van Grunsven, 2021; McLaren et al., 2018). Furthermore, by focusing on brightly lit urban centers, we may be underestimating the biological effects of ALAN, as light pollution remains understudied in rural, remote, and marine systems (Gaston et al., 2021). As such, the growing impact of ALAN has arisen as an area of focus within global change research (Davies & Smyth, 2018).

One area of study that has received notable attention is the impact of ALAN on migrating birds. Many studies have demonstrated various effects, yet we still lack strong consensus around the proximate and ultimate mechanisms that drive bird responses to light (Adams et al., 2021). For instance, there is ample evidence that ALAN attracts birds at various spatial scales (McLaren et al., 2018; Poot et al., 2008; Van Doren et al., 2021) and often disorients their sense of direction (Chernetsov, 2016; Gauthreaux, 1982). However, it remains unclear if these effects are the consequence of disruptions to avian perceptions of photoperiods (Kumar et al., 2017), stellar compasses (Foster et al., 2018),

or magnetic compasses (Muheim et al., 2016). Moreover, avian behavioral responses can be variable, including changes in flight height (May et al., 2017) or direction (Bruderer et al., 1999), and some lighting, such as flashing lights or lasers, even being shown to repel birds (Andelt et al., 1997; Cassidy, 2015). While it seems clear that ALAN can have profound effects on avian behavior, there are substantial gaps in our understanding of how and why these effects occur.

Beyond its mere presence, the degree to which the characteristics of lighting modulate its effect on birds is one such gap. A notable point of contention is the effects of different colors or, more specifically, wavelength spectra, on avian behavior. Early attempts to test this question along the Netherlands North Sea coastline suggested that birds were most attracted to light with long wavelengths, such as red light, and less affected by short wavelengths, such as blue and green lights (Poot et al., 2008). However, recent studies that employed systematic, automated methods for quantifying bird responses suggest that shorter wavelengths of blue, green, and white lights are more attractive to migrating birds (Evans et al., 2007; Rebke et al., 2019; Zhao et al., 2020). There may also be taxonomic or age-based variation in behavioral responses, as suggested by Syposz et al (2021), which found that breeding Manx Shearwaters (*Puffinus puffinus*) were more strongly repelled by blue and green light than other colors. Ultimately, our understanding of how birds respond to different spectra of light remains somewhat convoluted. Beyond providing insights into basic animal biology, physiology, and behavior, filling these gaps could have wide-reaching conservation implications. Migratory bird collisions with anthropogenic structures are a major source of mortality (Loss et al., 2015) and it is strongly suspected that ALAN plays a role in drawing birds

closer to those structures and hindering their ability to navigate (Lao et al., 2020; Parkins et al., 2015; Van Doren et al., 2021). The management of ALAN has emerged as an integral tool in migratory bird conservation, and identifying spectra-specific effects on bird behavior could inform more dynamic and effective management practices (Burt et al., 2023).

I designed a field experiment with the explicit goal of understanding how in-flight bird behavior is impacted by different spectra of ALAN. I used LED floodlights to emit ALAN across a remote, dark landscape in four color treatments (white, red, amber, and blue) during fall migration nights. Throughout my experiment, I recorded migratory bird flight behavior with a mobile, vertically looking radar. The specific objectives of this study were to understand 1) how in-flight bird behavior was affected by different spectra of ALAN and 2) the degree to which these effects are influenced by environmental conditions. Based on existing literature, I predicted that shortwave, white and blue light would be more attractive to birds than red and amber lights, and that this effect would be strongest when moon illumination was low, and cloud cover was high.

MATERIAL AND METHODS

Study system

I conducted my field experiment in Pawnee National Grassland, a 193,060-acre remnant shortgrass prairie managed by the National Forest Service. Weld County, in which Pawnee National Grassland is located, is situated in central, northern Colorado and is part of the High Plains ecosystem, dominated by drought tolerant, shortgrass prairie vegetation. Northern Colorado is a low-density migration traffic region relative to

the eastern continental United States (Dokter et al., 2018), but does serve as stopover habitat for birds along the North American central flyway and breeding habitat for many grassland species.

My study site was located within the eastern unit of Pawnee National Grassland (40.74°N, 104.03°W) (Figure 4.1). The site is far from urban centers or other major sources of ALAN, with the closest city, Sterling, with a population above 10,000 people being nearly 50km away. This setting allowed us to conduct my study with minimal interference from external ALAN contamination.

Lighting experiment design

I conducted an experiment from late August through late October of 2023 and 2024 to capture fall migration activity. I designed a lighting system that allowed us to manipulate the spectrum of a point ALAN source in a remote setting. Specifically, I powered two professional grade LED floodlights (Gopretty 800W LED Flood Light) with a portable generator. I positioned floodlights approximately 2m apart. I used 5.5-6mm thick polyester film lighting gels to change the wavelength of the floodlights and produce white, red, amber, and blue lighting treatments. I include detailed information and data regarding lighting spectral range and other characteristics of each treatment in my appendix (Supplemental Figure 4.1). Additionally, I used a handheld spectrometer and a dimmer to standardize the irradiance to approximately 8 W/m2 measured 1m from the floodlights.

In order to control for various spatio-temporal variables and isolate the effect of ALAN spectrum, I employed a color block study design adapted from (Rebke et al.,

2019) (Figure 4.2). I alternated between 15-minute control periods and 30-minute color treatment periods. During the 15-minute control periods, I turned off both spotlights, allowing birds to pass the area before starting a new treatment and creating a baseline comparison for each of the treatments. During treatment periods, I emitted a spectrum of ALAN from both spotlights, randomizing the sequence of treatments by using a random number generator. I considered a color block to be completed after all four treatments had been emitted and did not repeat a given treatment until starting a new block. I started my experiment 15 minutes after civil twilight and continued until the twilight of the following morning, pausing during inclement weather.

Monitoring in-flight responses with the BirdScan MR1

Throughout my experiment, I used the BirdScan MR1 (hereafter Birdscan) to quantify in-flight bird behavior (Figure 2). This vertically directed, mobile, 25 kW X-band (9.4 GHz, 3.2 cm wavelength) pulse radar system was explicitly designed to monitor and record animal movement in the lower atmosphere (Swiss Birdradar Solution, 2023). This radar system also collects high-resolution data on the echoes produced by each individual object. The features from these echoes can be used to classify objects as insects, bats, and various taxonomic and functional groups of birds. I used the short-pulse, antenna-rotating setting, which emits electromagnetic pulses with a pulse length of 81 ns and shot frequency of about 1800 Hz. The emitted pulses reflect off objects in the airspace, producing backscatter from an altitudinal range of 50m to approximately 1450 (Schmid et al., 2019; Weisshaupt et al., 2023). I deployed the BirdScan 3m away

from the spotlights with the intention of capturing in-flight bird behavior above and around my lighting setup.

Calculating behavior metrics and environmental covariates

I used the birdscanR R package (Haest et al., 2023) to extract and process in-flight bird behavior data in R (R Core Team, 2024). Specifically, I used a class selection filter to exclude insects, producing a dataset that included only bird echoes. Using these data, I characterized in-flight behavior in three response variable metrics: migration traffic rate, mean flight height, and mean flight direction. I defined migration traffic rate as the number of detected birds passing per hour across an imaginary 1km line, mean flight height as the mean altitude (m) of detected birds, and flight direction as the circular azimuthal mean (degrees) of detected birds. I calculated these metrics up to a maximum altitude of 800m at a 15-minute temporal resolution for each of the control and treatment periods. This process yielded one dataset that reflected in-flight bird behavior for all birds I detected.

Given evidence that environmental conditions, such as a moon illumination (Rodríguez & Rodríguez, 2009) and cloud cover (Ronconi et al., 2015) may influence how birds respond to ALAN, I included these variables in my models as coefficients. I used the calculateMoonlightIntensity function in the moonlit R package (Śmielak, 2023) to estimate the hourly moon illumination. This function predicts the intensity of moon illumination (lux) relative to an "average" full moon, while accounting for the elevation angle of the moon at a given ground location. I downloaded total cloud cover data from the National Centers for Environmental Prediction’s North American Regional

Reanalysis (NARR) for the grid cell containing my study site (Mesinger et al., 2006). These data reflect the fraction of the sky covered by clouds at all altitudinal levels expressed as a percentage and are estimated at a 3-hour temporal resolution.

Model-building and assessment

I fit two sets of generalized additive models (GAMs) to test my research objectives. My first set of models was designed to assess statistical support for bird responses to each color treatment relative to the preceding and succeeding “off” control periods. My second set of models was designed to assess potential differences in bird responses between color treatments. Across all models, I log-transformed migration traffic rate to satisfy model assumptions.

For my first set of models, I subset each dataset to treatment periods and the preceding and succeeding control period. Using these subsets, I fit GAMs for each of my three response variables and set the control periods as the intercept. I included the time after sunset (minutes) as a smooth term predictor, whether the light was on or off as a categorical predictor, cloud cover and moon illumination as continuous predictors, and date as a random effect using a basis spline. The resulting models allowed us to determine if bird behavior for each color treatment was statistically different than its paired control periods and estimate an effect size that accounted for variation explained by covariates.

For my second set of models, I subtracted the value for a behavioral metric during each control period from the value in its succeeding treatment period. I treated this calculated difference as the response variable in this set of GAMs and set the white

color treatment as the intercept. I reasoned that white light is a natural comparison point, given that it was my treatment without a filter and, more broadly, is often the default choice for lighting. I used all the same predictors as my first set of models. These models allowed us to determine differences between avian responses to color treatments and quantify the effects of environmental conditions on those responses. I used the gam.check function in the mgcv R package to ensure model convergence and to check fit diagnostics (Wood, 2017). Specifically, I used RMS GCV scores to assess convergence and p-values provided by basis dimension checking to adjust k-values that sufficiently captured smooth terms. Finally, I also visually inspected diagnostic plots to check for major violations of model assumptions.

RESULTS

Across two fall migration seasons, I conducted my experiment for a total of 31 nights. I collected data for 344 control periods and 344 corresponding treatment periods (n_{white}=92, n_{red}=83, n_{amber}=83, n_{blue}=86) recording a total of 78,243 bird echoes. Across the 31 nights, the mean migration traffic rate was 308 birds/hour. However, the distribution of migration traffic was heavily right-skewed, with many nights having low mean migration traffic rates (min=14 birds/hour*km) and few nights having high mean migration traffic rates (max = 1165 birds/hour*km).

Color treatment effects relative to control periods

I found that my white light treatment reduced the mean flight height relative to control periods (Est=-24.24$\pm$10.59, t=-2.29, p=0.02). I did not find an effect of other color

treatments on flight height or an effect of any color treatment on migration traffic rate or flight direction relative to control periods (Supplemental Table 4.1). I include residual diagnostic plots for the model showing the effect of white light treatment on flight height in my Appendix (Supplemental Figure 4.2).

Comparison of color treatment responses and environment effects

My models showed that white light treatments reduced mean flight height more than amber (Est=39.88±14.42, t=2.76, p=<0.01) and red (Est=31.22±14.41, t=2.16, p=0.03) treatments, but that this effect was marginal for blue treatments (Est=26.82±14.25, t=1.88, p=0.06). Residual inspection and data visualizations revealed that these differences were largely driven by long tails, with flight height responses centered on zero (Figure 4.3) (Supplemental Figure 4.3). I did not find an effect between color treatments with respect to migration traffic rate or flight direction (Supplemental Table 4.2). I also did not find an effect of moon illumination or cloud cover on bird responses to color treatments.

DISCUSSION

I conducted a field experiment to understand avian in-flight behavioral responses to different spectra of ALAN and the degree to which those responses are influenced by environmental conditions. I show that white light reduces the flight height for migrating birds and that this effect may be stronger than red, amber, and blue lighting. My research both provides support for previous findings and adds nuance to my understanding of how birds respond to ALAN. While I am cautious in my interpretations and want to be clear about the limitations of my experiment, my ability to demonstrate

avian responses in a low-density migration corridor could highlight that the effects of ALAN extend beyond brightly light, high traffic areas.

Overall, my results suggested that the white light treatment, which was composed of short wavelengths in the range of 430-450nm (~6,440-6740 kelvin), had the strongest effect on bird behavior. This finding adds to a growing literature showing that short-wavelength light has larger effects than long-wavelength lighting on nocturnally migrating birds in various contexts. Studies showing this have employed visual and acoustic monitoring (Evans et al., 2007), netting rates (Zhao et al., 2020), and thermal imagery (Rebke et al., 2019) to assess avian responses, focused largely on aggregation. My use of a vertically looking radar allowed us to monitor specific flight behavior and capture subtle flight height responses that may be overlooked through other monitoring techniques. To my knowledge, the only other study with comparable methods was the dissertation of d'Entremont (2015), which used X-band radar to determine that short wavelength lighting reduced flight height around wind turbines in northeastern British Columbia, and I find it encouraging that my results complement these findings. My blue light treatment was also primarily composed of a sharp peak at 430-450nm but was much narrower in spectral width than my white treatment. This may partially explain why the effect difference between white and blue treatments was weaker than red and amber lighting.

I was surprised that I did not find an effect of moon illumination nor cloud cover on bird responses to ALAN across any color treatment. While some studies have suggested that birds are more attracted to light when moon illumination is low (Bolshakov et al., 2013; Rodríguez & Rodríguez, 2009), others such as Poot et al

(2008) also failed to find an effect. While they attributed this to a small sample size, which may be applicable here, the effect of moon illumination may also be context specific. A systematic review of the effects of moon illumination on migratory organisms may be helpful in revealing generalizable ecological patterns. With respect to cloud cover, previous work has shown that high cover can amplify the spread of ALAN, thereby increasing its effects (Kyba et al., 2011). While I did include cloud cover as a covariate, I found it difficult to access data that matched the spatio-temporal resolution of my experiment. NARR provided cloud cover information at an approximately 32 kilometers spatial and 3-hour temporal resolution, both of which were coarser than my collected response data. This is important given that cloud conditions can be locally patchy and change rapidly. Data that more accurately reflect the conditions around small scale studies such as ours could be very valuable for future research efforts.

To that end, there were critical limitations of my study that should be considered when interpreting my results. While my intention was to isolate the effect of light spectrum, in practice ALAN is typically composed of a mix of sources ranging in spectrum and other characteristics. The combination of and interactions between ALAN sources and other environmental pollutants likely complicate bird responses. For example, Cabrera-Cruz et al (2019) used weather surveillance radar to determine that, contrary to their predictions, avian flight height increased when birds flew over urban areas in the eastern United States. Such findings highlight that avian responses to ALAN are complex and, while studies like ours that isolate one variable provide helpful insight, we must be careful in extrapolating such work into application. Further, the effect size I observed was relatively weak, with my models estimating that white light

reduced flight height by an average of 24m relative to a mean flight height of 374m (SD±106m). I suspect that this was at least partially due to my limited sample size in a low-density migration region (Dokter et al., 2018). Yet, in addition to being consistent with much of the broader literature, I submit that my findings may support the notion that ALAN's effects on wildlife behavior could be more widespread and pervasive than previously assumed (Gaston et al., 2021). ALAN is often discussed within the context of brightly lit, urban centers. The behavioral change I observed was subtle and likely would have been challenging to detect without high-resolution radar data. My ability to demonstrate an effect of a relatively small point source of ALAN could be indicative of isolated ALAN sources having widespread and important biological influences. In this regard, my results echo Gaston et al (2021) in calling for a more holistic consideration of how remote or mobile point sources of ALAN may be impacting wildlife distributions and behavior.

Given the connection between ALAN and bird collisions with anthropogenic structures, the management and mitigation of ALAN could play a prominent role in curbing the rapid decline of migratory birds. Van Doren et al. (2017), for example, demonstrated that turning off bright lights at a memorial center allowed for nocturnal migrants to pass through the area, informing a protocol of “off” periods when migration activity is high. At a larger scale, in response to research identifying areas where birds are most highly exposed to urban ALAN, many cities participate in ‘Lights Out’ campaigns, which seek to recruit members of the public to voluntarily reduce their ALAN emissions during migration seasons (Burt, Kelly, Fox, et al., 2023). When paired with forecasts of migration activity, such campaigns can even be targeted at specific nights

of high migration activity, optimizing public action (Horton et al., 2021). These examples not only elucidate the role that ALAN management could play in avian conservation, but also how that management can be refined by a stronger understanding of bird behavior. The growing consensus that short wavelengths more strongly effect birds could be integrated into conservation management. For example, prominent lighting could be filtered or replaced during migration seasons. As noted above, we should be careful in applying my findings and, more broadly, consider potential effects on non-avian wildlife and humans. Nonetheless, a stronger understanding of the relationships between animal behavior and ALAN is a promising research topic that could add flexibility to current lighting management schemes.

In conclusion, my study contributes to the growing body of evidence that ALAN influences avian behavior, particularly through the effects of short-wavelength light on flight height and migration traffic rate. My findings highlight that even small, isolated light sources can impact bird behavior, suggesting broader implications for ALAN management beyond urban centers. By refining our understanding of taxonomic and environmental nuances in avian responses to ALAN, we can better inform conservation strategies aimed at mitigating its impacts and supporting migratory bird populations.

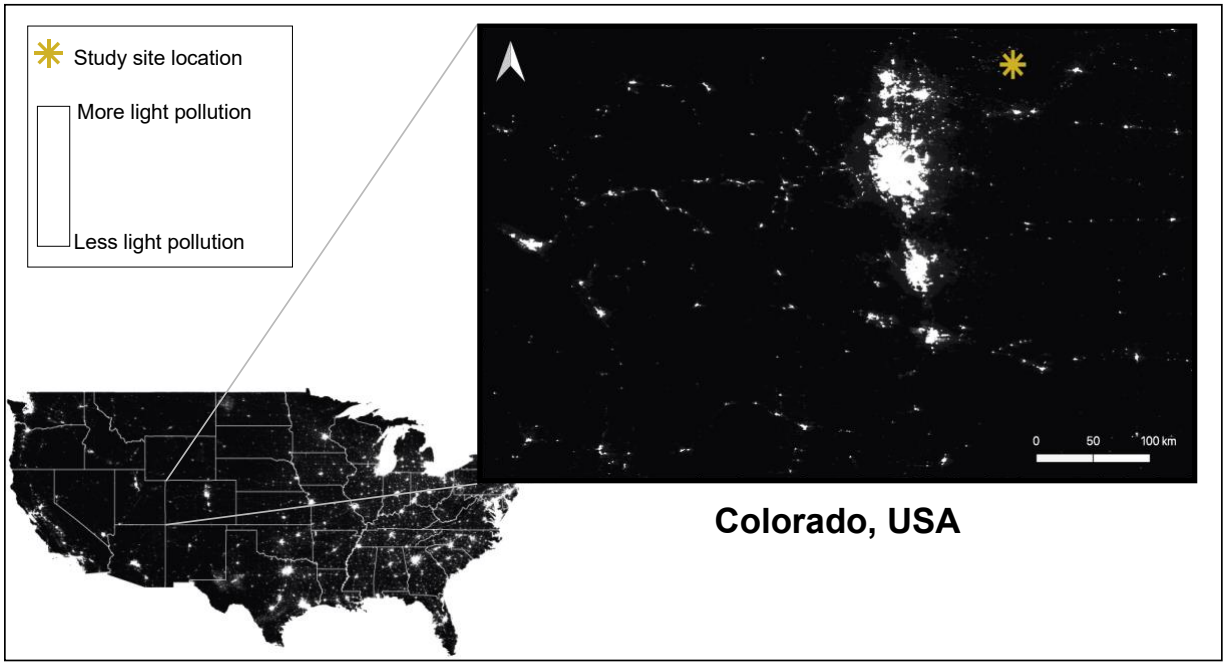

Figure 4.1 Map showing the study site location (yellow asterisk) for an experiment on the effects of different spectra of anthropogenic light at night on in-flight bird behavior. Light pollution data were taken from Visible Infrared Imaging Radiometer Suite (VIIRS) data, which is collected and made publicly available by the National Oceanic and Atmospheric Administration. VIIRS data are mapped over the continental United States, with a zoomed inset for the state of Colorado, in which the site is located.

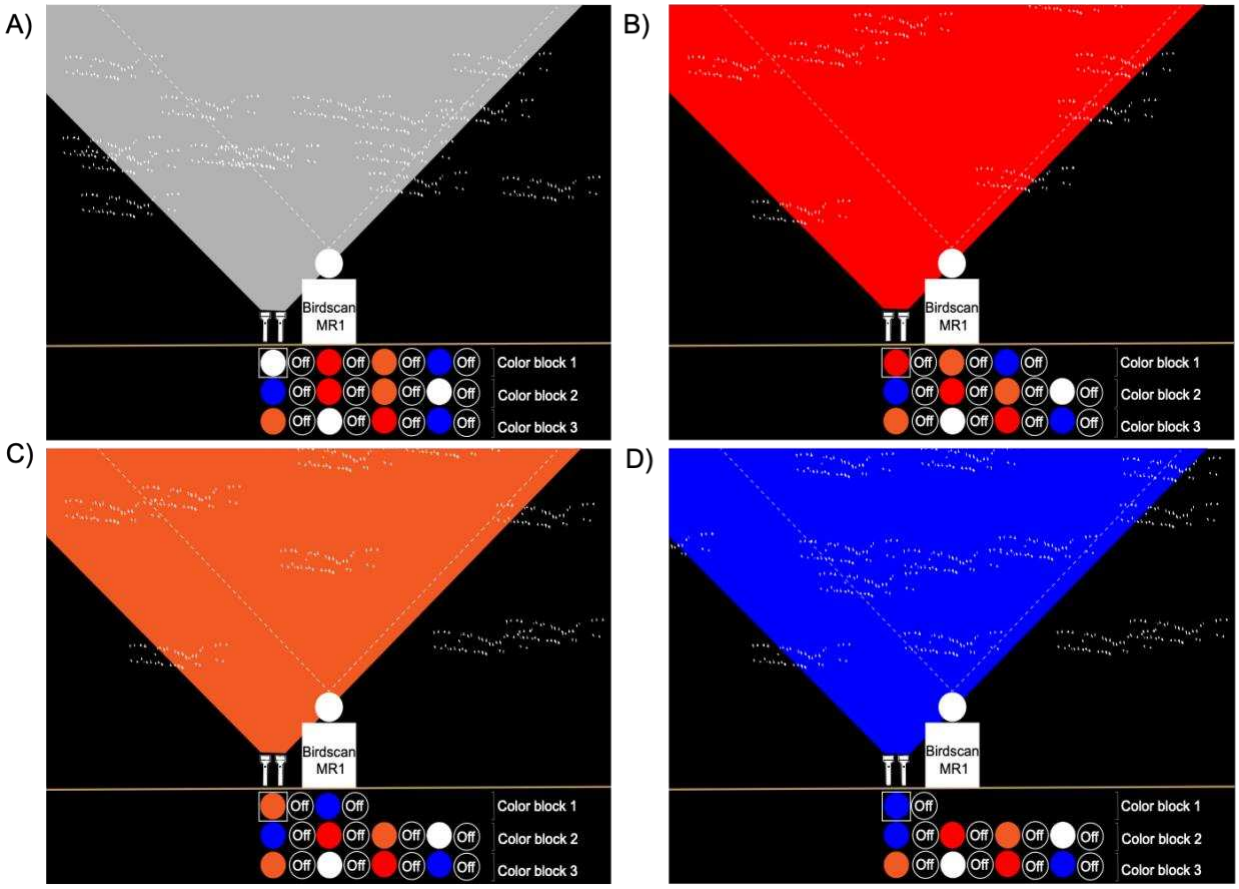

Figure 4.2 Experimental design for testing the effect of different spectra of artificial light at night on the in-flight behavior of nocturnally migrating birds. Professional grade spotlights emitted light into the sky and color treatments (A-white, B-red, C-amber, D-blue) were cycled every 30 minutes separated by 15-minute control periods when lights were turned off. The sequence of treatments was organized into color blocks, whereby colors were not repeated within a block and their order was randomized. The BirdScan MR1, a mobile radar designed to quantify activity in the atmosphere, was employed to collect bird behavior throughout the experiment.

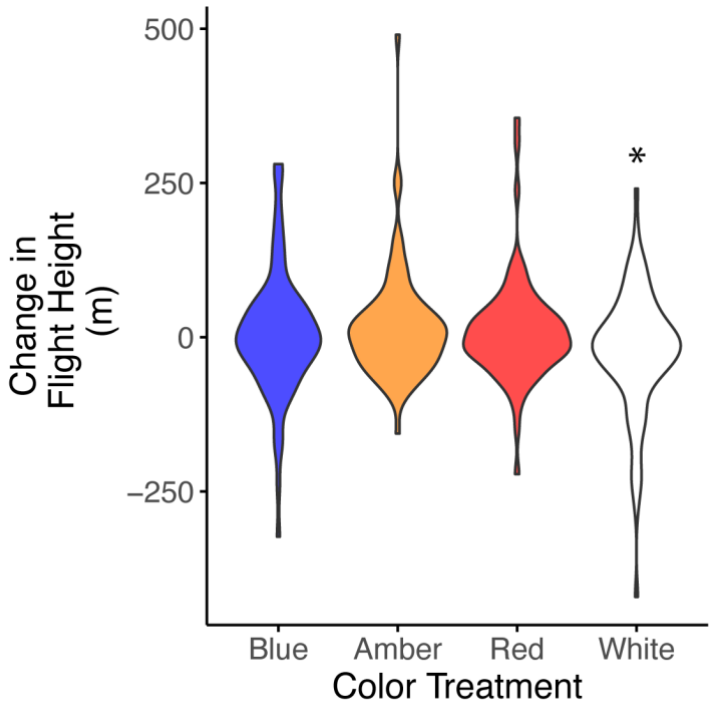

Figure 4.3 Violin plots showing the distribution of the changes in mean flight height for all detected nocturnally migrating birds in response to the emission of anthropogenic light for four color treatments. The x-axis represents the color treatment groups and the y-axis indicates the observed changes in flight height relative to the lights being off. Each violin plot illustrates the kernel density estimation of the data within each group, with the area scaled to reflect the sample size. An asterisk denotes a significant difference between treatment responses.

LITERATURE CITED

Adams, C. A., Fernández-Juricic, E., Bayne, E. M., & St. Clair, C. C. (2021). Effects of artificial light on bird movement and distribution: A systematic map. *Environmental Evidence*, *10*(1), 37. https://doi.org/10.1186/s13750-021-00246-8

Andelt, W. F., Woolley, T. P., & Hopper, S. N. (1997). *Effectiveness of barriers, pyrotechnics, flashing lights, and Scarey Man for deterring heron predation on fish*.

Aulsebrook, A. E., Jones, T. M., Mulder, R. A., & Lesku, J. A. (2018). Impacts of artificial light at night on sleep: A review and prospectus. *Journal of Experimental Zoology Part A: Ecological and Integrative Physiology*, *329*(8–9), 409–418. https://doi.org/10.1002/jez.2189

Bolshakov, C. V., Bulyuk, V. N., Sinelschikova, A. Y., & Vorotkov, M. V. (2013). *Influence of the vertical light beam on numbers and flight trajectories of night-migrating songbirds*.

Bruderer, B., Peter, D., & Steuri, T. (1999). Behaviour of migrating birds exposed to X-band radar and a bright light beam. *Journal of Experimental Biology*, *202*(9), 1015–1022. https://doi.org/10.1242/jeb.202.9.1015

Burt, C. S., Kelly, J. F., Fox, A. S., Jenkins-Smith, H. C., Leon-Corwin, M., Khalighifar, A., Trankina, G. E., Silva, C. L., & Horton, K. G. (2023). Can ecological forecasting lead to convergence on sustainable lighting policies? *Conservation Science and Practice*, *5*(4), e12920. https://doi.org/10.1111/csp2.12920

Burt, C. S., Kelly, J. F., Trankina, G. E., Silva, C. L., Khalighifar, A., Jenkins-Smith, H. C., Fox, A. S., Fristrup, K. M., & Horton, K. G. (2023). The effects of light

pollution on migratory animal behavior. *Trends in Ecology & Evolution*, *38*(4), 355–368. https://doi.org/10.1016/j.tree.2022.12.006

Cabrera-Cruz, S. A., Smolinsky, J. A., McCarthy, K. P., & Buler, J. J. (2019). Urban areas affect flight altitudes of nocturnally migrating birds. *Journal of Animal Ecology*, *88*(12), 1873–1887. https://doi.org/10.1111/1365-2656.13075

Cassidy, F. L. (2015, Fall). *The Potential of Lasers as Deterrents to Protect Birds in the Alberta Oil Sands and Other Areas of Human-Bird Conflict*. ERA. https://doi.org/10.7939/R3RV0DC06

Chernetsov, N. S. (2016). Orientation and navigation of migrating birds. *Biology Bulletin*, *43*(8), 788–803. https://doi.org/10.1134/S1062359016080069

d'Entremont, M. V. (2015). Response of Nocturnal Migrants To Variation in Artificial Lighting Around Wind Turbines. *University of Northern British Columbia*, *Dissertation*.

Davies, T. W., & Smyth, T. (2018). Why artificial light at night should be a focus for global change research in the 21st century. *Global Change Biology*, *24*(3), 872–882. https://doi.org/10.1111/gcb.13927

Dokter, A. M., Farnsworth, A., Fink, D., Ruiz-Gutierrez, V., Hochachka, W. M., La Sorte, F. A., Robinson, O. J., Rosenberg, K. V., & Kelling, S. (2018). Seasonal abundance and survival of North America's migratory avifauna determined by weather radar. *Nature Ecology & Evolution*, *2*(10), 1603–1609. https://doi.org/10.1038/s41559-018-0666-4

Evans, W. R., Akashi, Y., Altman, N. S., & Manville, A. M. (2007). Response of night-migrating songbirds in cloud to colored and flashing light. *North American Birds*, *60*(4), 476–488.

Foster, J. J., Smolka, J., Nilsson, D.-E., & Dacke, M. (2018). How animals follow the stars. *Proceedings of the Royal Society B: Biological Sciences*, *285*(1871), 20172322. https://doi.org/10.1098/rspb.2017.2322

Gaston, K. J., Ackermann, S., Bennie, J., Cox, D. T. C., Phillips, B. B., Sánchez de Miguel, A., & Sanders, D. (2021). Pervasiveness of Biological Impacts of Artificial Light at Night. *Integrative and Comparative Biology*, *61*(3), 1098–1110. https://doi.org/10.1093/icb/icab145

Gauthreaux, S. A. (1982). Age-Dependent Orientation in Migratory Birds. In F. Papi & H. G. Wallraff (Eds.), *Avian Navigation* (pp. 68–74). Springer. https://doi.org/10.1007/978-3-642-68616-0_7

Grubisic, M., & van Grunsven, R. H. (2021). Artificial light at night disrupts species interactions and changes insect communities. *Current Opinion in Insect Science*, *47*, 136–141. https://doi.org/10.1016/j.cois.2021.06.007

Haest, B., Hertner, F., Schmid, B., Preatoni, D., De Groeve, J., & Liechti, F. (2023). *birdscanR: Migration Traffic Rate Calculation Package for Birdscan MR1 Radars* [Computer software]. Zenodo. https://doi.org/10.5281/zenodo.7665531

Horton, K. G., Van Doren, B. M., Albers, H. J., Farnsworth, A., & Sheldon, D. (2021). Near-term ecological forecasting for dynamic aeroconservation of migratory birds. *Conservation Biology*, *35*(6), 1777–1786. https://doi.org/10.1111/cobi.13740

Kumar, J., Gupta, P., Naseem, A., & Malik, S. (2017). Light spectrum and intensity, and the timekeeping in birds. *Biological Rhythm Research*, *48*(5), 739–746. https://doi.org/10.1080/09291016.2017.1345449

Kyba, C. C. M., Ruhtz, T., Fischer, J., & Hölker, F. (2011). Cloud Coverage Acts as an Amplifier for Ecological Light Pollution in Urban Ecosystems. *PLoS ONE*, *6*(3), e17307. https://doi.org/10.1371/journal.pone.0017307

Lao, S., Robertson, B. A., Anderson, A. W., Blair, R. B., Eckles, J. W., Turner, R. J., & Loss, S. R. (2020). The influence of artificial light at night and polarized light on bird-building collisions. *Biological Conservation*, *241*, 108358. https://doi.org/10.1016/j.biocon.2019.108358

Loss, S. R., Will, T., & Marra, P. P. (2015). *Direct Mortality of Birds from Anthropogenic Causes*. https://doi.org/10.1146/annurev-ecolsys-112414-054133

May, R., Åström, J., Hamre, Ø., & Dahl, E. L. (2017). Do birds in flight respond to (ultra)violet lighting? *Avian Research*, *8*(1), 33. https://doi.org/10.1186/s40657-017-0092-3

McLaren, J. D., Buler, J. J., Schreckengost, T., Smolinsky, J. A., Boone, M., Emiel van Loon, E., Dawson, D. K., & Walters, E. L. (2018). Artificial light at night confounds broad-scale habitat use by migrating birds. *Ecology Letters*, *21*(3), 356–364. https://doi.org/10.1111/ele.12902

Mesinger, F., DiMego, G., Kalnay, E., Mitchell, K., Shafran, P. C., Ebisuzaki, W., Jović, D., Woollen, J., Rogers, E., Berbery, E. H., Ek, M. B., Fan, Y., Grumbine, R., Higgins, W., Li, H., Lin, Y., Manikin, G., Parrish, D., & Shi, W. (2006). North

American Regional Reanalysis. *Bulletin of the American Meteorological Society*, *87*(3), 343–360. https://doi.org/10.1175/BAMS-87-3-343

Muheim, R., Sjöberg, S., & Pinzon-Rodriguez, A. (2016). Polarized light modulates light-dependent magnetic compass orientation in birds. *Proceedings of the National Academy of Sciences*, *113*(6), 1654–1659. https://doi.org/10.1073/pnas.1513391113

Parkins, K. L., Elbin, S. B., & Barnes, E. (2015). Light, Glass, and Bird—Building Collisions in an Urban Park. *Northeastern Naturalist*, *22*(1), 84–94. https://doi.org/10.1656/045.022.0113

Poot, H., Ens, B. J., de Vries, H., Donners, M. A. H., Wernand, M. R., & Marquenie, J. M. (2008). Green Light for Nocturnally Migrating Birds. *Ecology and Society*, *13*(2). https://www.jstor.org/stable/26267982

R Core Team. (2024). *R Core Team (2022). R: A language and environment for statistical computing. R Foundation for Statistical Computing, Vienna, Austria. URL https://www.R-project.org/.* [Computer software].

Rebke, M., Dierschke, V., Weiner, C. N., Aumüller, R., Hill, K., & Hill, R. (2019). Attraction of nocturnally migrating birds to artificial light: The influence of colour, intensity and blinking mode under different cloud cover conditions. *Biological Conservation*, *233*, 220–227. https://doi.org/10.1016/j.biocon.2019.02.029

Rodríguez, A., & Rodríguez, B. (2009). Attraction of petrels to artificial lights in the Canary Islands: Effects of the moon phase and age class. *Ibis*, *151*(2), 299–310. https://doi.org/10.1111/j.1474-919X.2009.00925.x

Ronconi, R. A., Allard, K. A., & Taylor, P. D. (2015). Bird interactions with offshore oil and gas platforms: Review of impacts and monitoring techniques. *Journal of Environmental Management*, *147*, 34–45. https://doi.org/10.1016/j.jenvman.2014.07.031

Schmid, B., Zaugg, S., Votier, S. C., Chapman, J. W., Boos, M., & Liechti, F. (2019). Size matters in quantitative radar monitoring of animal migration: Estimating monitored volume from wingbeat frequency. *Ecography*, *42*(5), 931–941. https://doi.org/10.1111/ecog.04025

Seymoure, B. M., Buxton, R., White, J. M., Linares, C. R., Fristrup, K., Crooks, K., Wittemyer, G., & Angeloni, L. (2025). Global artificial light masks biologically important light cycles of animals. *Frontiers in Ecology and the Environment*, *n/a*(n/a), e2832. https://doi.org/10.1002/fee.2832

Śmielak, M. K. (2023). Biologically meaningful moonlight measures and their application in ecological research. *Behavioral Ecology and Sociobiology*, *77*(2), 21. https://doi.org/10.1007/s00265-022-03287-2

Swiss Birdradar Solution. (2023). *Radar System BirdScan MR1 | Swiss Birdradar Solution AG*. https://swiss-birdradar.com/systems/radar-birdscan-mr1/

Syposz, M., Padget, O., Willis, J., Van Doren, B. M., Gillies, N., Fayet, A. L., Wood, M. J., Alejo, A., & Guilford, T. (2021). Avoidance of different durations, colours and intensities of artificial light by adult seabirds. *Scientific Reports*, *11*(1), Article 1. https://doi.org/10.1038/s41598-021-97986-x

Van Doren, B. M., Willard, D. E., Hennen, M., Horton, K. G., Stuber, E. F., Sheldon, D., Sivakumar, A. H., Wang, J., Farnsworth, A., & Winger, B. M. (2021). Drivers of

fatal bird collisions in an urban center. *Proceedings of the National Academy of Sciences*, *118*(24), e2101666118. https://doi.org/10.1073/pnas.2101666118

Weisshaupt, N., Hervo, M., & Haest, B. (2023). Comparison of bird migration in a radar wind profiler and a dedicated bird radar. *Remote Sensing in Ecology and Conservation*, *n/a*(n/a). https://doi.org/10.1002/rse2.350

Wood, S. N. (2017). *Generalized Additive Models: An Introduction with R, Second Edition* (2nd ed.). Chapman and Hall/CRC. https://doi.org/10.1201/9781315370279

Zhao, X., Zhang, M., Che, X., & Zou, F. (2020). Blue light attracts nocturnally migrating birds. *The Condor*, *122*(2), duaa002. https://doi.org/10.1093/condor/duaa002

APPENDIX

Supplemental Table 1.1 Summary of the number of PPI pixels with a range adjustment factor (R) greater than 10, which were removed from the raster output of NEXRAD reflectivity as part of data processing. Mean, median, and standard deviation of the number of removed pixels are summarized by site.

Site	Mean	Median	SD
Elevated 1	1.222951	0	3.427616
Elevated 2	1.348770	0	3.769072
Elevated 3	1.896721	0	4.338769
Elevated 4	2.097541	0	4.478036
Elevated 5*	3.784426	1	5.104750
Flat 1	1.016803	0	3.710755
Flat 2	1.145082	0	3.574466
Flat 3	1.363525	0	3.886170
Flat 4	1.669262	0	4.488795
Flat 5	1.446721	0	3.913323

**An analysis of variance and subsequent Tukey's HSD test determined that cell removal was significantly higher at this site relative to all other sites*

Supplemental Table 1.2. Summary of the best supported linear model fit to the mean nightly of migration activity BirdScan MR1 and NEXRAD datasets. This model included the mean nightly BirdScan MR1 measures of density (birds/km^2) as a response variable. Mean nightly NEXRAD range-corrected reflectivity (cm^2/km^2) was included as a fixed predictor. The percentage of beam blockage and the distance of the BirdScan MR1 from the NEXRAD station were also included as fixed predictors with an interaction with NEXRAD range-corrected reflectivity.

*R code: lm(mean_dens~mean_corrected + dist*mean_corrected + block*mean_corrected)*

$$y_{it} = \beta_0 + \beta_1 * \mu_{corrected,it} + \beta_2 * distance_i + \beta_3 * blockage_i + \beta_4 \mu_{corrected,it} * distance_i + \beta_5 \mu_{corrected,it} * blockage_i + \epsilon_{it}$$

For mean density y at site *i* and date *t,* range-corrected reflectivity $(\mu_{corrected,it})$, distance from NEXRAD $distance_i$, and percentage beam blockage $blockage_i$.

	Estimate	Std. error	t-value	Pr(>|t|)
Intercept	8.699	1.483	5.865	9.57e-07 ***
mean_corrected	1.185	0.115	10.343	1.81e-12 ***
dist	1.149	1.530	0.751	0.458
block	-1.201	1.508	-0.796	0.431
mean_corrected:dist	0.042	0.110	0.382	0.704
mean_corrected:block	-0.117	0.108	-1.088	0.284

**** 0 < p <0.001*
*** 0.001 < p <0.01*
** 0.01 < p < 0.05*

Supplemental Table 1.3. Summary of the best supported linear mixed model fit to within night migration activity of BirdScan MR1 and NEXRAD datasets. This model included the mean BirdScan MR1 measures of density (birds/km^2) in 20-minute intervals as a response variable. Mean NEXRAD uncorrected reflectivity (cm^2/km^2) within the same interval was included as a fixed predictor, and the percentage of beam blockage and the distance of the BirdScan MR1 from the NEXRAD station were included as a three-way interaction with reflectivity. Date was included as a random intercept.

*R code: dens ~ eta_uncorrected + block_scaled*dist_scaled*eta_uncorrected + (1 | date)*

$$y_{it} = \beta_0 + \beta_{1,t} + \beta_2 * \mu_{uncorrected,it} + \beta_3 * blockage_i + \beta_4 * distance_i + \beta_5 * blocakge_i * distance_i + \beta_6 * \mu_{uncorrected,it} * blocakage_i + \beta_7 * \mu_{uncorrected,it} * distance_i + \beta_8 * distance_i * blockage_i * \mu_{uncorrected,it} + \epsilon_{it}$$

For mean density y at site *i* and timestep *t* range-corrected reflectivity $(\mu_{corrected,it})$, distance from NEXRAD ($distance_i$), and percentage beam blockage ($blockage_i$).

	Estimate	Std. error	t-value	p-value
Intercept	15.140	1.469	10.304	2.73e-13
mean_eta_uncorrected	0.557	0.057	9.813	< 2e-16
block_scaled	1.984	1.504	1.319	0.19394
dist _scaled	4.569	1.489	3.068	0.00371
block_scaled:dist_scaled	1.621	1.491	1.087	0.28301
mean_eta_uncorrected:block_scaled	-0.317	0.069	-4.581	5.38e-06
mean_eta_uncorrected:dist_scaled	-0.073	0.056	-1.316	0.18850
mean_eta_uncorrected:block_scaled:dist_scaled	-0.309	0.068	-4.507	7.56e-06

Supplemental table 1.4. Correlation coefficient summary between the proportion of migration activity between BirdScan MR1 and NEXRAD radar systems. The densities of each radar system were subset into 100m bins and calculated as a proportion of total activity across all altitudes. Densities were summarized into 20-minute periods as a unit of within-night comparison.

Height above sea level (100m bins)	Correlation coefficient	Sample size (20-minute periods)
1900	0.68	549
2000	0.67	647
2100	0.52	738
2200	0.45	738
2300	0.22	816
2400	0.30	815
2500	0.41	736
2600	0.41	576
2700	0.38	519
2800	0.20	343
2900	0.08	266

Supplemental Table 2.1 A list of the sampling, atmospheric, and terrestrial predictor variables used to predict bird migration density with gradient boosted trees.

Predictor	Class of variables	Resolution	Collection metrics	Cardinal directions
Ordinal date	Sampling	-	-	No
Time after sunset	Sampling	-	-	No
Distance from radar	Sampling	-	-	No
Elevation	Sampling	NASADEM (30 m)	-	No
Air temperature	Atmospheric	NARR (32 km) NAM (12 km)	2 m above ground, 800-1000 hPa	Yes
Geospatial height	Atmospheric	NARR (32 km) NAM (12 km)	Surface	Yes
Pressure	Atmospheric	NARR (32 km) NAM (12 km)	Surface, mean sea level	Yes
Relative humidity	Atmospheric	NARR (32 km) NAM (12 km)	2 m above ground	Yes
Total cloud cover	Atmospheric	NARR (32 km) NAM (12 km)	Entire atmosphere	Yes
Visibility	Atmospheric	NARR (32 km) NAM (12 km)	Surface	Yes
Zonal and meridional wind speed	Atmospheric	NARR (32 km) NAM (12 km)	10 m above ground, 800-1000 hPa	Yes
Enhanced Vegetation Index (EVI)	Terrestrial	MOD13A1 (500 m)	Aggregated to 2.9 km, and mean and standard deviation collected	No
Visible Infrared Imaging Radiometer Suite (VIIRS)	Terrestrial	VIIRS Nighttime lights (~500 m at the Equator)	Aggregated to 2.9 km, and mean and standard deviation collected	No
Water bodies	Terrestrial	MCD12Q1 (500 m)	Aggregated to 2.9 km, and relative percentage calculated	No

Grasslands	Terrestrial	MCD12Q1 (500 m)	Aggregated to 2.9 km, and relative percentage calculated	No
Permanent wetlands	Terrestrial	MCD12Q1 (500 m)	Aggregated to 2.9 km, and relative percentage calculated	No
Urban and Built-up Lands	Terrestrial	MCD12Q1 (500 m)	Aggregated to 2.9 km, and relative percentage calculated	No
Non-Vegetated Lands	Terrestrial	MCD12Q1 (500 m)	Aggregated to 2.9 km, and relative percentage calculated	No
Forests	Terrestrial	MCD12Q1 (500 m)	Aggregated to 2.9 km, and relative percentage calculated	No
Shrublands	Terrestrial	MCD12Q1 (500 m)	Aggregated to 2.9 km, and relative percentage calculated	No
Croplands	Terrestrial	MCD12Q1 (500 m)	Aggregated to 2.9 km, and relative percentage calculated	No
Savannas	Terrestrial	MCD12Q1 (500 m)	Aggregated to 2.9 km, and relative percentage calculated	No

Supplemental Table 3.1 Definitions and sources for three different definitions for "urban." Definitions are provided by both the United States Census Bureau and the National Center for Health Statistics, specifying criteria for Metropolitan Statistical Areas, Large Metropolitan Areas, and Census Urban Areas. Relevant links to original sources and downloading data are included for reference.

Definition	Institution	Definition	Link
Metropolitan Statistical Area	United States Census Bureau	Area with at least one urban area of 50,000 or more inhabitants.	https://www.census.gov/programs-surveys/metro-micro.html
Large Metropolitan Area	National Center for Health Statistics	Areas that have 1 million or more, including "central" and "fringe" metropolitan areas	https://www.cdc.gov/nchs/data-analysis-tools/urban-rural.html
Census Urban Area	United States Census Bureau	"Densely developed territory, and encompass residential, commercial, and other non-residential urban land uses. The Census Bureau delineates urban areas after each decennial census by applying specified criteria to decennial census and other data."	https://www.census.gov/programs-surveys/geography/guidance/geo-areas/urban-rural.html

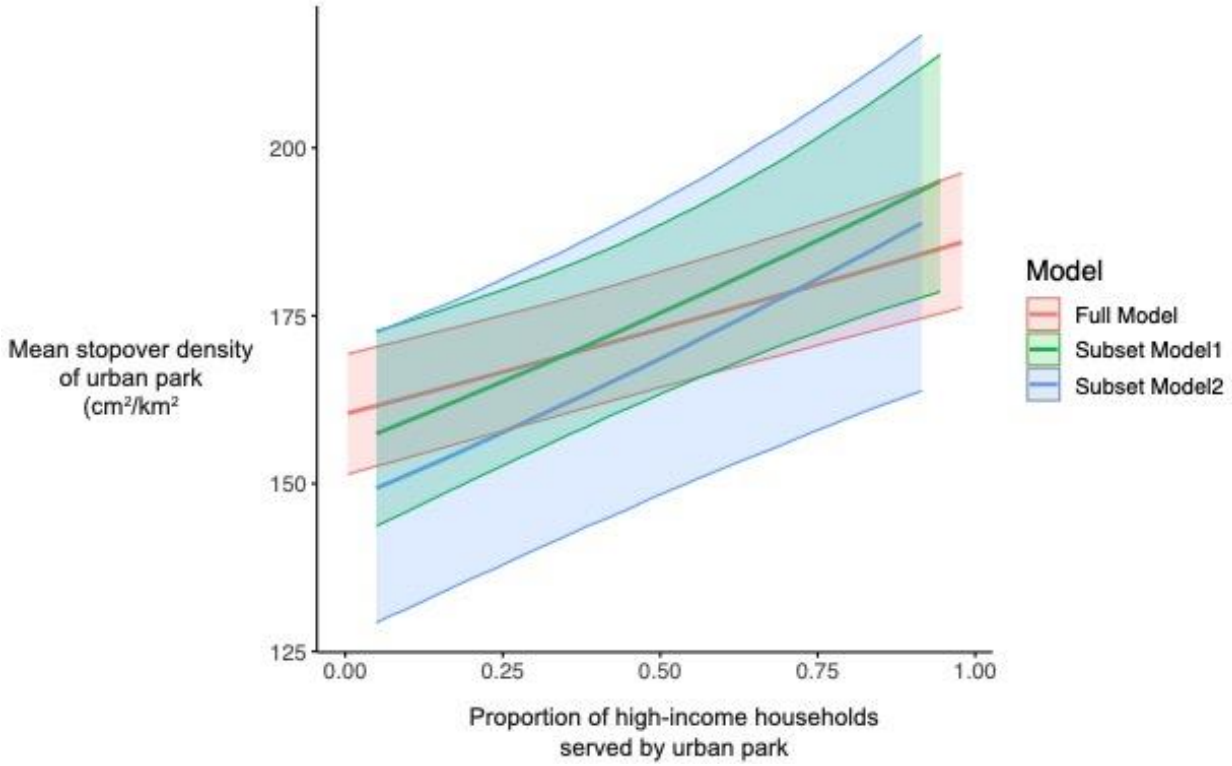

Supplemental Figure 3.1 Conditional effects of the proportion of high-income households within a 10-minute walking distance of a park on the estimated mean spring stopover density of migratory birds for that park. The slopes of these effects are shown for three Bayesian hierarchical models: a full model incorporating all parks (red line), a subset model including only parks larger than 1km2 (green line), and a further subset model including only cities with more than five parks larger than 1km2 (blue line). Shaded areas represent the 95% credible intervals for each model. A log link and Gamma family were used to model the positively skewed response variable.

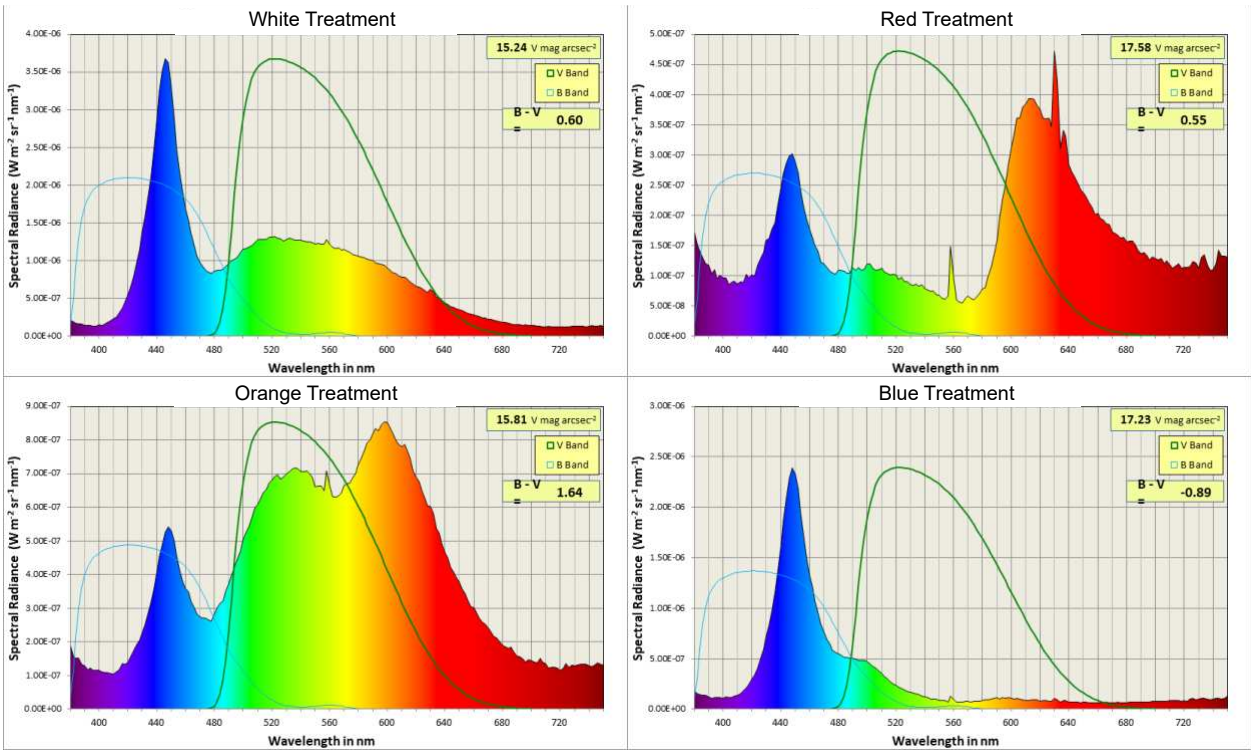

Supplemental Figure 4.1 *Summary of spectral radiance of the ALAN source used as a white, red, amber, and blue color treatments in a field experiment. Spectral radiance is plotted across wavelengths ranging from approximately 350 to 750 nm. The y-axis represents spectral radiance in units of W m−2 sr−1 nm−1W m−2sr−1nm−1, while the x-axis indicates wavelength in nanometers (nm).*

Supplemental Table 4.1 Summary of generalized additive model (GAM) coefficients for the effects of color on migration traffic rate, mean flight height, and mean flight direction for birds in flight. Estimates (± SE) represent the mean effect size for each color category. The t-values and corresponding p-values indicate the significance of these effects. Significant effects are denoted as follows: *p < 0.05.

	Color	Estimate (±SE)	t-value	p-value
Migration traffic rate				
	White	-0.01±0.09	-0.13	0.90
	Red	-0.08±0.10	-0.86	0.39
	Amber	0.01±0.10	0.08	0.94
	Blue	-0.06±0.10	-0.67	0.51
Flight height				
	White	-24.24±10.59	-2.29	0.02*
	Red	4.89±11.15	0.44	0.66
	Amber	6.58±10.75	0.61	0.54
	Blue	10.14±12.08	0.84	0.40
Flight direction				
	White	0.68±4.74	0.14	0.89
	Red	-2.96±5.17	-0.57	0.57
	Amber	-1.86±5.54	-0.34	0.74
	Blue	0.47±4.50	0.10	0.92

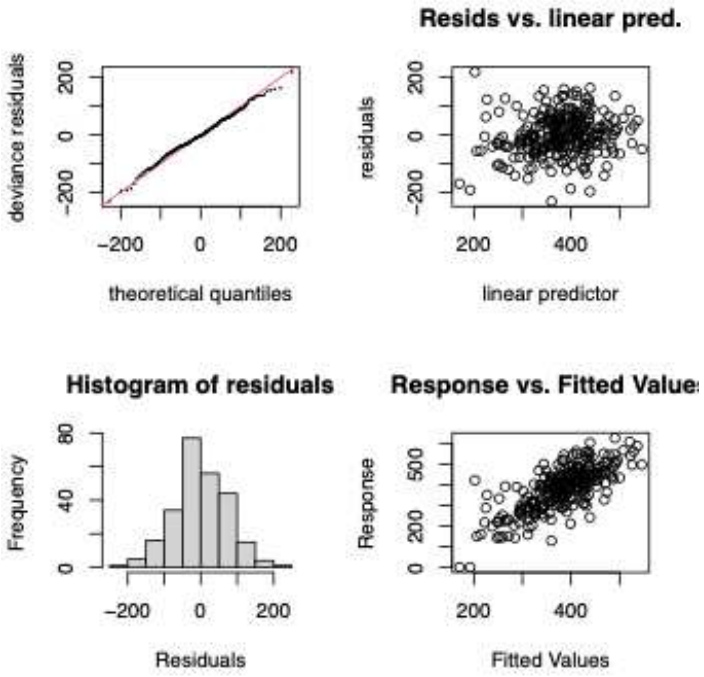

Supplemental Figure 4.2 Diagnostic plots for a Generalized Additive Model predicting the flight height of migratory birds based on multiple explanatory variables and smooth terms. Plots include a Q-Q plot of deviance residuals showing deviations from normality (top left), residuals versus the linear predictor to assess heteroscedasticity and model fit (top right), a histogram of residuals illustrating their distribution (bottom left), and a response versus fitted values plot to evaluate the agreement between observed and predicted values (bottom right).

Supplemental Table 4.2 Summary of generalized additive model (GAM) results for the change in migration traffic rate, flight height, and flight direction of birds aloft in response to artificial light at night treatments. Fixed effect estimates (± standard error), t-values, and p-values are provided for categorical color treatments (red, amber, and blue), cloud cover, and moon illumination. Smooth terms include time after sunset and Julian date, with effective degrees of freedom (edf), reference degrees of freedom (Ref.df), F-statistics, and p-values. Significant effects are denoted as follows: ·p < 0.10; *p < 0.05; **p < 0.01; ***p < 0.001

Migration traffic rate				
Fixed effects		*Estimate ±SE*	*t-value*	*p-value*
Red		-0.09 ±0.08	-1.11	0.27
Amber		-0.02 ±0.08	-0.27	0.78
Blue		-0.13 ±0.08	-1.52	0.13
Cloud cover		-0.00 ±0.00	-0.10	0.92
Moon illumination		0.07 ±0.19	0.40	0.69
Smooth terms	*edf*	*Ref.df*	*F*	*p-value*
Time after sunset	1.78	1.95	4.60	0.02*
Julian date	1.37	42.00	0.00	0.67
Flight height				
Fixed effects		*Estimate ±SE*	*t-value*	*p-value*
Red		31.22 ±14.41	2.16	0.03*
Amber		39.88 ±14.42	2.76	<0.01**

Blue		26.82 ±14.25	1.88	0.06·
Cloud cover		0.16 ±0.20	0.78	0.44
Moon illumination		-4.29 ±36.53	-0.12	0.91
Smooth terms	*edf*	*Ref.df*	*F*	*p-value*
Time after sunset	1.00	1	0.13	0.72
Julian date	8.92	42.00	0.24	0.26
Flight direction				
Fixed effects		*Estimate ±SE*	*t-value*	*p-value*
Red		-0.63 ±6.34	-0.10	0.92
Amber		1.33 ±6.38	0.21	0.84
Blue		5.72 ±6.31	0.91	0.37
Cloud cover		-0.05 ±0.09	-0.53	0.60
Moon illumination		-9.57± 17.24	-0.56	0.58
Smooth terms	*edf*	*Ref.df*	*F*	*p-value*
Time after sunset	1.00	1	0.78	0.38
Julian date	13.71	42.00	0.48	0.05*

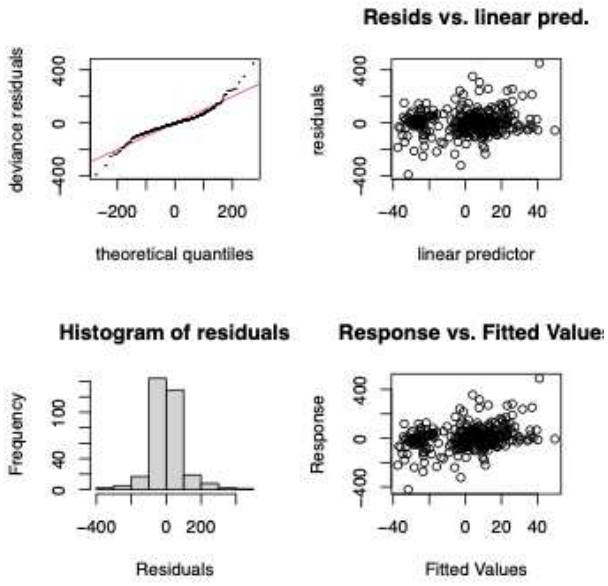

Supplemental Figure 4.3 Diagnostic plots for a Generalized Additive Model predicting the flight height of migratory birds based on multiple explanatory variables and smooth terms. Plots include a Q-Q plot of deviance residuals showing deviations from normality (top left), residuals versus the linear predictor to assess heteroscedasticity and model fit (top right), a histogram of residuals illustrating their distribution (bottom left), and a response versus fitted values plot to evaluate the agreement between observed and predicted values (bottom right).